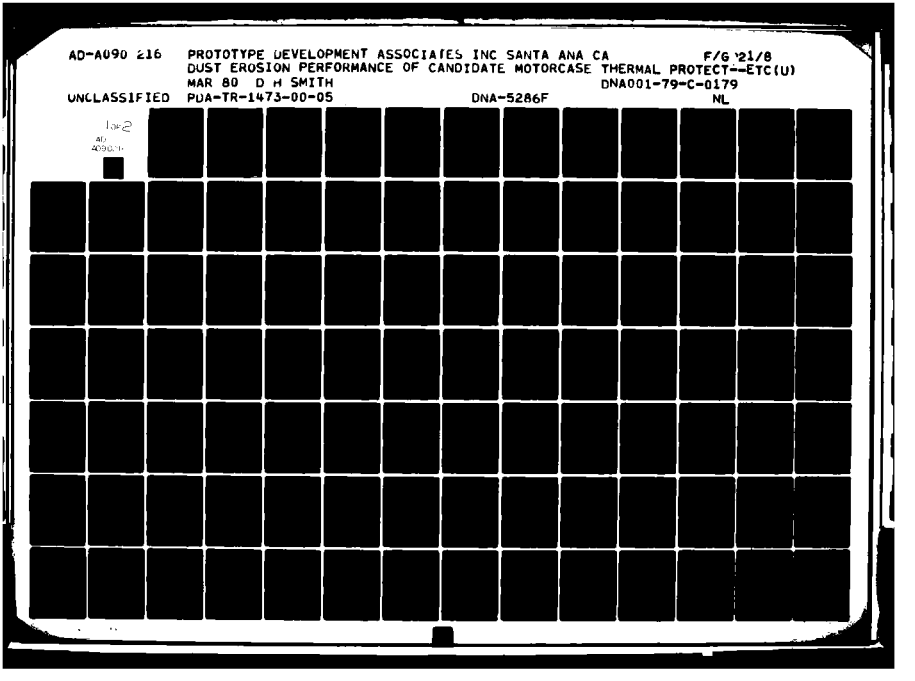
AD-A090 216
PROTOTYPE DEVELOPMENT ASSOCIATES INC SANTA ANA CA
F/G 21/8
DUST EROSION PERFORMANCE OF CANDIDATE MOTORCASE THERMAL PROTECT--ETC(U)
MAR 80 D H SMITH
DNA001-79-C-0179
UNCLASSIFIED
PDA-TR-1473-00-05
DNA-5286F
NL
1 of 2
AD
A090216

(12)

DNA 5286F

DUST EROSION PERFORMANCE OF CANDIDATE MOTORCASE THERMAL PROTECTION MATERIALS

D. H. Smith
Prototype Development Associates, Inc.
1740 Garry Avenue, Suite 201
Santa Ana, California 92705

10 March 1980

Final Report for Period 1 January 1979—1 October 1979

CONTRACT No. DNA 001-79-C-0179

THIS WORK SPONSORED BY THE DEFENSE NUCLEAR AGENCY
UNDER RDT&E RMSS CODE B342079464 N99QAXAI41006 H2590D.

Prepared for
Director
DEFENSE NUCLEAR AGENCY
Washington, D. C. 20305

Destroy this report when it is no longer needed. Do not return to sender.

PLEASE NOTIFY THE DEFENSE NUCLEAR AGENCY, ATTN: STTI, WASHINGTON, D.C. 20305, IF YOUR ADDRESS IS INCORRECT, IF YOU WISH TO BE DELETED FROM THE DISTRIBUTION LIST, OR IF THE ADDRESSEE IS NO LONGER EMPLOYED BY YOUR ORGANIZATION.

UNCLASSIFIED

SECURITY CLASSIFICATION OF THIS PAGE (When Data Entered)

REPORT DOCUMENTATION PAGE

READ INSTRUCTIONS BEFORE COMPLETING FORM

1. REPORT NUMBER: DNA 5286F	2. GOVT ACCESSION NO: AD90216
3. RECIPIENT'S CATALOG NUMBER:	
4. TITLE (and Subtitle): DUST EROSION PERFORMANCE OF CANDIDATE MOTORCASE THERMAL PROTECTION MATERIALS	5. TYPE OF REPORT & PERIOD COVERED: Final Report for Period 1 Jan 79—1 Oct 79
6. PERFORMING ORG. REPORT NUMBER: PDA-TR-1473-00-05	
7. AUTHOR(s): D. H. Smith	8. CONTRACT OR GRANT NUMBER(s): DNA 001-79-C-0179
9. PERFORMING ORGANIZATION NAME AND ADDRESS: Prototype Development Associates, Incorporated, 1740 Garry Avenue, Suite 201, Santa Ana, California 92705	10. PROGRAM ELEMENT, PROJECT, TASK AREA & WORK UNIT NUMBERS: Subtask N99QAXAI410-06
11. CONTROLLING OFFICE NAME AND ADDRESS: Director, Defense Nuclear Agency, Washington, D.C. 20305	12. REPORT DATE: 10 March 1980
	13. NUMBER OF PAGES: 160
14. MONITORING AGENCY NAME & ADDRESS (if different from Controlling Office)	15. SECURITY CLASS. (of this report): UNCLASSIFIED
	15a. DECLASSIFICATION DOWNGRADING SCHEDULE

16. DISTRIBUTION STATEMENT (of this Report)

Approved for public release; distribution unlimited.

17. DISTRIBUTION STATEMENT (of the abstract entered in Block 20, if different from Report)

18. SUPPLEMENTARY NOTES

This work sponsored by the Defense Nuclear Agency under RDT&E RMSS Code B342079464 N99QAXAI41006 H2590D.

19. KEY WORDS (Continue on reverse side if necessary and identify by block number)

Erosion
Materials
Motorcase
Test Results

20. ABSTRACT (Continue on reverse side if necessary and identify by block number)

A study was conducted to evaluate the erosion performance of candidate motorcase thermal protection materials for advanced missiles. Available data were compiled and evaluated and empirical expressions were developed to describe the erosion performance of two of the leading candidate materials (VAMAC 15J and Kevlar-epoxy). These expressions then were applied to predict the flight response of these two materials for two design flight trajectories and a simulated freestream dust environment. Finally, a number of available ground

DD FORM 1 JAN 73 1473 EDITION OF 1 NOV 65 IS OBSOLETE

UNCLASSIFIED

SECURITY CLASSIFICATION OF THIS PAGE (When Data Entered)

20. ABSTRACT (Continued)

test facilities were evaluated for use in performing erosion tests of materials for ascent flight. Recommendations were made for the optimum facilities to accomplish different types of test objectives.

PREFACE

The work described in this report was conducted by Prototype Development Associates, Inc. (PDA), Santa Ana, California, for the Defense Nuclear Agency (DNA) under contract number DNA001-79-C-0179. Captain A.T. Hopkins was the DNA Contracting Officer's Representative. The technical effort at PDA was performed under the direction of Mr. M.M. Sherman, Program Manager. Mr. D.H. Smith served as the Principal Investigator. Important contributions to the effort were provided by Messrs. J.L. Schmidt and J.E. Dunn of PDA's technical staff. PDA also is indebted to the following individuals who provided valuable assistance and cooperation in obtaining and interpreting the data contained herein: Mr. A.W. Zimmerman (TRW), Mr. G.P. Johnson (MDAC), Mr. G.H. Burghart (SAI), Mr. H.F. Lewis (AEDC), and Dr. W. Barry (The Aerospace Corp.).

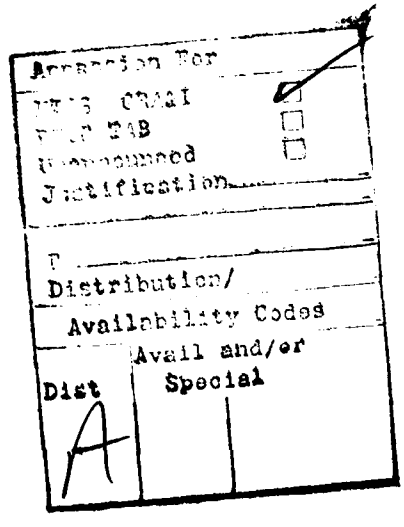

TABLE OF CONTENTS

TABLE OF CONTENTS - (Continued)

LIST OF ILLUSTRATIONS

LIST OF ILLUSTRATIONS - (Continued)

LIST OF TABLES

Conversion factors for U. S. customary to metric (SI) units of measurement.

To Convert From	To	Multiply By
angstrom	meters (m)	1.000 000 X E -10
atmosphere (normal)	kilo pascal (kPa)	1.013 25 X E +2
bar	kilo pascal (kPa)	1.000 000 X E +2
barn	meter^2 (m^2)	1.000 000 X E -28
British thermal unit (thermochemical)	joule (J)	1.054 350 X E +3
cal (thermochemical)/cm^2§	mega joule/m^2 (MJ/M^2)	4.184 000 X E -2
calorie (thermochemical)§	joule (J)	4.184 000
calorie (thermochemical)/g§	joule per kilogram (J/kg)*	4.184 000 X E +3
curie§	giga becquerel (GBq)†	3.700 000 X E +1
degree Celsius‡	degree kelvin (K)	$t_K = t°_C + 273.15$
degree (angle)	radian (rad)	1.745 329 X E -2
degree Fahrenheit	degree kelvin (K)	$t_K = (t°_F + 459.67)/1.8$
electron volt§	joule (J)	1.602 19 X E -19
erg§	joule (J)	1.000 000 X E -7
erg/second	watt (W)	1.000 000 X E -7
foot	meter (m)	3.048 000 X E -1
foot-pound-force	joule (J)	1.355 818
gallon (U. S. liquid)	meter^3 (m^3)	3.785 412 X E -3
inch	meter (m)	2.540 000 X E -2
jerk	joule (J)	1.000 000 X E +9
joule/kilogram (J/kg) (radiation dose absorbed)§	gray (Gy)*	1.000 000
kilotons§	terajoules	4.183
kip (1000 lbf)	newton (N)	4.448 222 X E +3
kip/inch^2 (ksi)	kilo pascal (kPa)	6.894 757 X E +3
ktap	newton-second/m^2 ($N-s/m^2$)	1.000 000 X E +2
micron	meter (m)	1.000 000 X E -6
mil	meter (m)	2.540 000 X E -5
mile (international)	meter (m)	1.609 344 X E +3
ounce	kilogram (kg)	2.834 952 X E -2
pound-force (lbf avoirdupois)	newton (N)	4.448 222
pound-force inch	newton-meter (N·m)	1.129 848 X E -1
pound-force/inch	newton/meter (N/m)	1.751 268 X E +2
pound-force/foot^2	kilo pascal (kPa)	4.788 026 X E -2
pound-force/inch^2 (psi)	kilo pascal (kPa)	6.894 757
pound-mass (lbm avoirdupois)	kilogram (kg)	4.535 924 X E -1
pound-mass-foot^2 (moment of inertia)	kilogram-meter^2 ($kg·m^2$)	4.214 011 X E -2
pound-mass/foot^3	kilogram-meter^3 (kg/m^3)	1.601 846 X E +1
rad (radiation dose absorbed)§	gray (Gy)*	1.000 000 X E -2
roentgen§	coulomb/kilogram (C/kg)	2.579 760 X E -4
shake	second (s)	1.000 000 X E -8
slug	kilogram (kg)	1.459 390 X E +1
torr (mm Hg, 0° C)	kilo pascal (kPa)	1.333 22 X E -1

*The gray (Gy) is the accepted SI unit equivalent to the energy imparted by ionizing radiation to a mass of energy corresponding to one joule/kilogram.
†The becquerel (Bq) is the SI unit of radioactivity: 1 Bq = 1 event/s.
‡Temperature may be reported in degree Celsius as well as degree kelvin.
§These units should not be converted in DNA technical reports; however, a parenthetical conversion is permitted at the author's discretion.

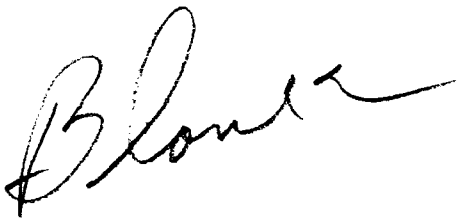

SECTION 1.0
INTRODUCTION AND SUMMARY

Advanced missiles may have to survive ascent flight through an erosive freestream dust environment which would impose potentially severe performance constraints on the various external protection materials (EPMs). This requirement has resulted in a number of test programs designed to evaluate candidate materials for this application by obtaining data for use in deriving analytical expressions for erosion performance predictions.

Since the dust that could be encountered ranges in size from microscopic particles to pebbles nearly an inch in diameter, tests of both continuous dust erosion and single pebble impacts have been conducted. The tests were performed by McDonnell-Douglas Astronautics Company (MDAC); TRW, Inc.; and Science Applications, Inc. (SAI), at facilities operated by the Arnold Engineering Development Center (AEDC) and by SAI.

Included in the various ground test programs were candidate materials to provide external thermal protection for the vehicle shroud, extendible nozzle exit cone (ENEC), and motorcases. This report contains a compilation (Appendix A) of all the available data from these test programs. In addition, studies were performed to define the erosive environment that will be experienced by the motorcases during flight and to derive analytical expressions to predict the flight response of some of the primary candidate motorcase materials.

One group of materials of particular interest for motorcase protection consists of ethylene/acrylic elastomers with the trade name VAMAC. Several types of VAMAC have been considered which differ in details of their manufacturing processes and in the relative amounts of components and additives, such as carbon black. At the time that the analyses reported herein were performed, the formulation of most interest was designated VAMAC 15J by MDAC. The available data for this material were examined and an empirical expression was derived to predict its erosion response in freestream dust environments. This correlation is shown to represent the upper bound of the data bases, from both the AEDC and the SAI test facilities. A correlation of dust erosion data for Kevlar-epoxy, the basic motorcase material, also was derived; and Kevlar-epoxy was found to have erosion resistance similar to that of VAMAC 15J. A correlation was obtained for the impact of large pebbles on both VAMAC and Kevlar-epoxy, and it was concluded that the deepest crater expected in flight would be less than 0.015-inch deep.*

*This conclusion is based on the available data and will be evaluated further in a system proof test to be performed in the Holloman rocket sled facility under a separate contract.

An evaluation of the expected flight erosion environment was conducted, and it was found that, depending on the trajectory, the shock layer will reduce motorcase erosion by 30 to 60 percent and will prevent any particles smaller than 200 to 600μ in diameter from impacting the surface. In light of these analyses, facilities for further booster ascent flight erosion testing were evaluated, and the following facilities were recommended:

- AEDC Dust Erosion Tunnel
- Bell Aerospace Rotating Arm
- SAI Powder Gun
- Sandia Laboratories or Holloman AFB Rocket Sled

SECTION 2.0
FACILITIES

Data from three types of erosion tests were evaluated during this program: 1) continuous dust erosion tests, 2) pebble impact tests, and 3) tests employing several sequential salvos of small dust-size particles. The continuous dust erosion tests were conducted at the Dust Erosion Tunnel (DET) at the Arnold Engineering Development Center (AEDC) near Tullahoma, Tennessee. Both of the other two types of tests were performed at the Science Applications, Inc. (SAI) Electro-Optics and Impact Laboratory in Santa Ana, California. These facilities are described in this section. A full listing of the test data is given in Appendix A.

2.1 CONTINUOUS DUST EROSION TESTS

2.1.1 Facility Description

The DET is a continuous-flow, arc-heated wind tunnel located in the Engine Test Facility (ETF). High-pressure air supplied from the von Karman Facility (VKF) high-pressure air system is heated in a 5 MW arc heater. Dust particles are injected upstream of the nozzle throat and aerodynamically accelerated in a low-expansion-rate hypersonic nozzle. A multiple-mount model positioning system with nine stings is enclosed in a test cabin and injects models into the tunnel flow. An exhaust connection is provided through a diffuser to the ETF exhaust plant. The tunnel is water-cooled. Schematics of the tunnel and model positioning system are shown in Figures 1 and 2 (from Reference 1).

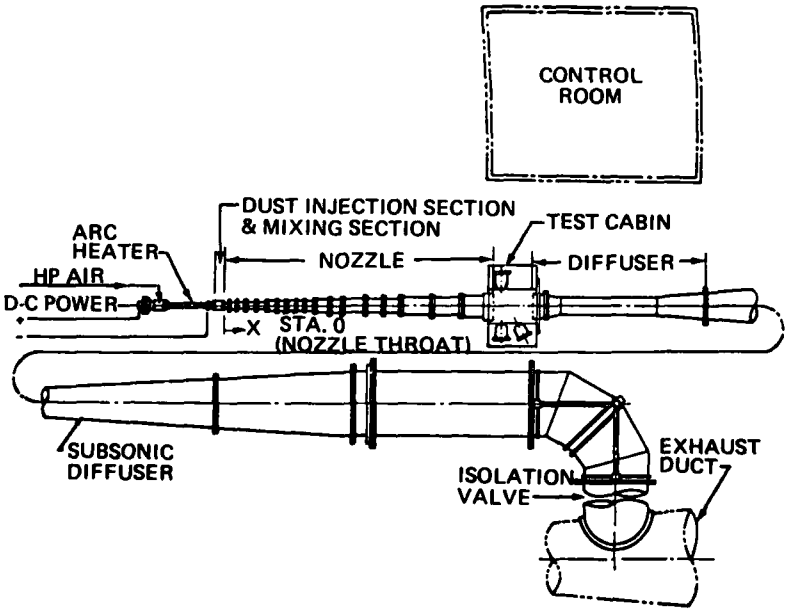

Figure 1. Schematic view of AEDC Dust Erosion Tunnel.

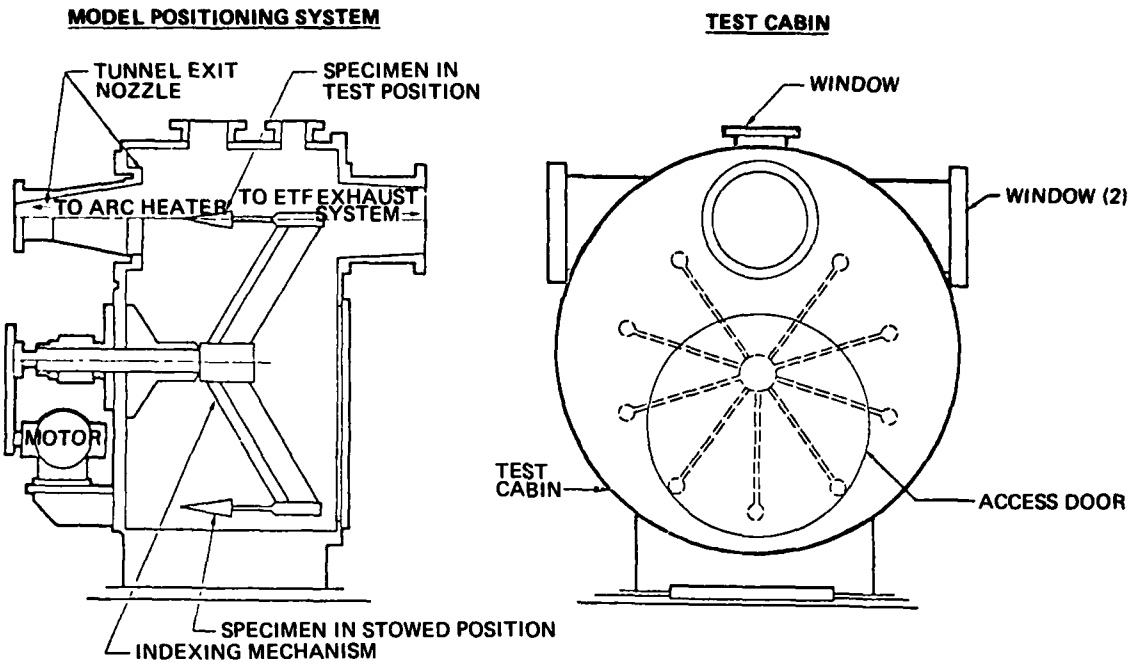

Figure 2. DET test cabin and model positioning system.

Controls for the dust dispenser and the model positioning system are located in a control room along with all recording and indication equipment necessary to evaluate the arc heater and tunnel test condition parameters. Instrumentation for recording tunnel and model parameters consists of 36-channel oscillographs and several strip chart recorders. Pyrometers and many types of high-speed motion-picture cameras with frame speeds up to 5000 fps are available for model observation. Front surface temperatures of the earlier shroud specimens were obtained with an infrared pyrometer which responds to temperatures in the range from 230°F to 800°F. The backfaces of some of the models used in this program were instrumented with one or more thermocouples. Facilities for pre- and post-test photographing and weighing of the erosion specimens are provided. Other equipment required for the conduct of the tests were screens to sieve the particulate.

A variety of equipment has been used to characterize the dust cloud in the DET test cabin. This equipment includes a laser holographic system, a laser doppler velocimeter, impact bars, and cloud bars. The current program relied primarily on prior calibrations of the dust environment. However, supplementary data were obtained with impact bars, and holographic runs were made at one point during the present tests to provide an accurate calibration of the facilities. A detailed description of the DET and its calibration is contained in Reference 1.

2.1.2 Test Conditions

Erosion tests for the external protection materials (EPMs) were conducted in the DET using two different chamber pressures and three different particle sizes. Since the particles are accelerated by the air flow, this provides six possible impact velocities, although only four of the combinations were actually used.

A calibration program, described in Reference 2, obtained holographic data on 650-micron and 50-micron (nominal diameter) particles for the 1,000 psi chamber pressure condition. These data were used in that program to define statistically equivalent clouds of uniform diameter spherical particles having the same overall particle density and average values of mass/particle, kinetic energy/particle, and kinetic energy/mass as the actual clouds. Table 1 summarizes the results of that study. Where possible, statistically equivalent particle parameters are listed in this report. This required adjusting the freestream particle concentrations reported in References 3, 4, and 5 because particle concentration is a derived quantity based on the total mass flow of particles divided by the particle velocity. Since no holography was done for the 300 psi chamber pressure condition, the particle velocities listed for those tests were obtained with the following expression:

$$V\ (300\ \text{psi}) = V_{\text{NOMINAL}}\ (300\ \text{psi}) \left[\frac{V_{\text{STAT EQ}}\ (1{,}000\ \text{psi})}{V_{\text{NOM}}\ (1{,}000\ \text{psi})}\right] \qquad (1)$$

$$= 2{,}140\ \text{ft/sec}$$

Since no holography was done for the 200-micron nominal diameter particles at any condition, nominal values of the particle diameter and velocity are listed for those tests. However, whenever possible, it is important to use the statistically equivalent velocity rather than the nominal velocity to correlate DET erosion data. If the mass loss ratio is assumed to be of the form $G \sim k\ V^2$, then the value of k derived for 650-micron particles using the nominal velocities will be 50 percent higher than that derived using the statistically equivalent velocity.

Because no calibration data for the conditions of the ENEC and shroud nosetip tests were available, nominal conditions are listed for those tests.

2.1.3 Particles

The particles used for all the DET tests reported herein were produced by crushing 98- to 99-percent pure fused cubic MgO crystals. The resulting particulate then was washed with alcohol and screened several times to obtain a batch of particles with sizes concentrated near the desired nominal size. The particles are irregular both in shape and in size.

Table 1. Dust cloud characteristics for $p_o \cong 1{,}000$ psi, $h_o \cong 500$ Btu/lbm (Reference 2).

DUST	NOMINAL CLOUD (CONST DIAM)	REAL DUST CLOUD		STATISTICALLY EQUIVALENT CLOUD – CONSTANT DIAMETER, SMOOTH MgO SPHERES
		BEFORE INJECTION (PHOTOMICROGRAPH)	IN FLIGHT (HOLOGRAPHY)	
650 μm MgO	D_p = 650 μm	550 ≤ D_p ≤ 950 μm (91 %, 650 ≤ D_p ≤ 850 μm) (92 % Mass, 650 ≤ D_p ≤ 850 μm)	50 ≤ D_p ≤ 900 μm (64 %, 50 ≤ D_p ≤ 300 μm) (86 % Mass, 600 ≤ D_p)	D_p = 438 μm
	$V_{p_{calc}}$ = 2,400 ft/sec		V_p = 2,200 - 4,500 ft/sec, all particles = 2,200 - 3,300 ft/sec, 650 μm particles	V_p = 2,937 ft/sec
50 μm MgO	D_p = 50 μm	5 ≤ D_p ≤ 150 μm (90 %, 5 ≤ D_p ≤ 50 μm) (88 % Mass, 50 ≤ D_p ≤ 100 μm)	20* ≤ D_p ≤ 160 μm (70 %, 40 ≤ D_p ≤ 100 μm) (73 % Mass, 80 ≤ D_p ≤ 140 μm)	D_p = 94 μm
	$V_{p_{calc}}$ = 3,950 ft/sec		V_p = 3,220 - 5,150 ft/sec, all particles = 3,850 - 4,950 ft/sec, 50 μm particles	V_p = 4,125 ft/sec

*Lower resolution limit of holography system used with nominal 50 μm dust is 20 to 40 μm, depending on position of particle and hologram quality. Particles below this limit in size are not recorded.

2.1.4 Model Descriptions

All of the flat test specimens were 2-inch diameter discs which were mounted in wedge-shaped model holders, as illustrated in Figure 3. The specimen retainer surrounding the test specimen was made of the same materials as the 2-inch disc to avoid edge effects and to get a one-dimensional mass loss. The backface of the test sample materials of each test specimen was instrumented with one thermocouple at the center of the disc, as shown in Figure 4. The model holders support two test specimens, and each model holder is sting-mounted to one of the nine struts of the model positioning system.

The hemisphere models had a diameter of 3 inches and a nominal thickness of 0.050 inch. The backface of each hemisphere was instrumented with two thermocouples located side-by-side near the model stagnation point. Each hemisphere was sting-mounted to one of the nine struts of the model positioning system.

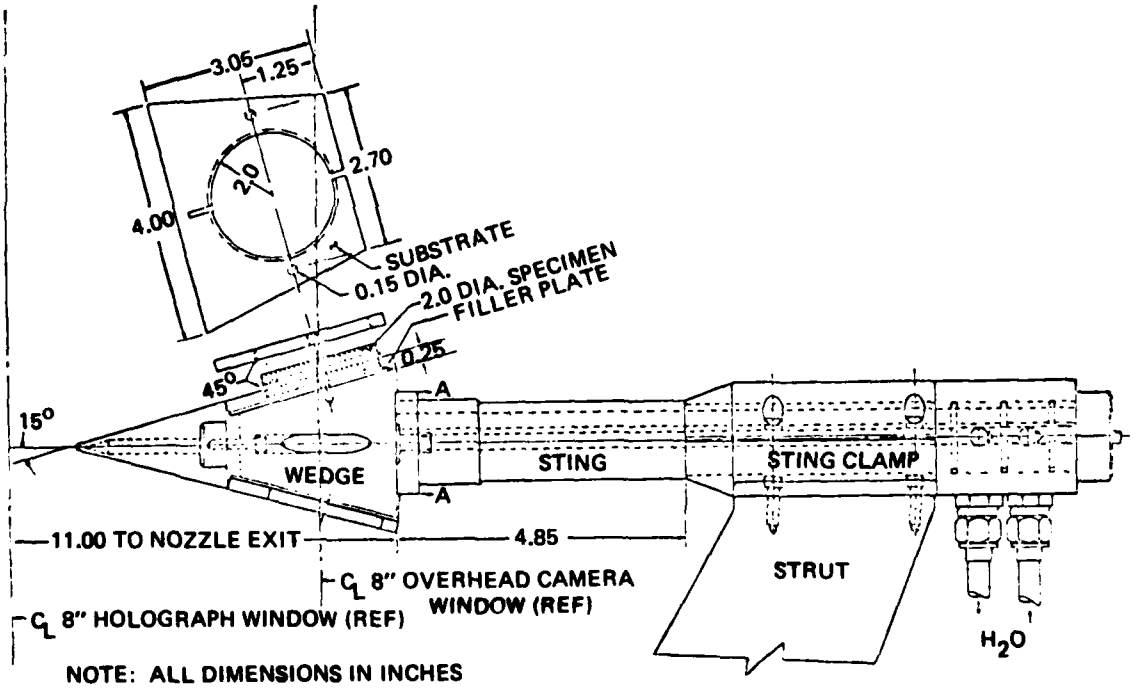

Figure 3. Wedge model holder and sting support for DET tests.

2.1.5 Tare Data

Tare data obtained in these tests are summarized in Table 2 (from Reference 6). If it is assumed that tare sample weight change is due primarily to outgassing, contamination, and handling, then tare weight change may be only a weak function of material. The standard deviation of the weight change for all of the samples taken together is

0.055 gram. Comparing this value to the weight losses measured for the erosion tests, it is found that the accuracy for all tests performed at impact angles of 9 degrees or greater should be very good. However, the 4-degree impact angle data are generally questionable.

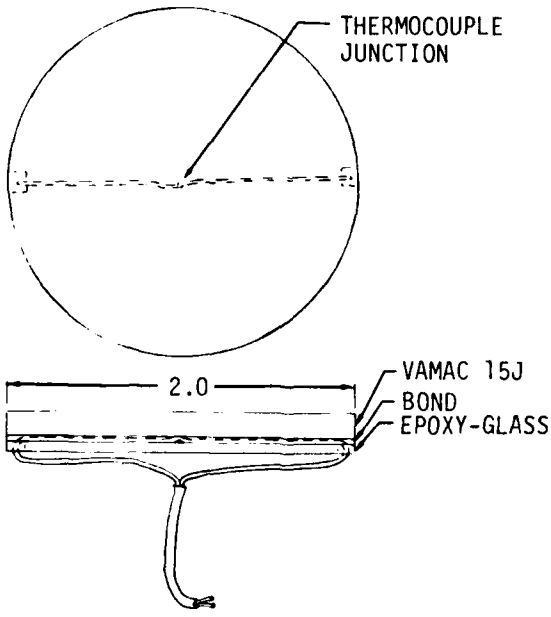

Figure 4. DET model.

2.2 PEBBLE IMPACT TESTS

2.2.1 Facility Description

The pebble impact experiments were conducted in the Science Applications, Inc. (SAI) Electro-Optics and Impact Laboratory located in Santa Ana, California. The launcher used in this test program is a powder gun consisting of a variable volume powder chamber to which launch barrels of various sizes can be attached on one end and a 30/06 rifle action mechanism mounted on the opposite end. A plastic diaphragm separates the powder chamber and the launch barrel. The operating sequence is to place a sabot holding the pebble and the diaphragm in the breech of the barrel, secure the powder chamber, place a custom loaded 30/06 rifle cartridge into the gun, and finally fire the gun with an electric solenoid.

The primary instrumentation used in the tests is a light screen system for measuring projectile velocity. With this system, time is measured by counting the pulses of a very accurate electronic clock. Two screens are placed five feet apart to sense the passing of the projectile. As the projectile passes over the first screen, a signal is

Table 2. TARE data.

Reference 6: p_o = 1,000 lb/in^2

Δt = 40 sec

θ = 9 degrees

Material Name	Weight Change,* Δm(g)	
	Run 5A h_o = 552 Btu/lb	Run 6A h_o = 493 Btu/lb
Ke/VAMAC	0.014	0.005
VAMAC	0.039	-0.023*
Alternate VAMAC	0.105	0.010
Ke/VITON	0.043	-0.035*
VITON	0.039	-0.028*
Ke/TBR	0.008	-0.053*
TBR	0.007	-0.026*

* Negative indicates weight gain.

Reference 4: Run 9

p_o = 992 lb/in^2

h_o = 507 Btu/lbm

Material Name	Angle (deg)	Δt (sec)	Δm (g)
TBR II	4	40	0.105
TBR II	9	60	0.140
KePVF/.75 PVF +0.25 E_p NOV	9	60	0.075

Avg = 0.025

$$\sigma = \sqrt{\frac{1}{N-1} \sum_{1}^{N} (\bar{K} - K_i)^2} = \sqrt{\frac{0.0480}{16}} = 0.055$$

sent to command an electronic device to start counting the pulses. When the projectile passes the second screen, a signal is sent to stop the pulse counting and to convert the pulse count number into a velocity reading. The velocity is then displayed on a digital readout. To preclude the possibility of a false command due to the shock wave which precedes the projectile, a backup system of paper screens containing conductive wires is employed to ensure accurate velocity measurement. A schematic of the velocity measuring systems is shown in Figure 5.

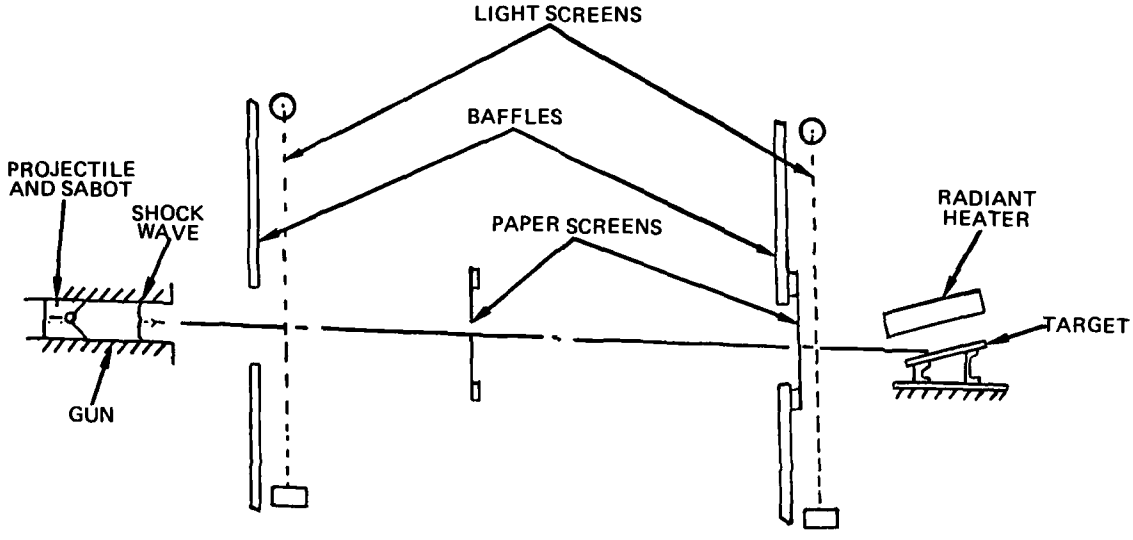

Figure 5. SAI pebble test facility and projectile velocity measuring systems.

2.2.2 Pebbles

Spherical pebbles made from Tonalite, a type of granite from a core sample taken near Cedar City, Utah, were used for most tests on this program, although a few shots were fired with glass spheres.

2.2.3 Model Description

The samples tested were rectangles, typically 6-inches square, although other sizes were also used. Some samples were bonded to substrates simulating the motorcase and interstage skirt structure, while others had no back surface support.

2.3 SALVO DUST EROSION TESTS

The salvo dust erosion tests are performed by SAI in essentially the same manner as the pebble impact tests except that the salvo tests are conducted inside an evacuated tube, and the paper screens that provided the pebble test backup velocity data are not used. A number of small particles (weighed and counted) is placed in the sabot and fired

at the target. The sample is then removed from the apparatus and weighed. This procedure is typically repeated at least four times for each sample, and each measurement represents a data point. Since the mass loss on a single shot is very small, each test sample has an identical tare sample used to determine weight change due to other effects, such as outgassing and water absorption. The test and tare samples are stored together, placed in the test vacuum chamber at the same time, and weighed at the same times. The reported weight losses from each shot actually are the differences between the test sample and the tare sample weight changes.

Blank

SECTION 3.0
DATA CORRELATION

Both the dust erosion and the pebble impact data were correlated during this program. A number of tests of different varieties of EPMs have been conducted at the DET. At the time of this study, the majority of the data were for a formulation designated VAMAC 15J. Therefore, based on these data, an expression to predict the flight erosion of VAMAC 15J was derived.

A second material that was evaluated in this effort is the Kevlar-epoxy motorcase material itself, since erosion protection can be provided by simply increasing the motorcase thickness. This would probably be the least expensive approach, although it could result in a substantial weight penalty. An erosion correlation for this material also was derived from DET data.

During ascent, the materials may encounter debris varying in size from microscopic dust to pebbles nearly an inch in diameter. It has been shown analytically that the mass fraction of large pebbles is so small that they account for relatively little of the erosion mass loss. This conclusion does not preclude the possibility that a few impacts by large pebbles could cause deep craters that would be a threat to the survival of the vehicle, even though the total mass removed is small due to the small number of these craters. Therefore, crater depth correlations were derived for both VAMAC 15J and Kevlar-epoxy based on impact data obtained at SAI with spherical granite pebbles.

3.1 VAMAC 15J DUST EROSION CORRELATION

Useful correlations of measured erosion data require accurate knowledge of both the particle impact parameters (particle diameter, impact velocity, and impact angle) and the target material conditions (surface temperature and internal temperature distribution). A brief study was performed to evaluate these parameters for the wedge test models and the DET test conditions used in the subject test programs. The study considered: 1) the effects of the wedge shock layer on the particle velocity and impact angle, 2) the possible surface shielding effect of debris from upstream particle impacts, 3) the influence of kinetic energy deposition on the surface heat flux, and 4) the effects of variations in particle size and freestream concentration on impact velocity.

3.1.1 Shock Layer Effects

A two-dimensional analysis was conducted of particles traveling through the shock layer of the DET wedge model holder. Various combinations of particle velocity and size

were evaluated. Since the change in gas velocity across the wedge shock is relatively small, the principal effect of the shock layer is to turn the particles; however, this effect was found to be negligible for particles greater than 10 microns in diameter. Figure 6 shows the computed turning angles experienced by a range of particle sizes traveling through the shock layer of a 14-degree half-angle sharp wedge.

3.1.2 Debris Shielding

A study of debris shielding on flat plates has resulted in a simple analytic technique that has been used to define a non-dimensional parameter for evaluating the onset of shielding effects. Both the analytic technique and the non-dimensional parameter are described in Appendix B. The analytic technique was used to evaluate one DET run for each of the two particle sizes used. The results are shown in Figure 7, and it can be seen that the probability of shielding is negligible in both cases.

3.1.3 Heating

No direct measurements of kinetic energy deposition are available for the materials tested, and convective heating has not been calibrated for the 300 psi chamber pressure test condition. Fortunately, the models tested in the program described in Reference 4 had thermocouples installed, as shown in Figure 4. The responses of these thermocouples were used to evaluate both kinetic energy deposition and convective heating.

3.1.3.1 Kinetic Energy Deposition

Kinetic energy deposition was evaluated using data from tests run with 50-micron particles, since kinetic energy deposition is proportional to velocity cubed and the 50-micron particles are traveling approximately 40 percent faster than the 650-micron particles. The principal analytic tool used in this study was the PDA Ablation Conduction and Erosion (PACE) code. This code solves the one-dimensional heat conduction equation for multiple materials, including convection, radiation, independent external and/or internal heat flux, erosion, ablation, and internal decomposition. For these analyses, constant material properties were used, and no ablation or decomposition was considered. Material properties used are listed below:

Material	Thickness (inch)	Density (lb/ft^3)	Conductivity (Btu/ft-sec-°R)	Specific Heat (Btu/lb-°R)
VAMAC 15J (Reference 3)	0.18	81	0.000083	0.40
Epoxy-glass	0.05	118	0.000069	0.25

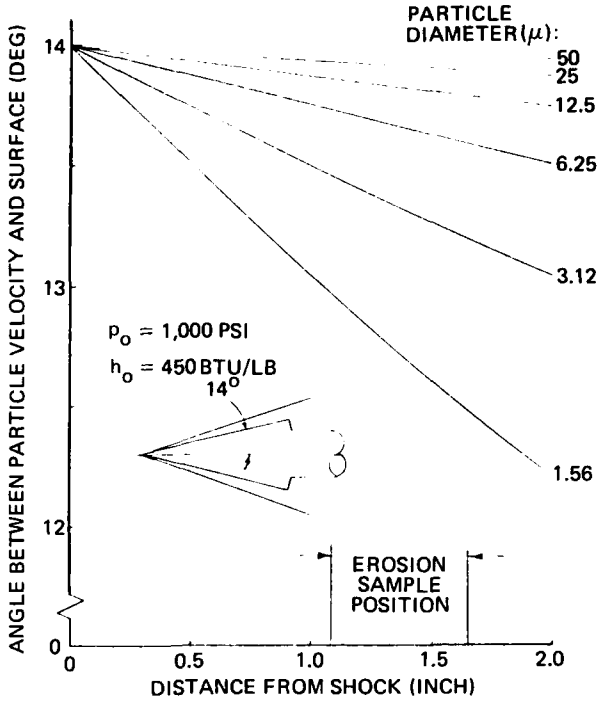

Figure 6. Shock layer effects in the DET.

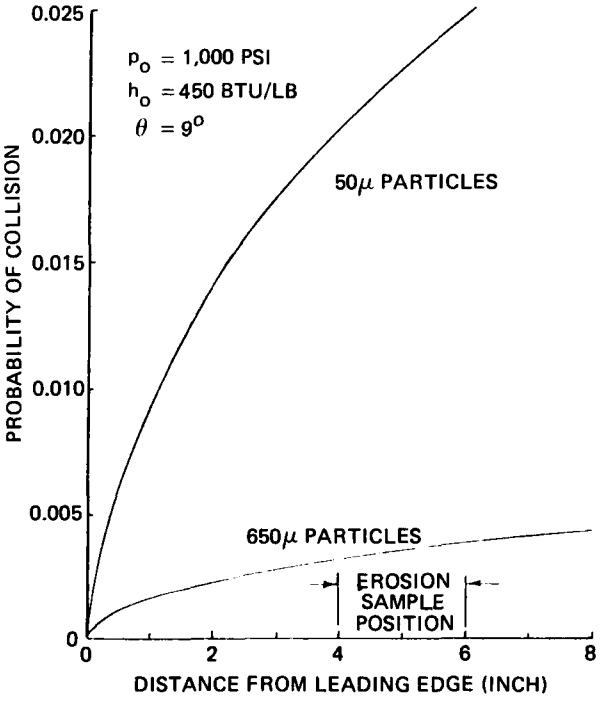

Figure 7. Probability of incoming particle colliding with debris in DET.

In Reference 4, it was shown that good agreement with the response of the thermocouples in two models was obtained by assuming a kinetic energy accommodation coefficient (C_{KF}) of 0.7 sin θ, resulting in an energy deposition rate due to particle impacts of:

$$\dot{q} = \dot{q}_{KE} = \frac{62.4 \times 10^{-6}}{(32.2)\ (778)} \cdot C_{KE} \cdot 1/2\ \rho_\infty V_p^3 \sin\theta \qquad (2)$$

$$= 8.7 \times 10^{-10}\ \rho_\infty V_p^3 \sin^2\theta$$

in which ρ_∞ and V_p are dust density (g/m^3) and velocity (ft/sec), respectively, and θ is impact angle. In this study all of the models tested with 50-micron particles were analyzed both with the above kinetic energy deposition expression and with no kinetic energy deposition. The results are compared to the measured thermocouple responses in Figures 8 through 14. Several conclusions are evident from these figures.

- Predicted and measured temperatures generally agree well, indicating that the material properties and the convective heating model are accurate.
- The predictions using Equation 2 appear to match the measured data somewhat better than the predictions with no kinetic energy deposition.
- The differences between the two sets of predictions are too small to provide a firm definition of the kinetic energy deposition.
- Since no difference at all is observable between the two sets of predictions for either the 4-degree wedge data (due to the sine-squared dependence) or the 30-degree wedge data (due to the short test times), no conclusions on angular dependence can be drawn.

3.1.3.2 Convective Heating

Convective heating in the DET has been calibrated for the 1,000 psi chamber pressure condition (Reference 1). These data are shown in Figure 15, along with the calculated kinetic energy heating for two typical test conditions.

Initial calculations for the 300 psi test condition were made using the 1,000 psi heating modified by the square root of the pressure to reflect the Reynolds number dependence of laminar convection. This substantially underpredicted the observed temperature histories, and it was found that the best agreement was obtained using:

$$\dot{q}\ (300\ \text{psi}) = 0.91\ \dot{q}\ (1{,}000\ \text{psi}) \qquad (3)$$

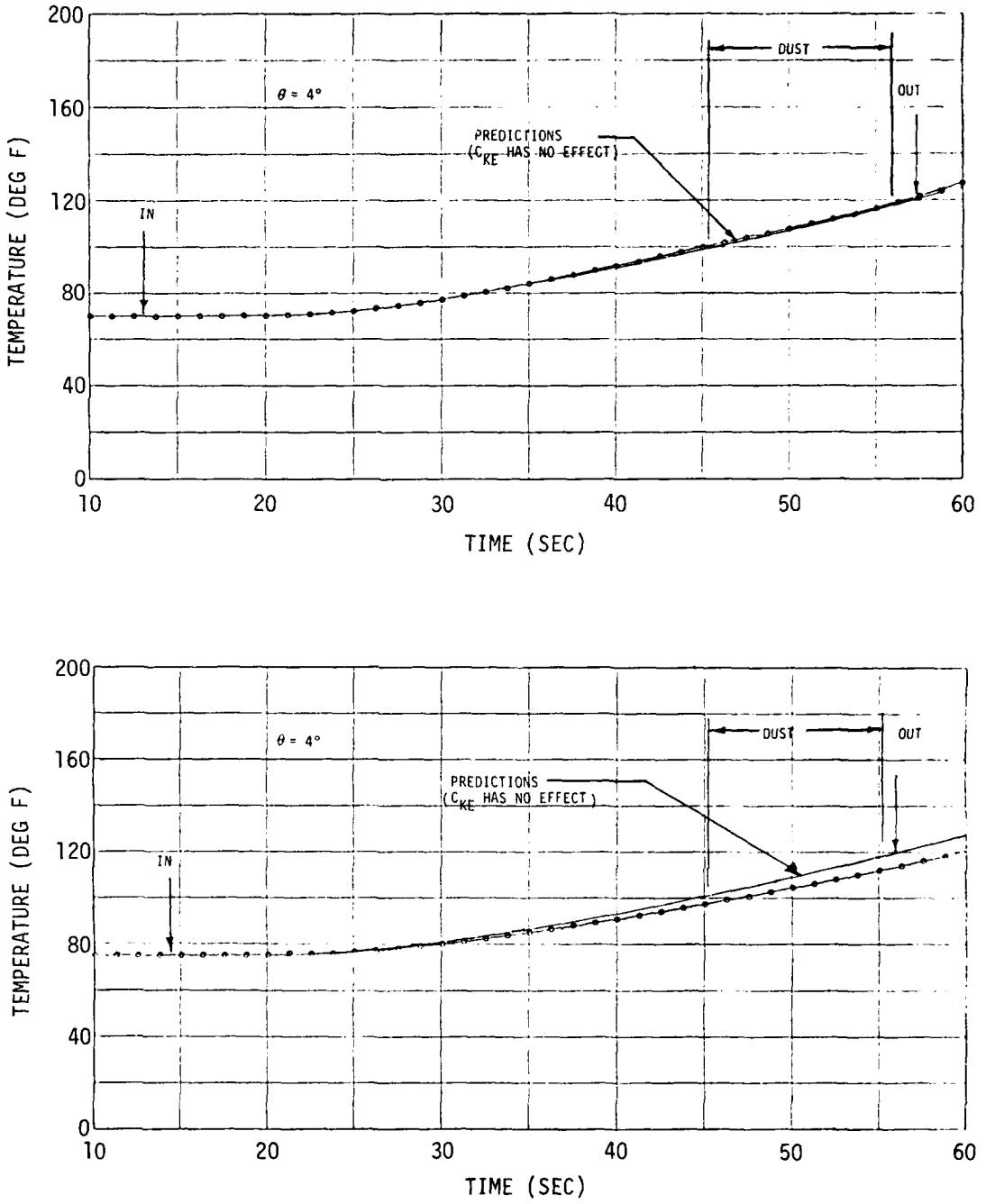

Figure 8. Kinetic energy method comparison: 4-deg angle.

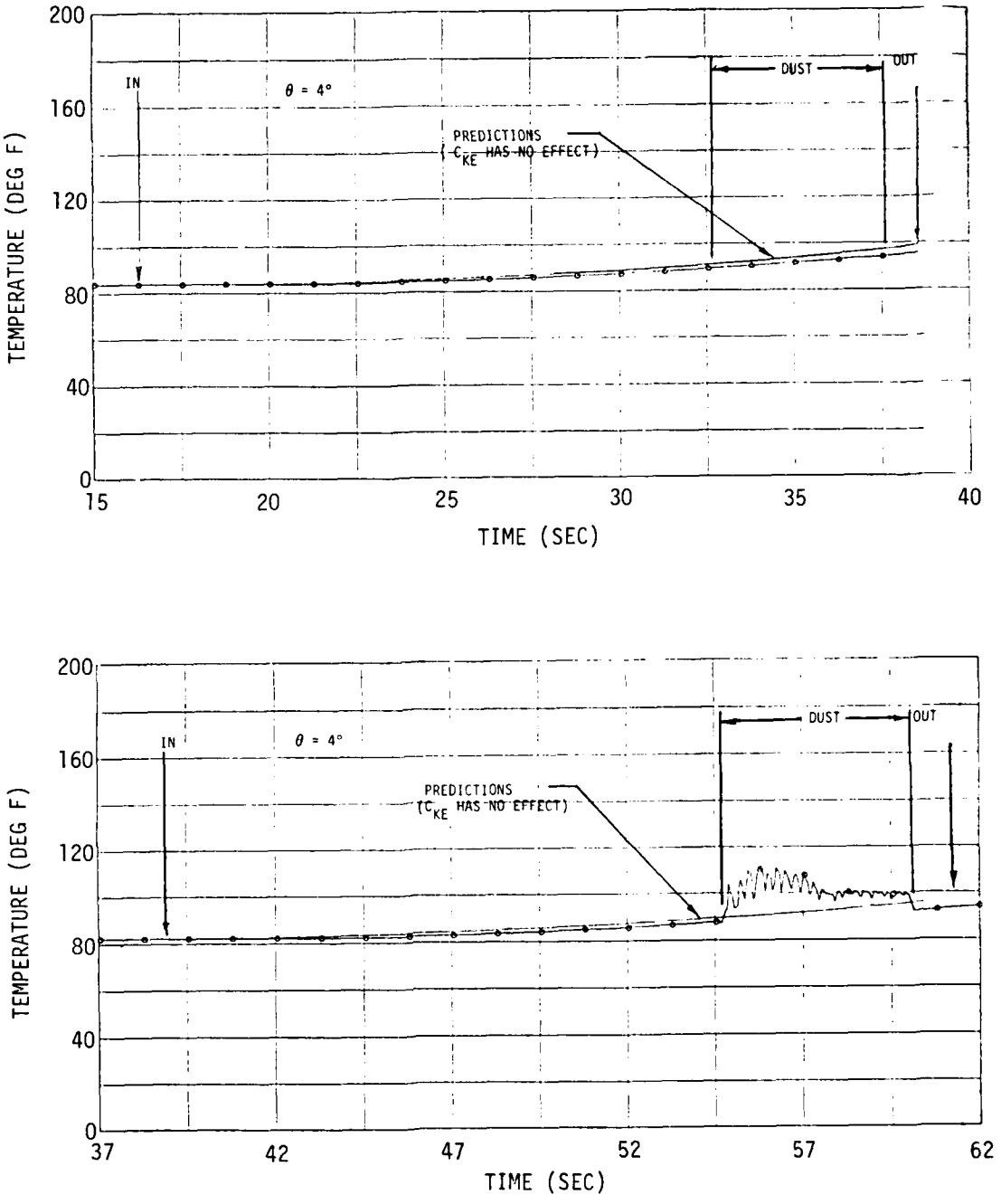

Figure 9. Kinetic energy method comparison: 4-deg angle.

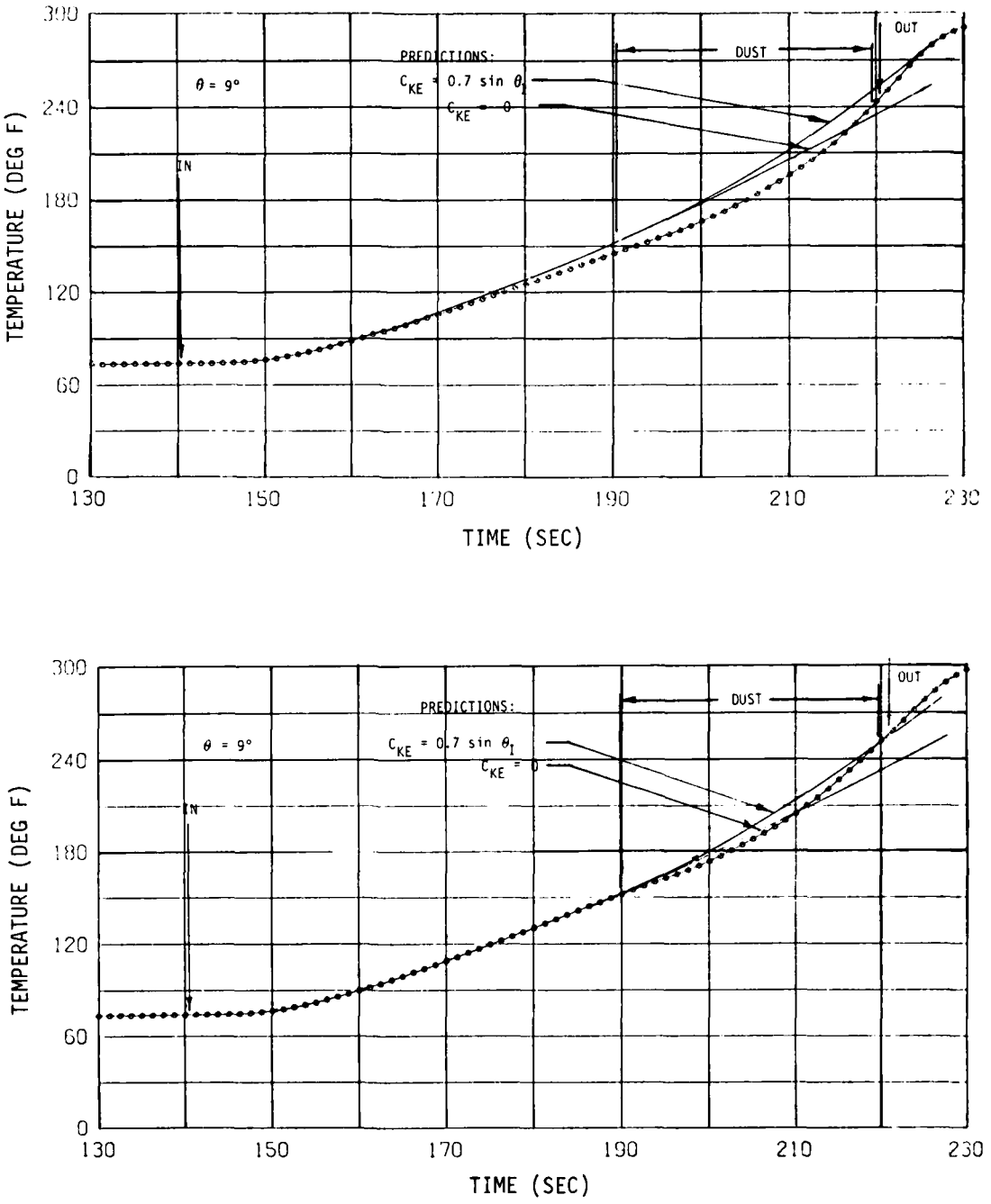

Figure 10. Kinetic energy method comparison: 9-deg angle.

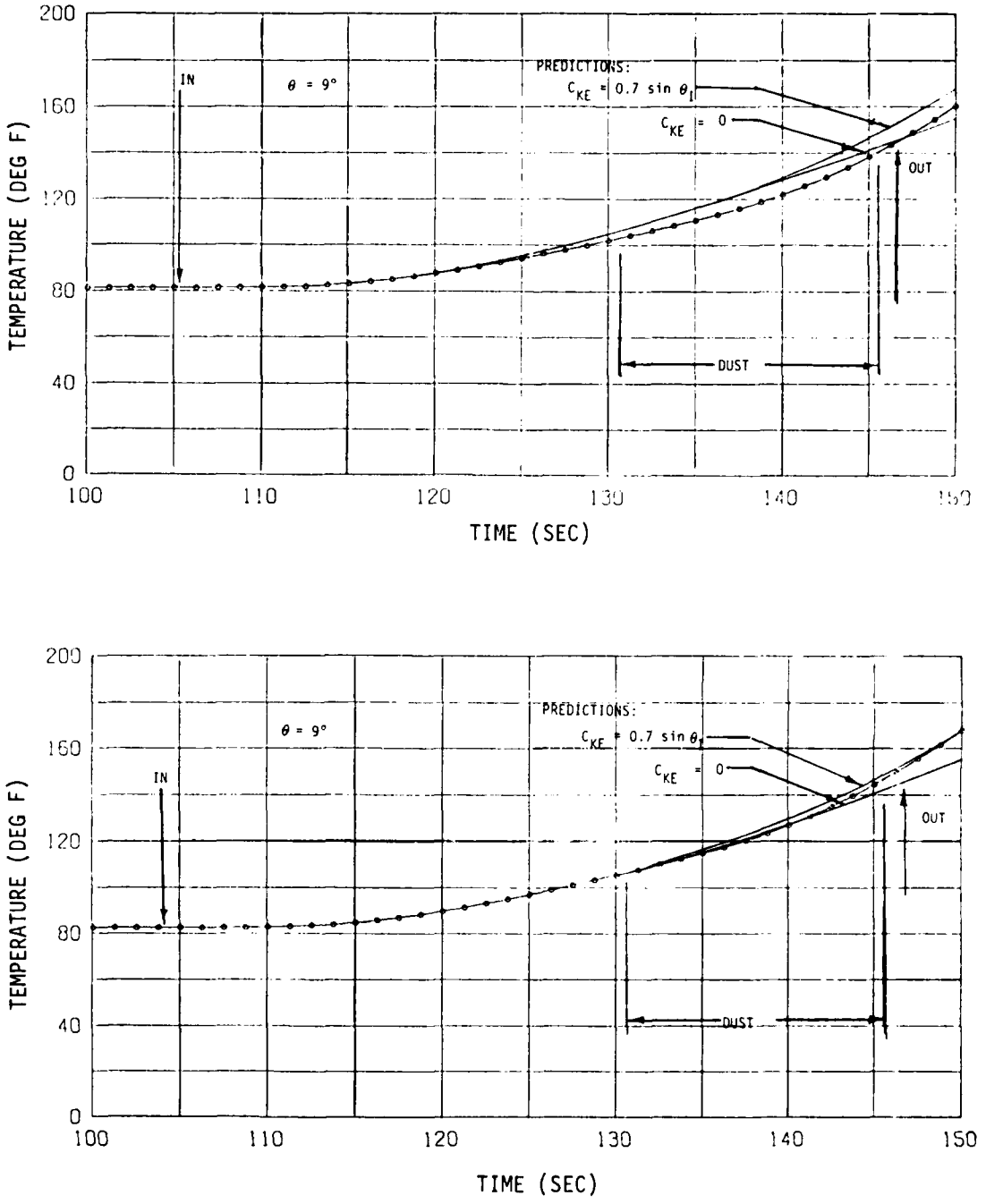

Figure 11. Kinetic energy method comparison: 9-deg angle.

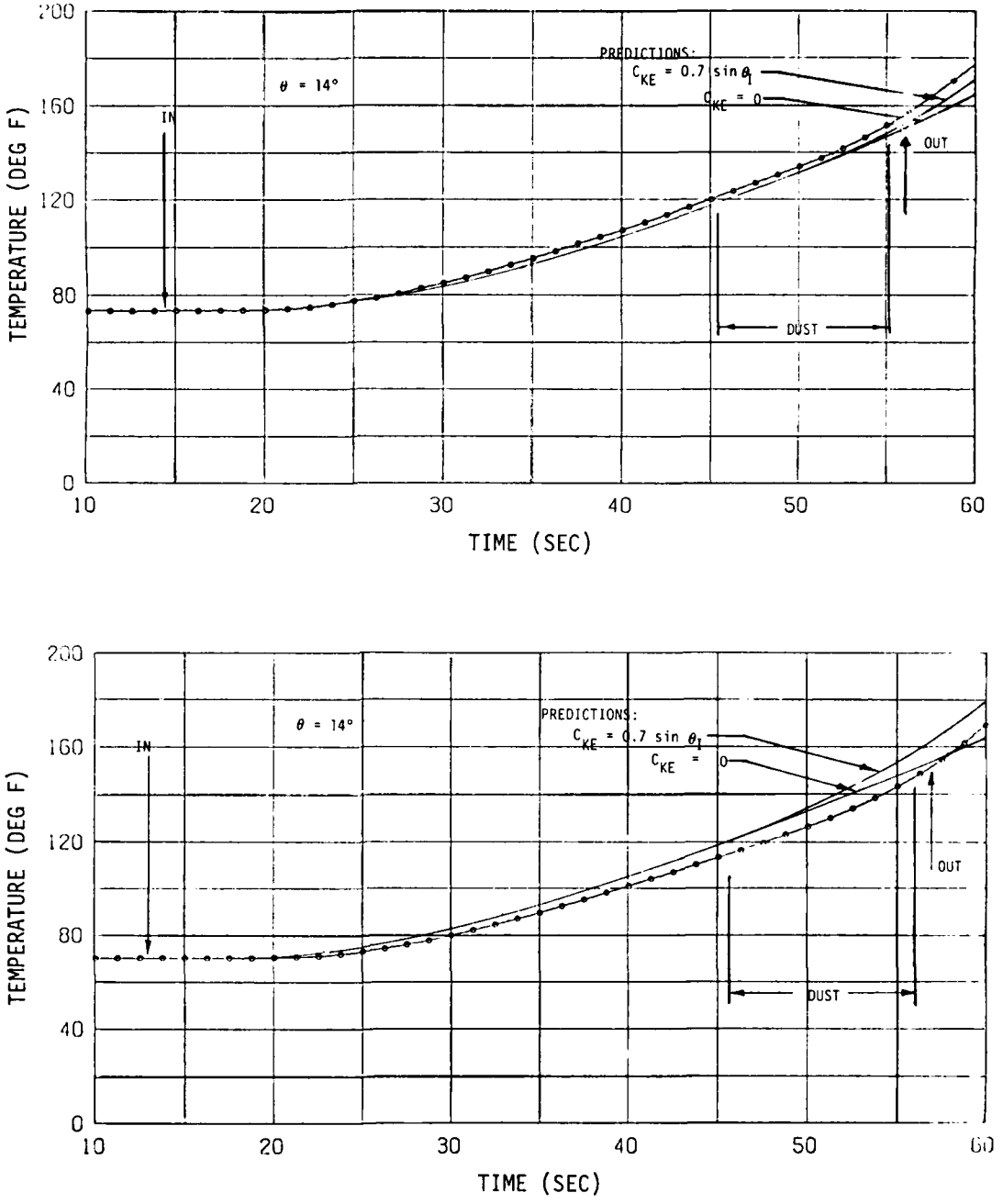

Figure 12. Kinetic energy method comparison: 14-deg angle.

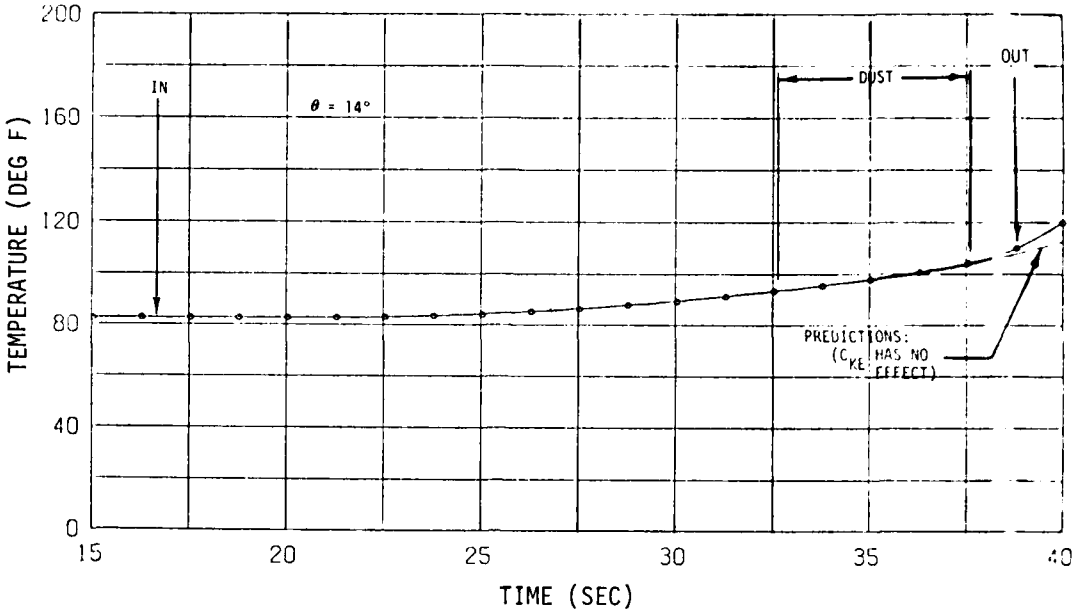

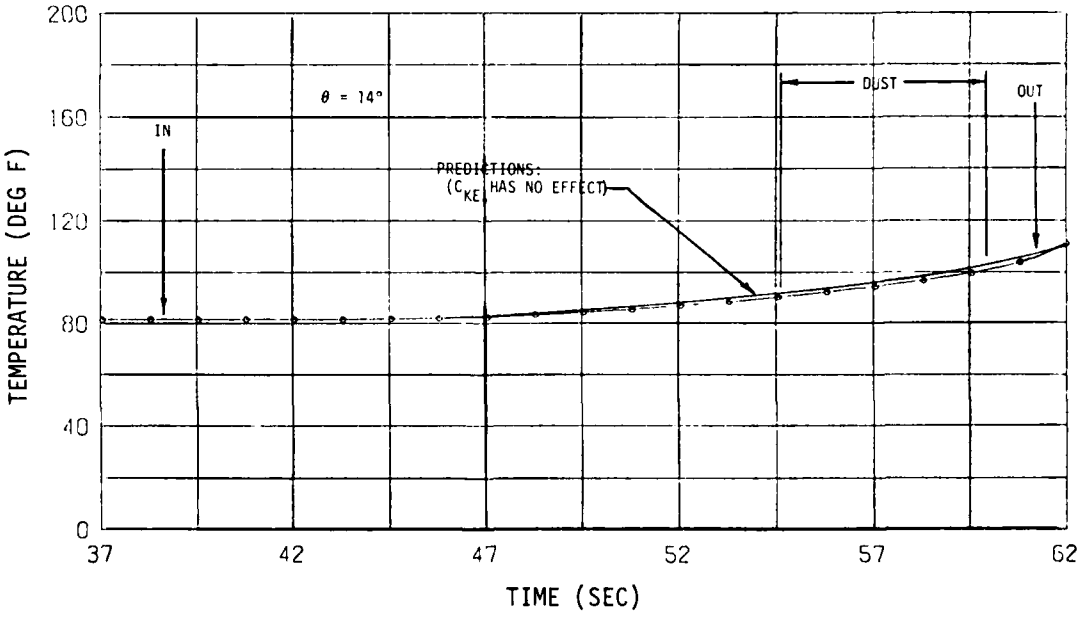

Figure 13. Kinetic energy method comparison: 14-deg angle.

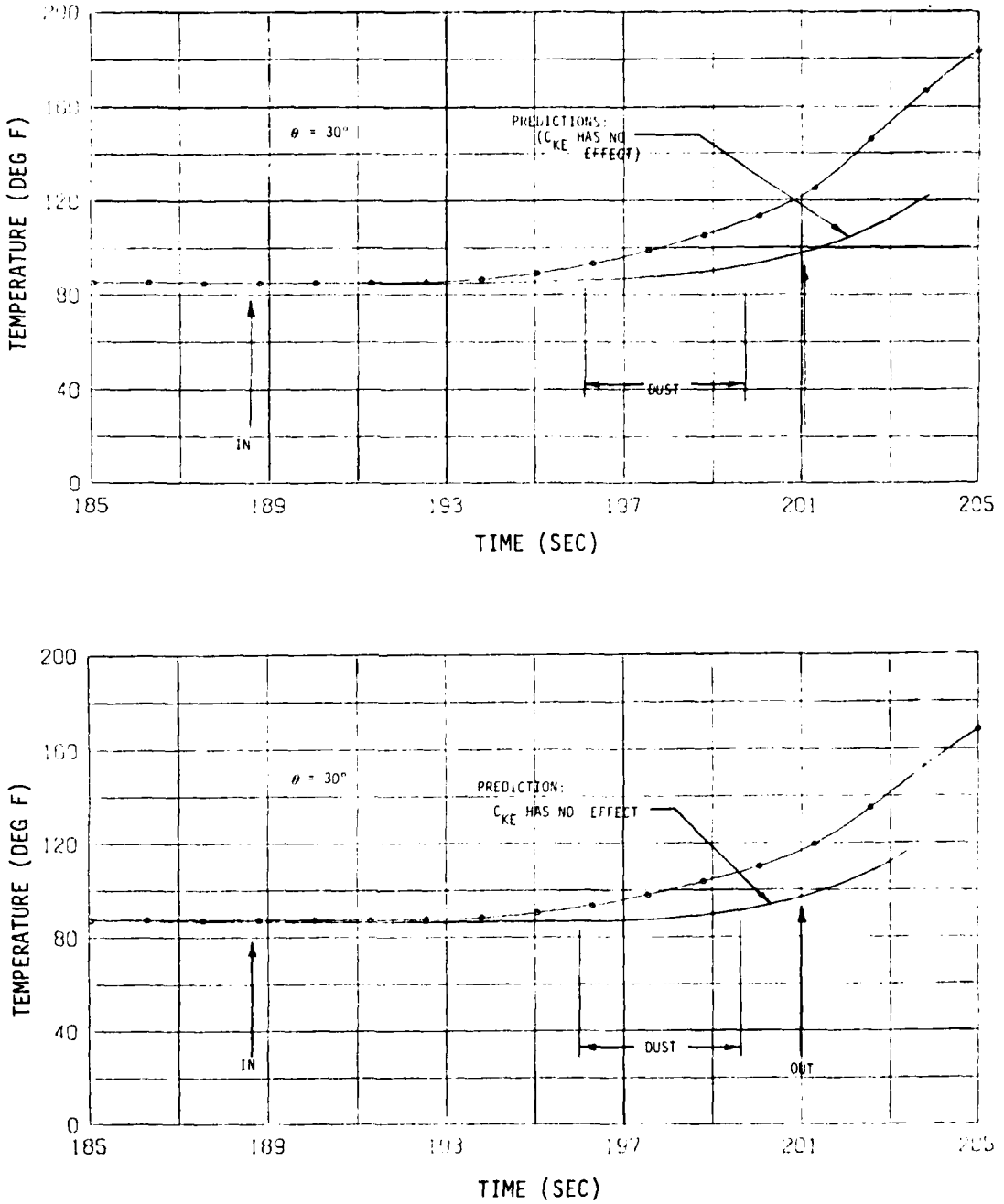

Figure 14. Kinetic energy method comparison: 30-deg angle.

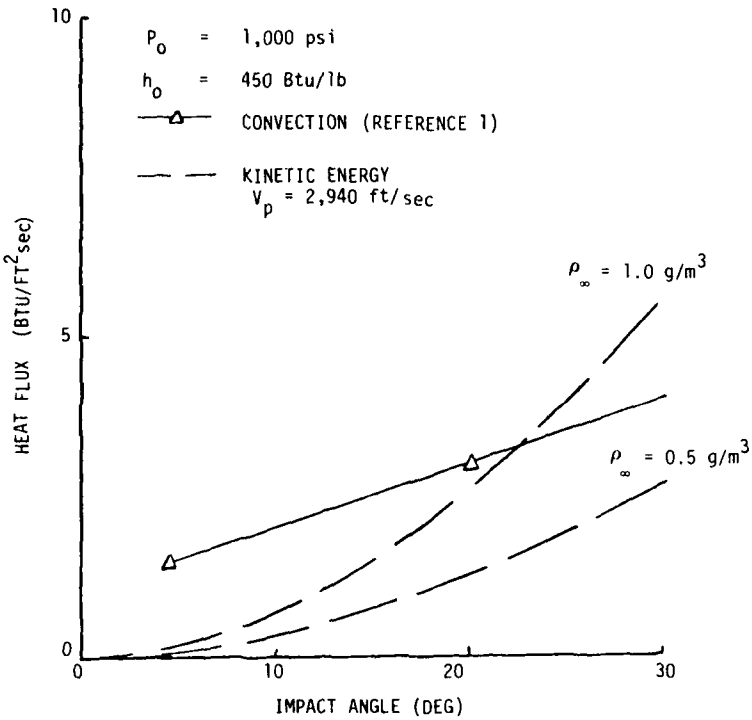

Figure 15. Convective heating in DET.

The temperature history shown in Figure 16 for the AEDC Run 7 (TRW Series, Reference 4) compares a measured thermocouple history to predictions using the above two methods. The relatively high heating for 300 psi probably is due to turbulence. The tunnel wall turbulent boundary layer grows to the tunnel centerline at 300 psi, but does not at 1,000 psi. All further analyses of 300 psi tests were done using the above equation for heating.

AEDC Run 3 (TRW Series) was found to be anomalous. Figure 17 shows that the predictions significantly underpredict the temperature rise. Reference 7 indicated that some 300 psi runs in the MDAC series also appeared to experience very high heating (these runs were not reported in the MDAC test report). It was concluded at that time that ice forming in the airflow measurement venturis caused the facility control electronics to malfunction. Run 3 has not been included in any of the following correlations.

3.1.4 Particle Velocity

The conclusions described in this section used the statistically equivalent particle velocities discussed in Section 2.1.

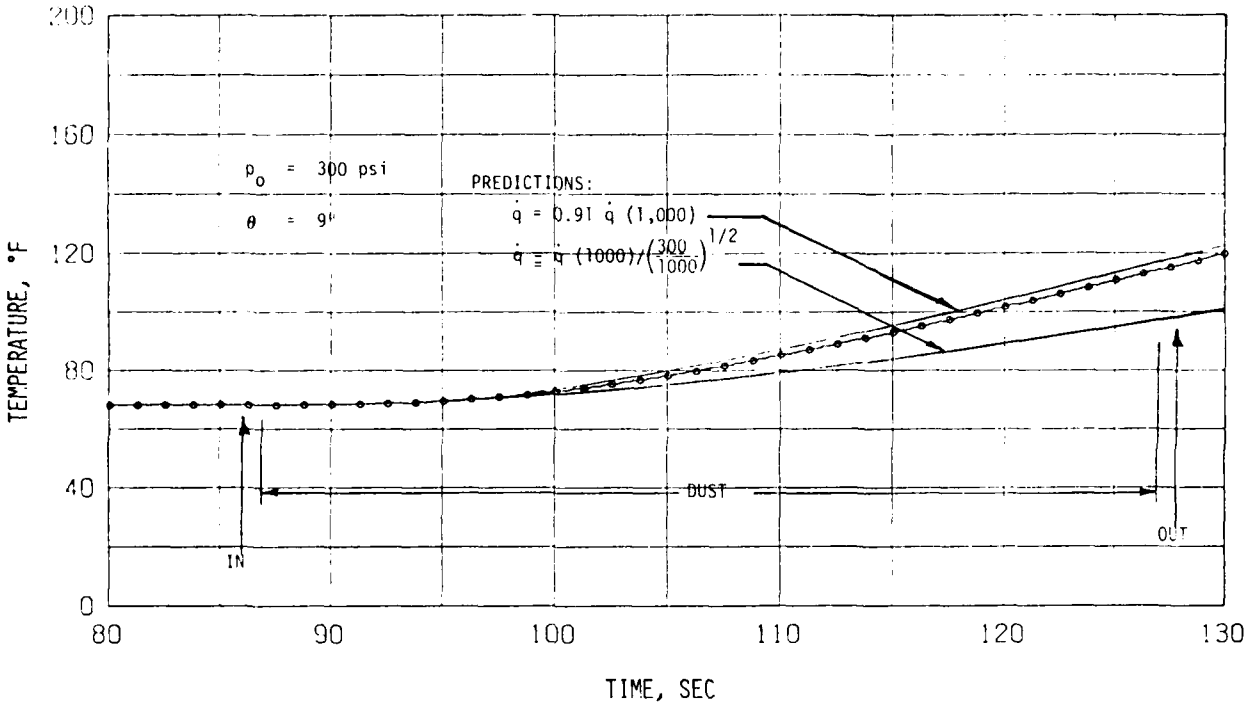

Figure 16. Convective heating model comparison (p_o = 300 psi).

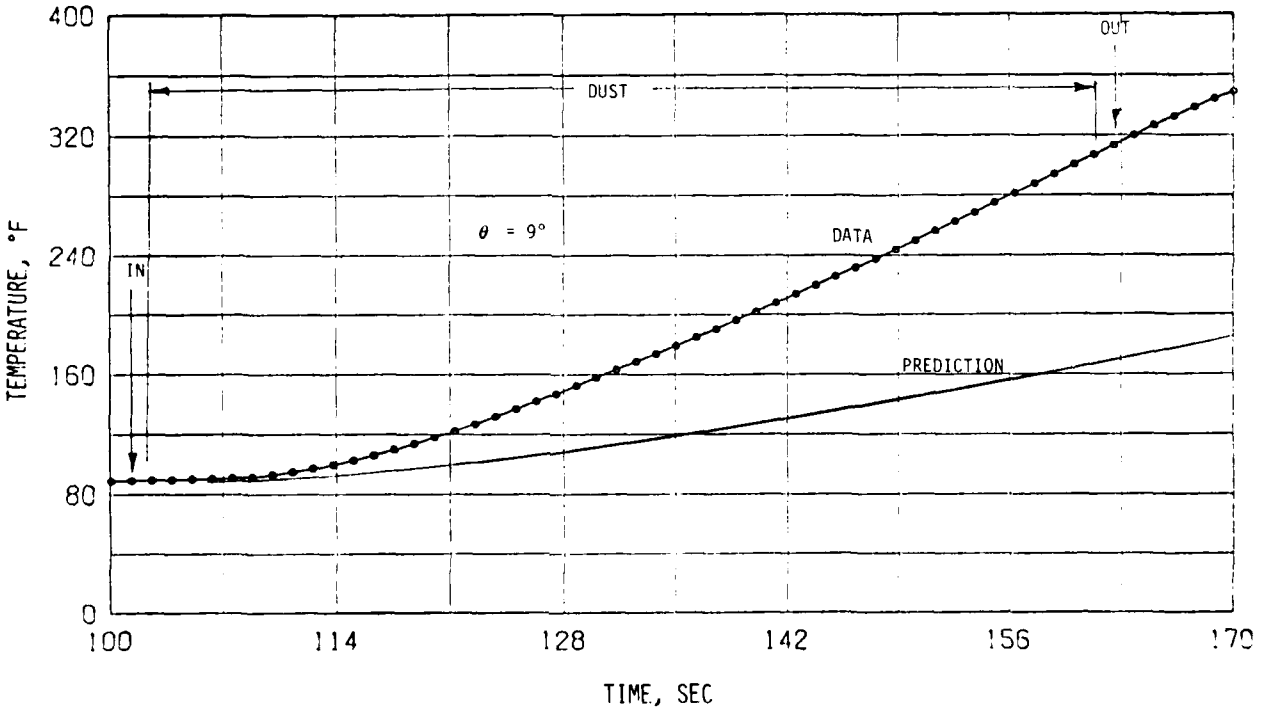

Figure 17. AEDC run 3 data trace.

3.1.5 Correlation

A seven-step procedure was used in the data correlation:

1. Calculate surface temperature histories for all models using observed mass loss ratios (constant during run) for each model.
2. Plot mass loss ratio (G) versus predicted surface temperature during erosion.
3. Obtain function f(T) to describe the effect of temperature on mass loss.
4. Plot G/f(T), using observed G and predicted f(T), versus velocity to obtain velocity dependence.
5. Similarly, plot G/[f(T) · velocity function] versus impact angle to obtain impact angle dependence.
6. Repeat Step 1 using erosion model derived in Steps 2 through 5.
7. Plot predicted G's versus observed G's to evaluate model.

The results of Steps 1 through 3 are shown in Figure 18. Each of the surface temperature range bars shown represent the range from the lowest to the highest surface temperature predicted for a single test sample during the erosion period. The two functions shown as dashed lines both were used in attempting to correlate the mass loss data, and the results are shown in Figure 19. The temperature function $f_2(T)$ was selected because the resultant velocity variation is more credible than that resulting from $f_1(T)$. The squared dependence on velocity was chosen even though it does not fit the 50-micron particle data well. This was done for several reasons:

- The function selected is an upper bound.
- It will be shown in Section 4.0 that the majority of the flight erosion for the erosion-critical Trajectory A occurs below 3 kft/sec, in the velocity range where the squared dependence gives best agreement with the data.
- The poor correlation of the 50-micron data may be due to some other parameter (such as particle size) that cannot be varied independently.

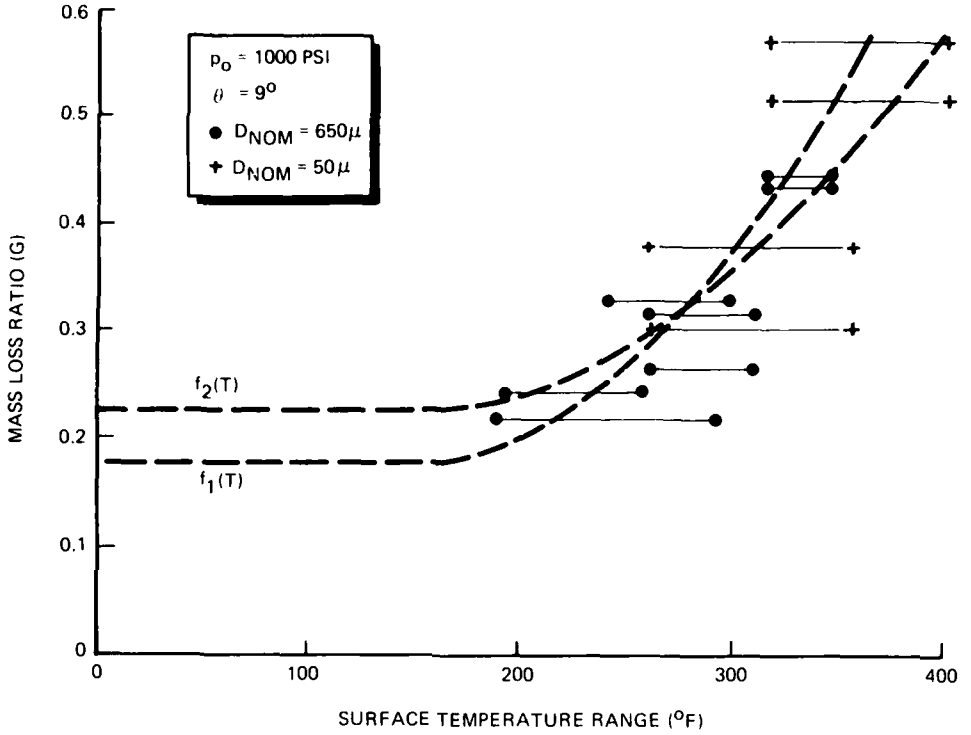

Figure 18. Influence of surface temperature on erosion. 7901325

$\theta = 9^o$

SYMBOL	P_o (PSI)	$D_{NOM}(\mu)$
●	1000	650
○	300	650
+	1000	50

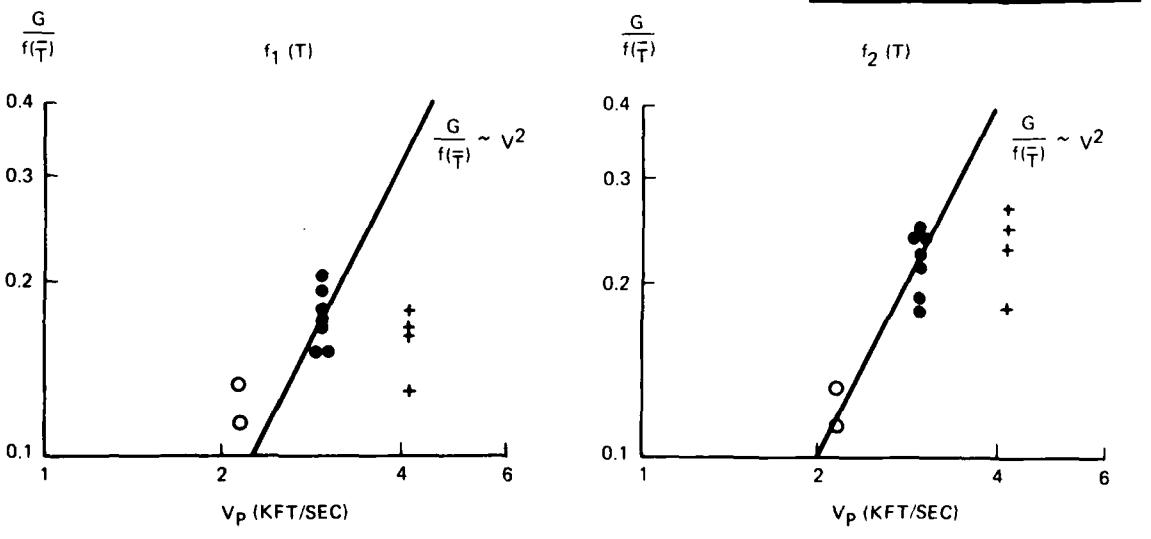

7901324

Figure 19. Influence of velocity on erosion.

The mass loss data then were corrected for both temperature and velocity, and are plotted against impact angle in Figure 20. It is noted that the correlation is very poor for the 30-degree data. However, it will be shown in Section 4.0 that this is not critical, since less than 15 percent of the erosion predicted for Trajectory A occurs at impact angles above 15 degrees.

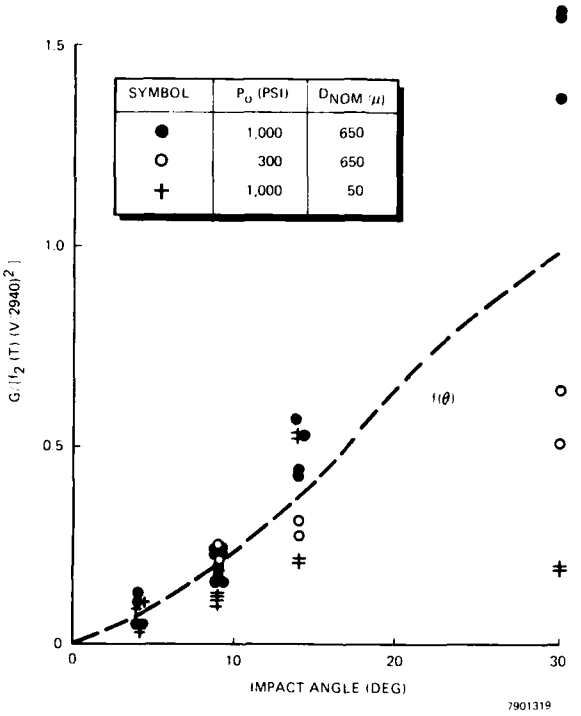

Figure 20. Influence of impact angle on erosion.

The resultant expression for the erosion of VAMAC 15J is:

$$G = 1.15 \times 10^{-7} V^2 [1 + 2.5 \times 10^{-5} (T-150)^2] f(\theta) \quad (4)$$

with a kinetic energy accommodation coefficient (see Equation 2) of:

$$C_{KE} = 0.7 \sin\theta \quad (5)$$

where $f(\theta)$ is a tabular function shown graphically in Figure 20. Erosion for all of the DET tests was then calculated using Equations 4 and 5, and the predicted and measured mass losses were compared in Figure 22. The agreement is actually somewhat better than might be expected from Figures 20 and 21. The reason for this is that the assumed temperature dependence tends to limit the erosion; i.e., as erosion increases, the surface temperature drops, thereby decreasing G.

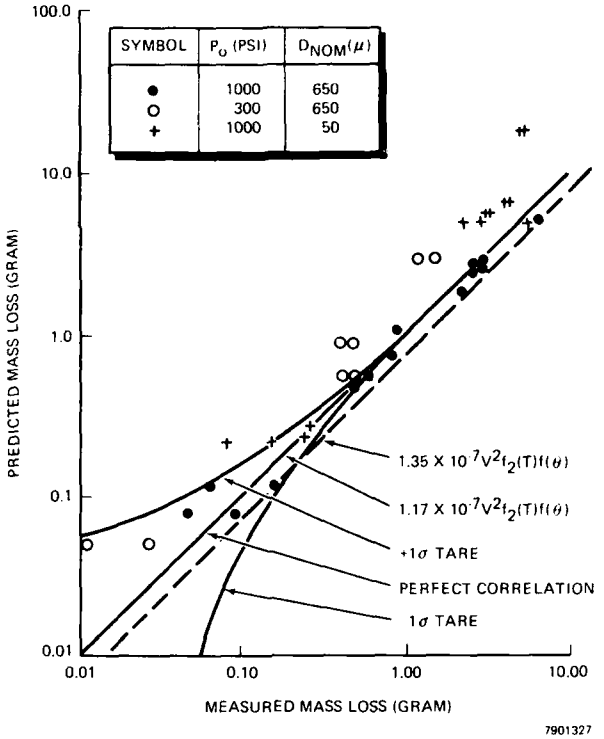

Figure 21. VAMAC 15J erosion data correlation evaluation.

It was found that by multiplying the constant in Equation 4 by 1.15, the resultant correlation, also shown in Figure 21, represents an upper bound to all DET data. This correlation is selected as the final expression recommended for conservative design predictions:

$$G = 1.35 \times 10^{-7} V^2 [1 + 2.5 \times 10^{-5} (T-150)^2] f(\theta) \quad (6)$$

3.1.6 Applicability to Salvo Data

Following the development of the above correlation, salvo erosion data were obtained on several VAMAC materials. These data are compared to the predictions of Equation 5 in Figures 22 through 25, and the correlation is seen to be conservative in almost every case.

3.2 KEVLAR-EPOXY DUST EROSION CORRELATION

The DET data reported in Reference 4 are correlated here as a function of velocity, impact angle, and particle size. Due to the relatively limited data base it was impossible to estimate the effect of surface temperature.

The effect of impact angle is shown in Figure 26. These data have been fit mathematically by the straight line:

$$G = G_{9^\circ} + 0.0353 (\theta - 9) \quad (7)$$

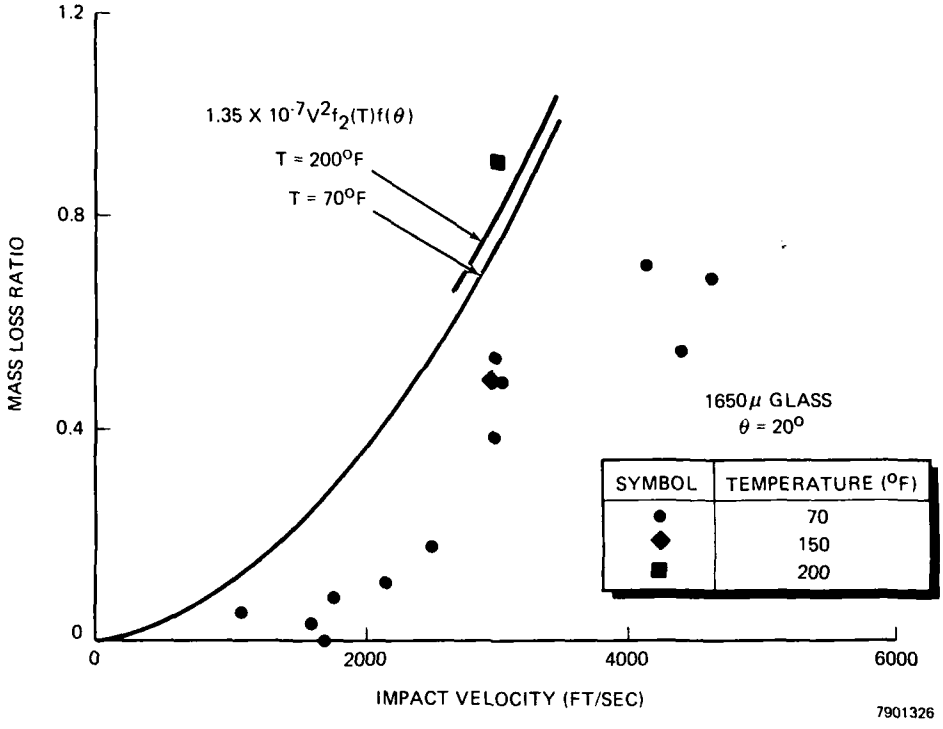

Figure 22. Comparison of VAMAC 15J salvo test erosion data with DET correlation (velocity effect).

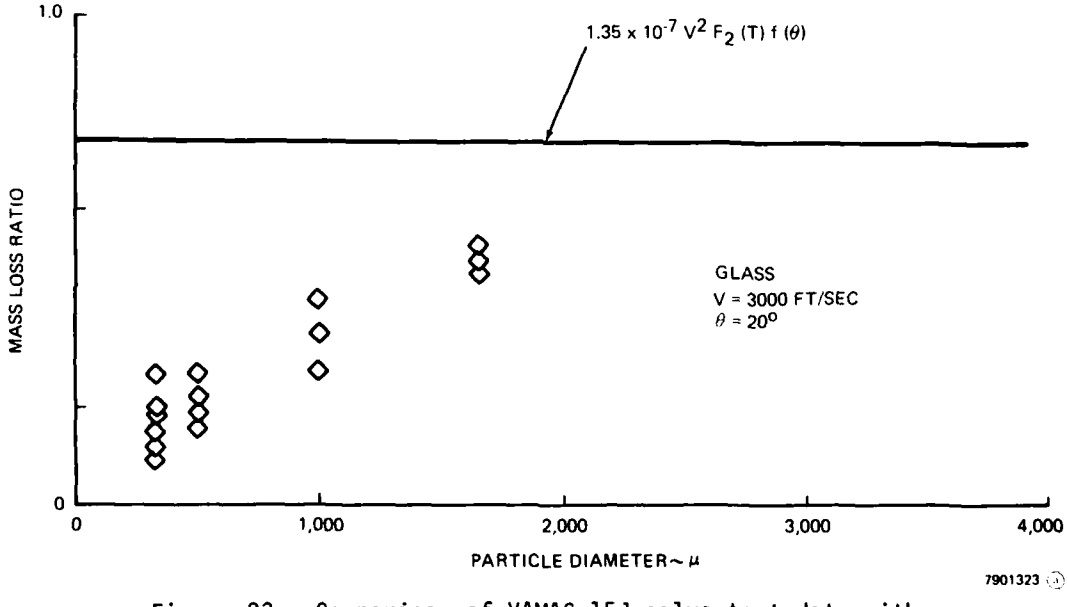

Figure 23. Comparison of VAMAC 15J salvo test data with DET correlation (particle diameter effect).

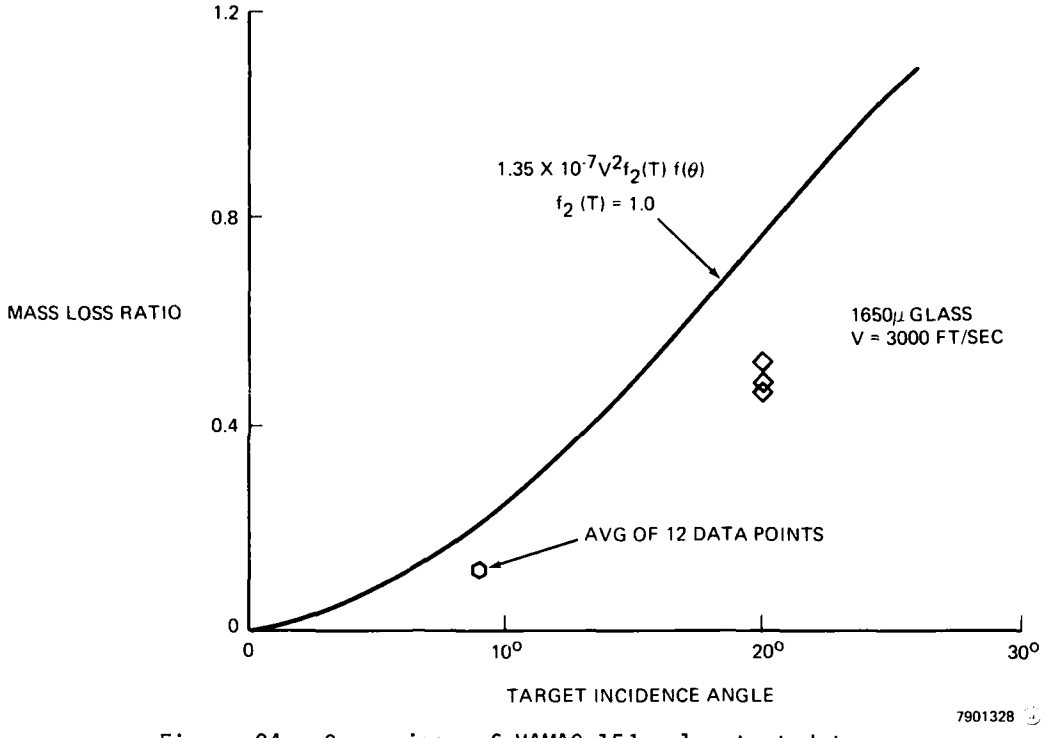

Figure 24. Comparison of VAMAC 15J salvo test data with DET correlation (angle effect).

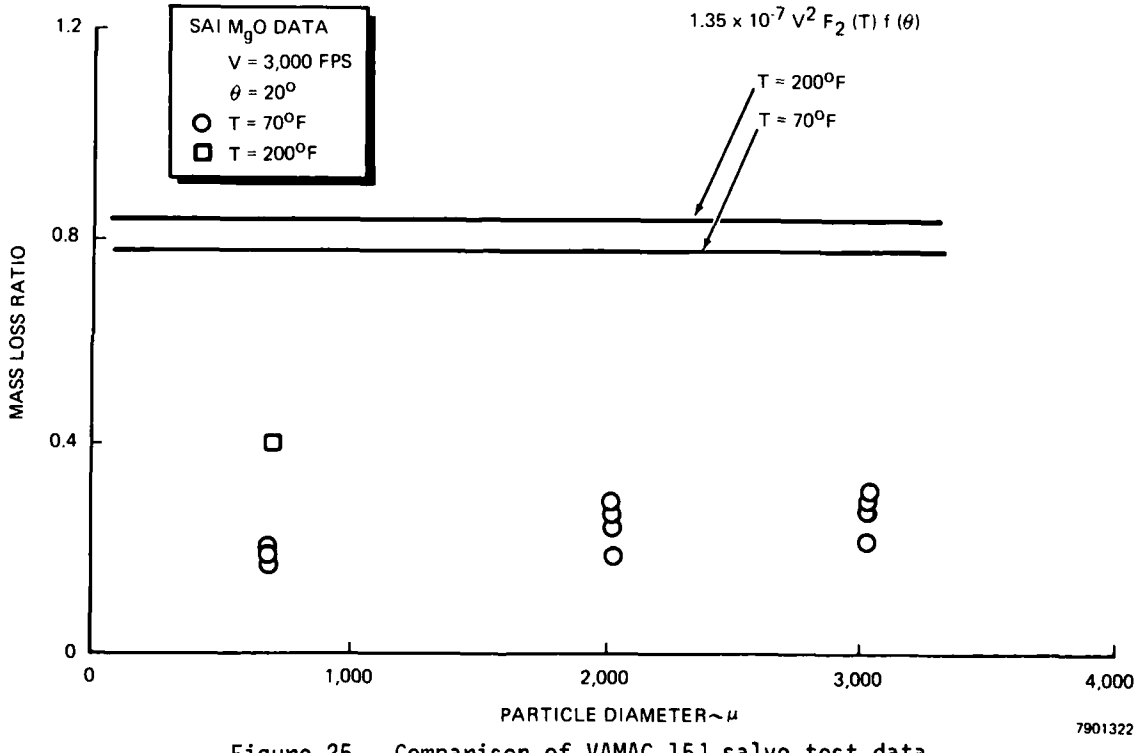

Figure 25. Comparison of VAMAC 15J salvo test data with DET correlation (MgO data).

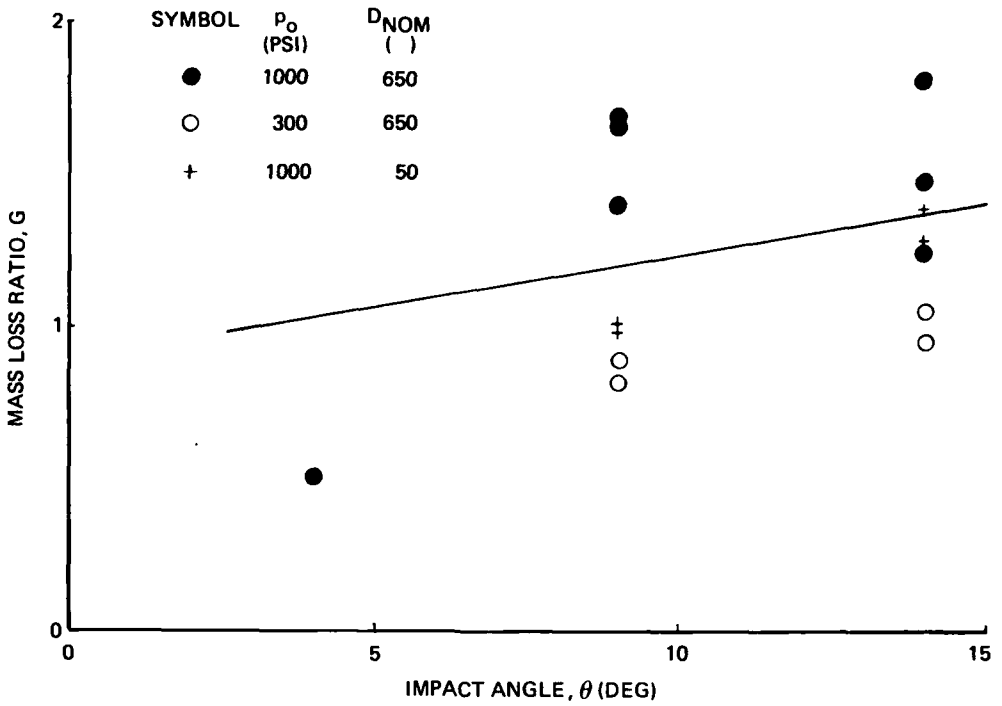

Figure 26. Influence of impact angle on Kevlar-epoxy erosion.

in which G is mass loss ratio, and θ is impact angle in degrees. Note that some of the scatter in Figure 26 is due to the fact that different velocity data are plotted together.

To eliminate the effect of impact angle, the data were then divided by the above function, evaluated for the appropriate impact angle, and the results are plotted in Figure 27 as a function of velocity. A particle size dependence is suggested by the fact that the 2,140 ft/sec data and the 2,950 ft/sec data (all 650μ particles) are well fit by a velocity-squared curve, while the 4,125 ft/sec data (50μ particles) not only do not fall on that curve, but actually show generally lower erosion than the 2,950 ft/sec data. To describe this data in a simple manner, the velocity-squared curve shown in Figure 27 was fit through the 650μ data, and the difference between the value of that function evaluated at 4,125 ft/sec and the average of the 50μ data was used to derive the following particle size function:

$$\frac{G}{G_{650\mu}} = 0.21 + 0.0018\ D \qquad (8)$$

in which D is particle diameter in microns. Note that the actual diameters for the two particle sizes were determined to be 438μ and 94μ, as discussed in Section 2.1. These latter values were used to derive Equation 8.

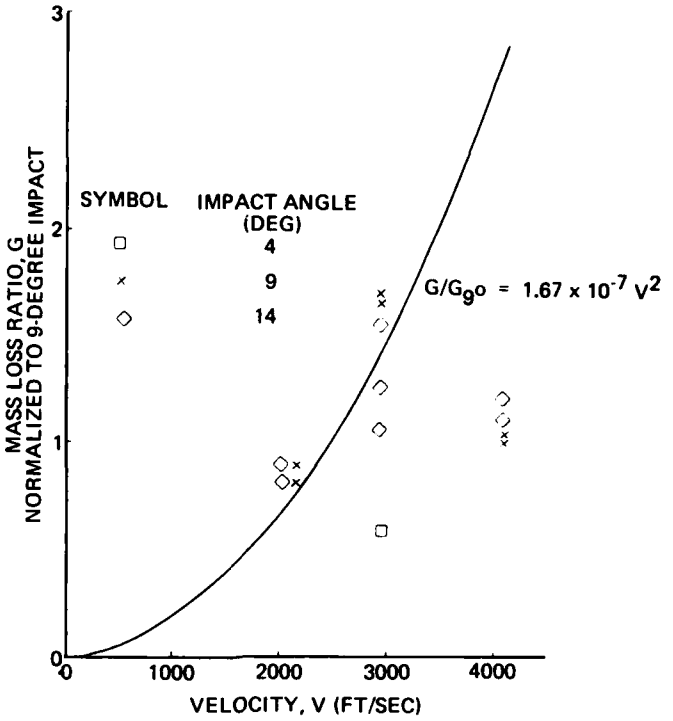

Figure 27. Influence of velocity on Kevlar-epoxy erosion.

Combining the impact angle, velocity, and particle size functions yields the expression for the erosion mass loss of Kevlar-epoxy:

$$G = 0.26 \times 10^{-7} V^2 (1 + 0.04 \theta) (1 + 0.0086 D) \quad (9)$$

Erosion rates for all of the tests used in developing this correlation were then calculated with this model, and the predicted and measured mass loss ratios are compared in Figure 28. Equation 9 is seen to correlate the data reasonably well.

3.3 VAMAC 15J AND KEVLAR-EPOXY PEBBLE IMPACT CORRELATION

Pebble impact data for VAMAC 15J and Kevlar-epoxy are presented in References 3 and 5, respectively. These data were obtained using the Science Applications, Inc. (SAI) 28mm smooth-bore powder gun and machined sperhical tonalite granite pebbles.

3.3.1 VAMAC 15J

The majority of the VAMAC pebble data were obtained for VAMAC samples which were reinforced with Kevlar or graphite fibers in addition to the carbon black contained in all VAMAC materials. However, since the data indicate that the fibers may actually degrade erosion resistance, only the unreinforced VAMAC 15J was considered here. Unfortuantely, the mass losses in the pebble impact expression for this material is derived partially from the correlation of the DET data for room temperature specimens:

$$G = 1.35 \times 10^{-7} V^2 F(\theta) \quad (10)$$

in which $f(\theta)$ is the graphical function shown earlier in Figure 21.

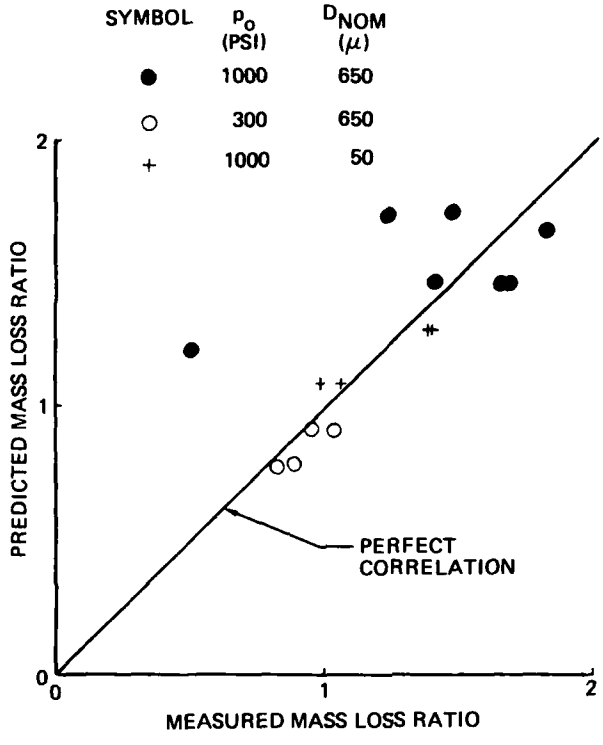

Figure 28. Kevlar-epoxy erosion data correlation evaluation.

Oblique impacts typically produce shallow roughly elliptical craters. Treating the mass loss at the center of such a crater one-dimensionally, the maximum crater depth (d) is:

$$d = G \frac{\rho_p}{\rho_t} D \sin \theta \quad (11)$$

in which D is pebble diameter, and ρ_p and ρ_t are pebble and target densities, respectively.

3.3.2 Kevlar-Epoxy

In contrast to the VAMAC 15J samples, Kevlar-epoxy samples lost significant mass in the pebble impact tests. Very little data are given in the references for Kevlar-epoxy; however, there is a large amount of data on Kevlar-phenolic. It was expected that Kevlar-epoxy and Kevlar-phenolic would have similar erosion properties, and the following data evaluation shows this is the case. Consequently, the correlation was actually performed using Kevlar-phenolic data.

The impact data are shown in Figure 29 for Kevlar-epoxy and in Figures 30 through 32 for Kevlar-phenolic. To eliminate particle diameter as a parameter, the crater depth was non-dimensionalized by the particle diameter. The local failure mechanism associated with break-through is different from that associated with impact damage to a thick specimen. Since the actual motorcase is several times thicker than the impact samples, only data for particles that did not break through the sample are shown.

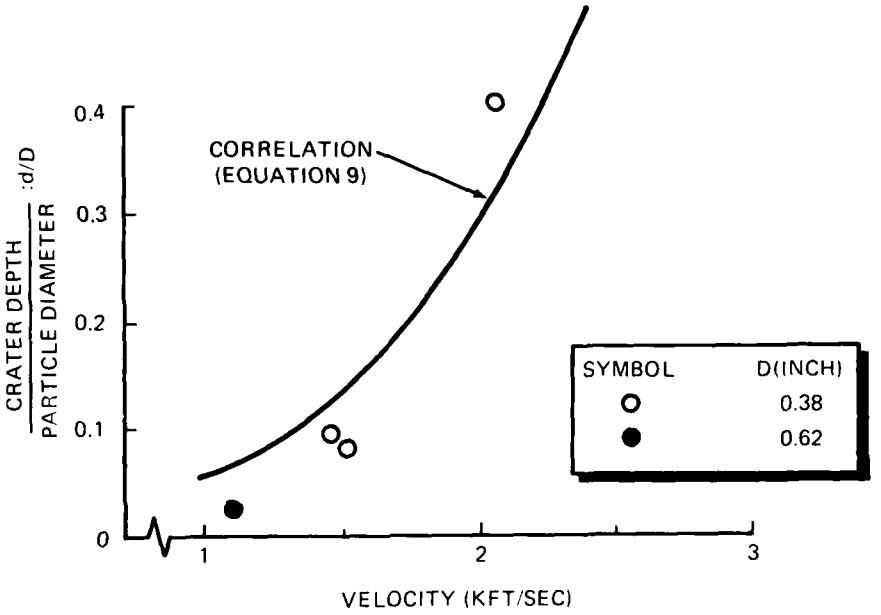

Figure 29. Kevlar-epoxy 20-degree pebble impact data.

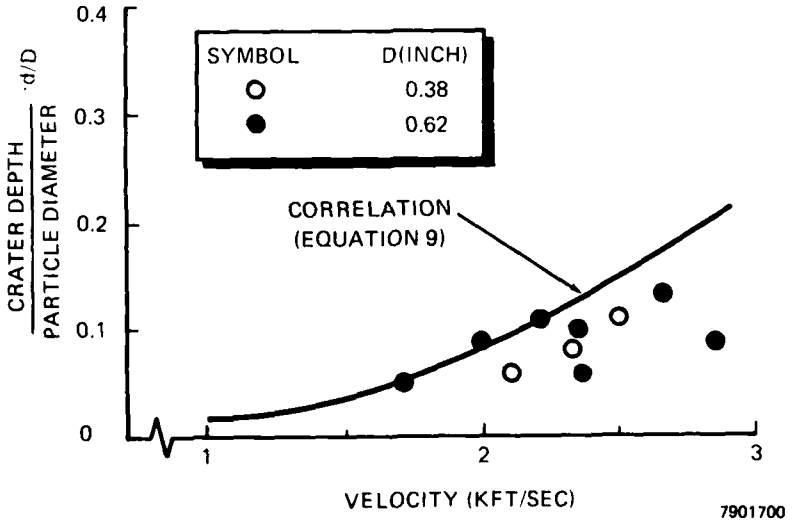

Figure 30. Kevlar-phenolic 6-degree pebble impact data.

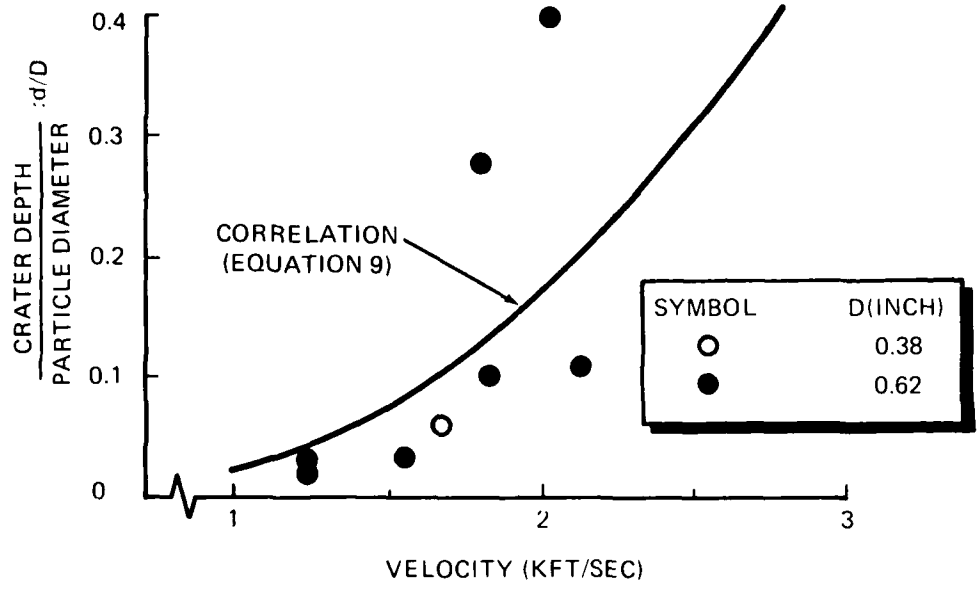

Figure 31. Kevlar-phenolic 12-degree pebble impact data.

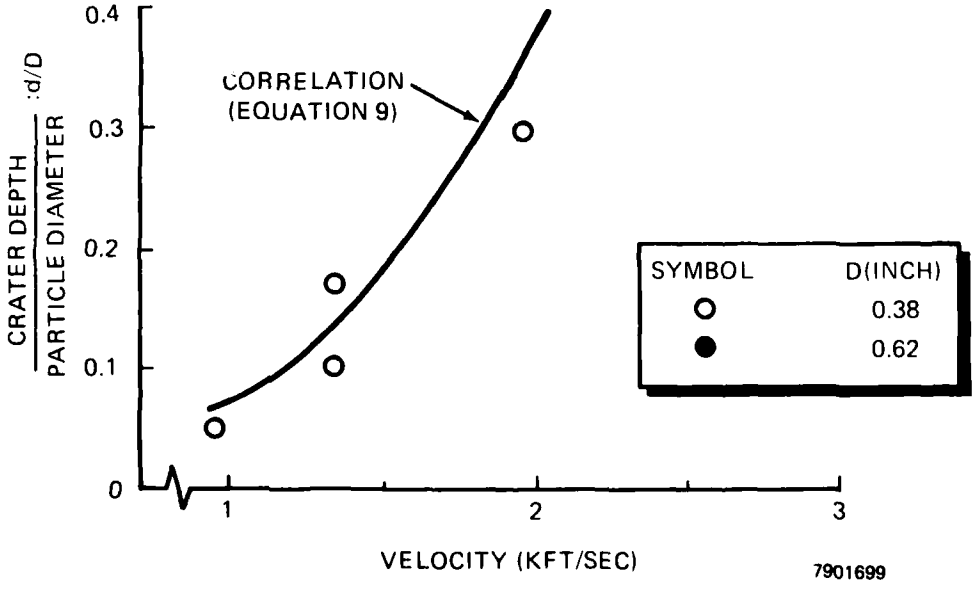

Figure 32. Kevlar-phenolic 30-degree pebble impact data.

SECTION 4.0
FLIGHT PREDICTIONS

The erosion of VAMAC 15J was predicted for two trajectories (Section 4.1) and one atmospheric dust profile, using the temperature-dependent erosion model described in Section 3.1. Erosion was calculated both with and without the influence of the shock layer on the particles. The shock layer is calculated to reduce erosion by 30 percent on one trajectory and by 50 percent on the other trajectory. Erosion also was calculated with and without the effect of material temperature in the erosion model. When the temperature function is set equal to 1.0, the erosion predicted for the two trajectories is reduced by 4 percent and by 30 percent relative to the nominal predictions for the two trajectories.

Pebble impacts for both VAMAC and Kevlar-epoxy were evaluated, and no craters deeper than 0.010 inch were predicted.

No debris shielding analyses were performed for flight because the debris shielding analysis currently does not have a collision model. The smallest particles in the flight dust profile specified are so numerous that virtually every incoming particle will collide with one or more of them. Consequently, the limiting analysis performed for the DET tests, which assumed all equal-sized particles, is not applicable to the flight case.

4.1 ENVIRONMENT

Motorcase erosion calculations were performed for two trajectories, which are designated as A and B. Trajectory B includes the effects of worst-case winds. Figure 33 illustrates both trajectories. The dust profile (identical for both trajectories) is defined in Reference 3.

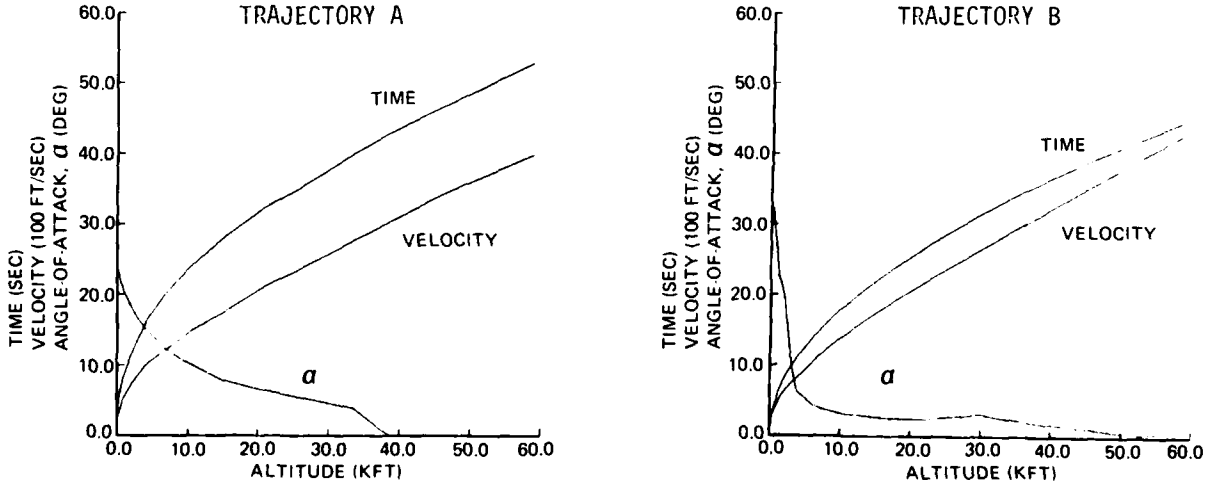

Figure 33. Design trajectories.

4.2 IN-VACUO EROSION

The in-vacuo erosion predictions (i.e., the effects of the shock layer are ignored) are shown in Figures 34 and 35 for the two trajectories. To show the influence of particle size, the predictions are subdivided into particle size ranges that produce roughly equal erosion increments for Trajectory A. Trajectory A clearly is the more severe with respect to erosion. The principal reason for this difference is the difference in the angle-of-attack histories. Because of the angular dependence used in the erosion model, the predicted erosion rate varies approximately as the square of the impact angle. Consequently, even though the angle-of-attack (AOA) persists much longer in Trajectory B, the higher average AOA prior to 40,000 ft altitude in Trajectory A produces more than twice the total erosion predicted for Trajectory B.

4.3 SHOCK LAYER EFFECTS

An approximate analysis was performed (Reference 8) to estimate the effects of the shock layer on the trajectories of the impinging dust particles. The analysis was restricted to the windward meridian and used a tangent-cone procedure (Figure 36) to describe the shock wave shape. The shock shapes on the three-angle shroud were superimposed, with the intersection points determined from Mach-line projections. The flowfield in each region was based on a tangent-wedge calculation, with a pseudo-wedge angle defined by the tangent-cone shock angle. Two-dimensional trajectories then were computed for the particles by neglecting crossflow deflection and vehicle roll effects. The particle drag coefficients were based on the data correlations in Reference 9 for smooth spheres.

This procedure was designed to provide a conservative estimate of the actual particle erosion, since each approximation tends to underpredict the deflection of the particles away from the body. A partial exception to this rule is the use of the tangent-cone shock approximation which overpredicts the shock standoff distance on the windward meridian (although this is offset to some extent by overpredicting the streamline turning effects). However, for the trajectory times of most importance; i.e., when the angle-of-attack is less than 5 degrees, the tangent-cone shock shape approximation is most accurate.

Particle trajectories were computed over the axial region from the end of the shroud to the end of Stage One for both trajectories. Figure 37 shows typical results for the two trajectories, and leads to the following observations:

For Trajectory A:

1. Aerodynamic shielding in the shock layer reduces erosion on the windward meridian from 0.026 inch to 0.017 inch.

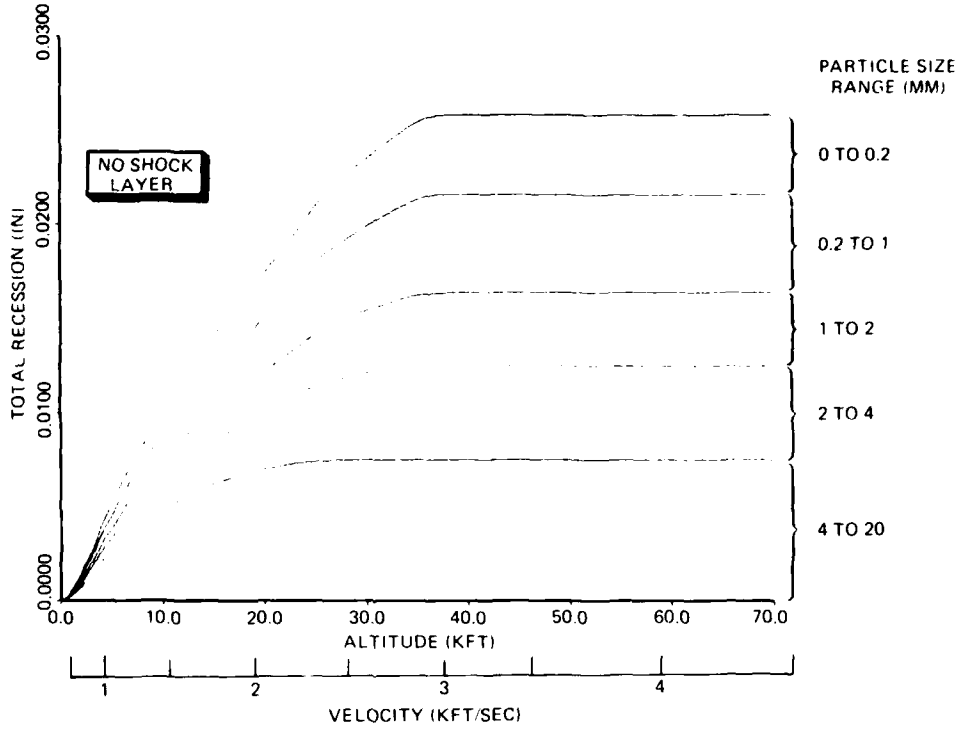

Figure 34. VAMAC 15J motorcase erosion (Trajectory A).

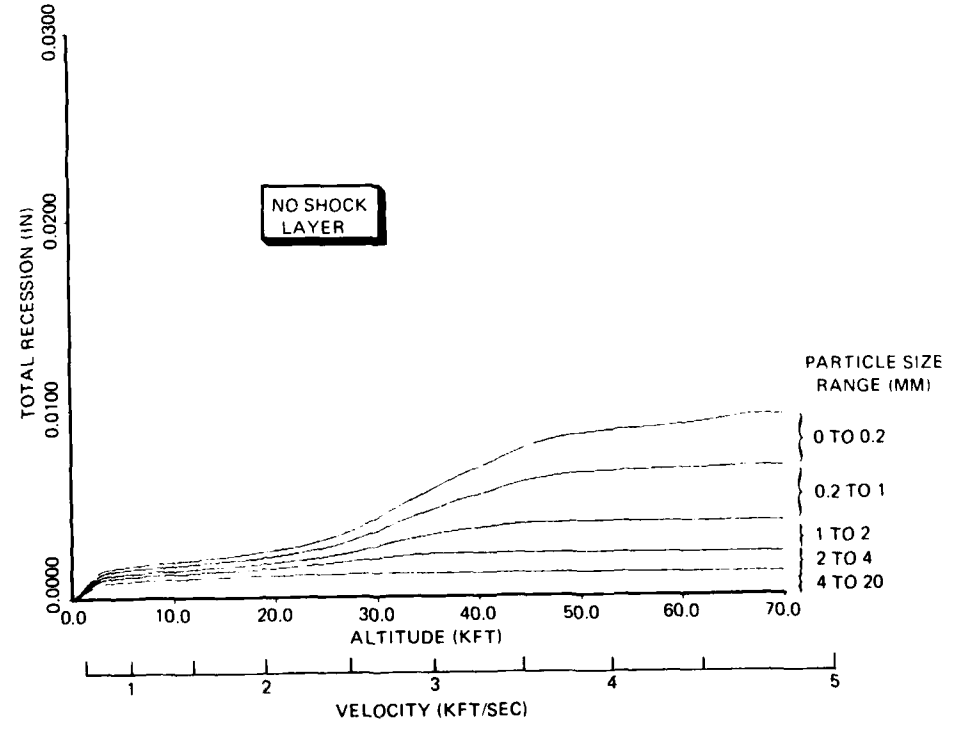

Figure 35. VAMAC 15J motorcase erosion (Trajectory B).

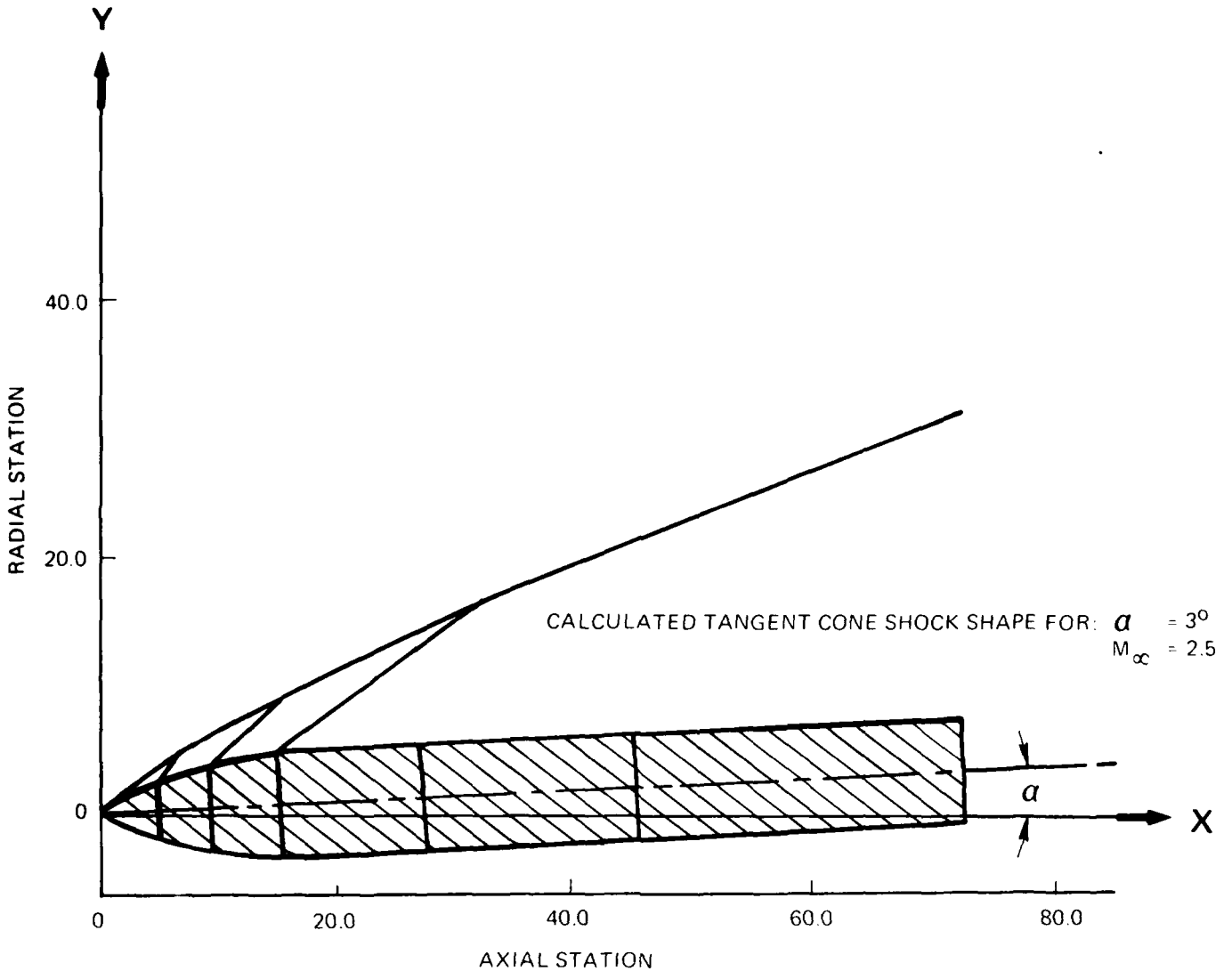

Figure 36. Schematic of vehicle shock layer.

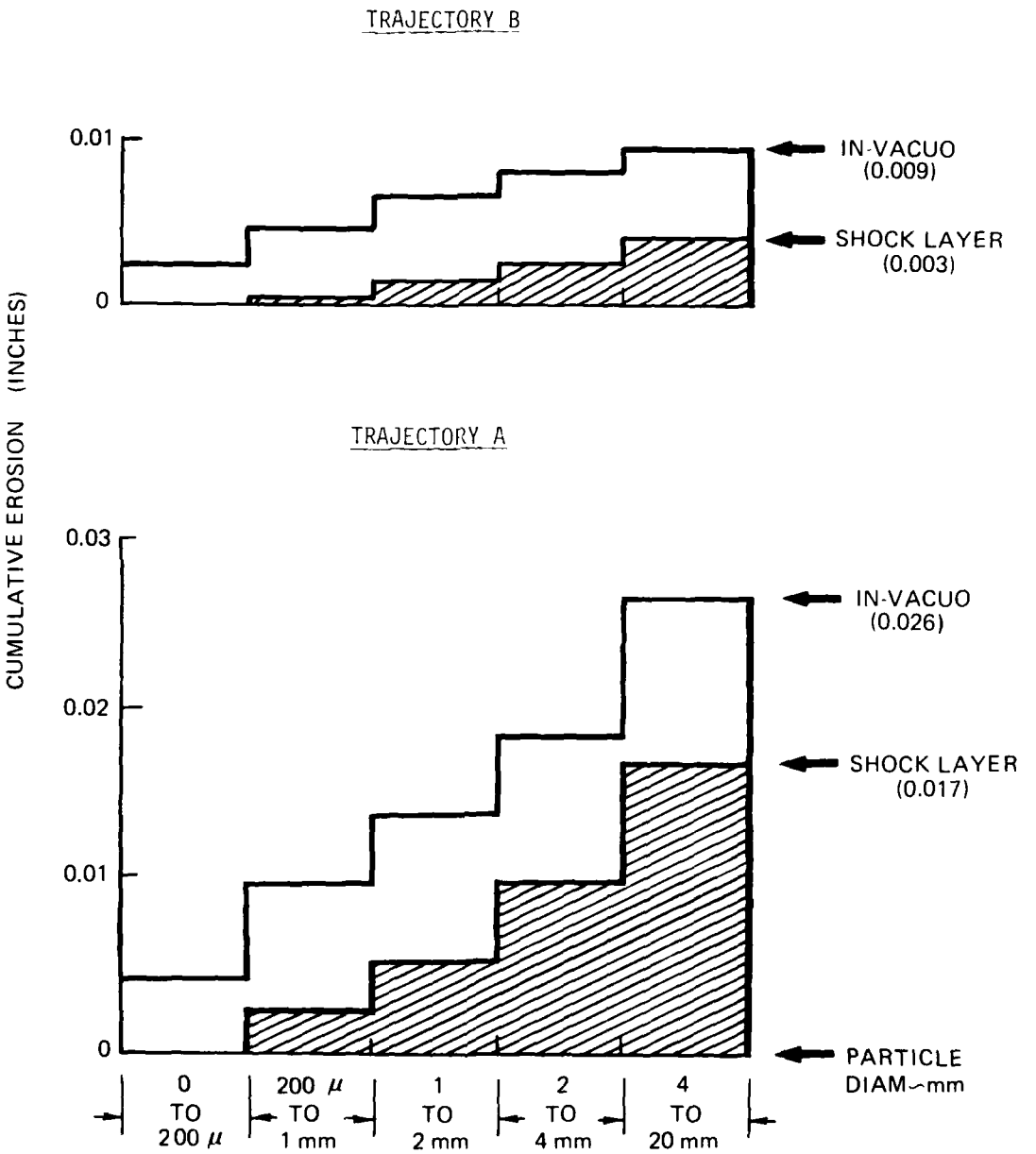

Figure 37. Influence of shock layer on motorcase erosion.

2. Particles smaller than 1000μ contribute less than 13 percent of total erosion.

3. Essentially all erosion occurs at velocities less than 3000 ft/sec.

For Trajectory B:

1. Aerodynamic shielding in the shock layer reduces erosion on the windward meridian from 0.009 inch to 0.003 inch.

2. Particles smaller than 1000μ contribute less than 7 percent of total erosion.

3. Ninety percent of the erosion occurs at velocities less than 3000 ft/sec.

Thus, the shielding effect produced by aerodynamic deflection of particles in the shock layer produces a significant reduction in predicted motorcase erosion depth for both trajectories; although the effect is much greater for Trajectory B because of its smaller, longer duration angle-of-attack history. Future design analyses should account for these shock layer effects, although it may be necessary to develop improved techniques to describe the flowfield and particle interactions over the complex body shapes of interest. The results also indicate that ground test erosion programs should concentrate mostly on particles larger than 1000μ and on impact velocities below 3000 ft/sec.

4.4 WALL TEMPERATURE EFFECTS

The motorcase surface temperature histories predicted for the two trajectories, including the calculated effects of heating due to particle kinetic energy deposition, are shown in Figure 38. Erosion histories were calculated both with the temperature dependence function $f_2(T)$, described earlier in Section 3.1, and with the temperature function set equal to 1.0 (i.e., no material temperature dependence). The results of those calculations are compared in Table 3.

4.5 PEBBLE IMPACT PREDICTIONS

The maximum crater depth histories were calculated for both VAMAC 15J and Kevlar-epoxy using the erosion models described in Section 3.3. Because the angles-of-attack at the low altitudes where pebbles may be encountered are much larger for Trajectory A than for Trajectory B, only Trajectory A was evaluated. The results are shown in Figure 39. Peak crater depths occur at different altitudes for the two materials due to the different angular dependence functions used. Since $f(\theta)$ used in the VAMAC 15J

correlation is approximately proportional to sin θ, the VAMAC 15J crater depth is approximately proportional to sin θ squared, while the Kevlar-epoxy crater depth is correlated by sin θ to the first power. This difference in angular dependence may be due partly to the use of DET data to predict VAMAC 15J crater depths. However, it should be noted that comparison of the Kevlar-epoxy data and the VAMAC 15J data from the DET indicates that the mass loss of Kevlar-epoxy actually is less sensitive to impact angle than is the mass loss of VAMAC 15J.

The maximum crater depths expected for the trajectory and particle size distributions analyzed are 0.009 inch for VAMAC 15J and 0.013 inch for Kevlar-epoxy. These craters are not expected to pose a hazard to the vehicle.

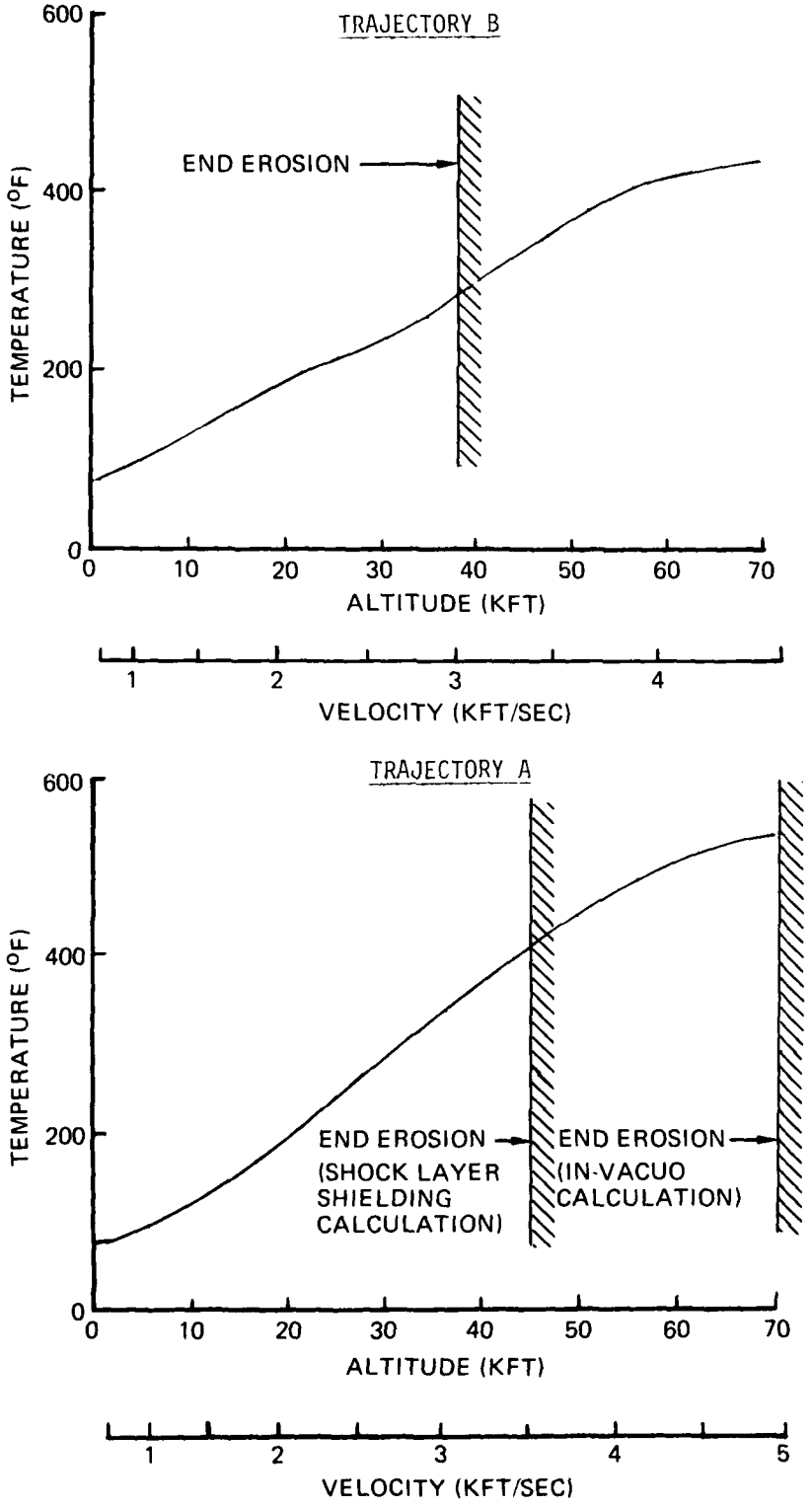

Figure 38. Motorcase surface temperature histories.

Table 3. Effect of temperature on flight erosion predictions.

Trajectory	Shock Layer Effects	Surface Temperature Function	Predicted Erosion (Inch)
A	No	1.0	0.025
↓	No	$f_2(T)$	0.026
	Yes	1.0	0.0165
	Yes	$f_2(T)$	0.0173
B	No	1.0	0.0063
↓	No	$f_2(T)$	0.0095
	Yes	1.0	0.0029
	Yes	$f_2(T)$	0.0034

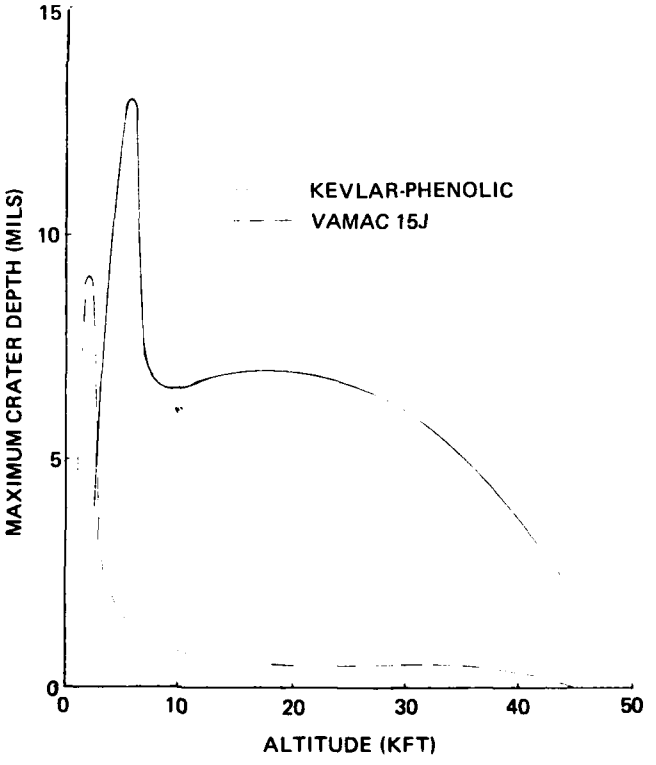

Figure 39. Crater depth history.

Blank

SECTION 5.0
RECOMMENDATIONS FOR FUTURE TESTING

A study has been performed to evaluate several existing facilities for use in performing erosion tests of candidate external thermal protection materials. The evaluation considered such factors as flight simulation capability, performance characterization, flexibility of test conditions, and cost. As a result of this study, it is recommended that material screening tests and relative performance comparison tests be conducted in the Bell Aerospace Corporation rotating arm facility and in the Dust Erosion Tunnel (DET) at the Arnold Engineering Development Center (AEDC). Tests to obtain detailed information for development of analytical erosion models should be performed at the Bell rotating arm facility and at the Science Applications, Inc. (SAI) powder gun facility. Finally, materials/system performance verification tests should be conducted using a rocket-powered sled (e.g., at Holloman AFB or at Sandia Laboratories, Albuquerque).

Five basic types of facilities were considered: particle-seeded arc-jets, powder guns, ballistic ranges, rocket sleds, and rotating arms. A summary of facility capabilities is shown in Table 4. The relative advantages and limitations of each type of facility are discussed in the following paragraphs.

5.1 ARC-JETS

Several particle-seeded arc-jets currently are used for reentry erosion testing including the AEDC High Enthalpy Ablation Test (HEAT) facility, the Avco 10 MW facility, and the AEDC DET. However, the only such facility that can produce the desired particle velocities without unacceptably high convective heating (for ascent flight simulation), is the DET. The DET has the further advantage of being able to provide essentially continuous flow. Tests at conditions producing very low erosion rates can be conducted successfully by extending the test duration until measurable mass losses have been achieved. The principal disadvantage of the facility (shared by all particle-seeded jets) is that calibration of the particle environment (particle size, velocity, and distribution) is very difficult and time consuming. The particles appear to break up during injection, so that the effective particle size can only be determined accurately by holography. Particle velocity is proportional to the particle size (since the particles are drag-accelerated by the gas stream), as well as to the gas flow conditions (enthalpy and chamber pressure). In principle, almost all conditions of interest can be simulated in the DET; however, in practice it is very difficult to vary any single particle or flow parameter independently. Consequently, testing has primarily been conducted at only a few calibrated conditions.

Because of the difficulties associated with calibrating the particle impact conditions and in varying individual test parameters, the DET is not generally satisfactory for tests supporting the development of analytical erosion models. However, since a large number of samples can be tested in a single run, DET tests are relatively inexpensive and the facility is well suited for material screening tests and for obtaining material performance comparisons.

5.2 POWDER GUNS

The mass removed by the impact of a single particle at ascent flight conditions is so small that it is generally less than the tare mass change due to handling the sample. Therefore, with the possible exception of tests with large pebbles, single particle impact tests are generally impractical for ascent erosion studies. Consequently, SAI has developed a multiple particle salvo test in which a number of particles are launched simultaneously. The particles initially are contained in a sabot which is accelerated by a powder gun. A typical test sequence consists of impacting the sample with four (or more) salvos of particles and weighing the sample after each salvo. Each salvo is considered to be a data point for purposes of computing the approximate test cost listed in Table 4.

This technique has been found to be reasonably effective and to have the advantages that particle size and velocity, as well as target temperature, can be varied independently and measured accurately. The principal disadvantages are: 1) due to the sharp reduction in mass loss with impact angle, the tare mass change can introduce substantial errors at low impact angles and velocities, and 2) model temperatures are limited to the range in which no permanent material degradation occurs.

5.3 BALLISTIC RANGES

Ballistic ranges are widely used for reentry erosion testing for two reasons: 1) no other type of facility can duplicate high performance flight velocity and aerodynamic heating simultaneously, and 2) no other type of facility can produce hypersonic impacts by snowflakes and water droplets. The principal disadvantages of ballistic ranges are high cost, short test time, and the difficulty of obtaining accurate in-flight measurements of the mass loss.

Unfortunately, the features that make ballistic ranges attractive for reentry are of minor importance for ascent flight applications. The principal advantages for ascent flight testing are that the particle environment can be controlled accurately, and the impact velocity can be determined accurately. In addition, it often is possible to recover the models for accurate measurements and examination.

Table 4. Multiple particle impact ground simulation facilities.

APPLICATION	FACILITY	MODEL SIZE	PARTICLE VELOCITY (ft/sec)	PARTICLE SIZE (mm)	PARTICLE DENSITY (gm/m^3)	
SCREENING	-AEDC RANGE G- Guided Rail Track with Dust Shakers	2.5" Diameter Flat, Cone or Pyramid	4000 - 18000	0.2 → 1 Dust concentrated in 120 ∿3 inch curtains. Actual density ≈30 times average density.	0.1 → 2 (average) Increase to 6 possible	
SCREENING	-AEDC DET- Arc-Heated Tunnel with Injected Particles	2" - 4" Flat, Wedges, Cone	2000 - 5500	0.05 - 2.0	1 - 30	
SCREENING	-HOLLOMAN- Supersonic Sled Piercing Dust Loaded Nets	14" x 24" Wedge 7" Diameter Cone	to 4200 to 8000	Unlimited. Only 1 - 3 Used to date	> 2	
SYSTEM VERIFICATION OR SCREENING	-SANDIA ROCKET SLED-	18" Diameter 8" Diameter	0 → 3500* 6500 *Tests proposed to simulate flyout profile.	Unlimited	TBD	
SCREENING AND IMPACT THEORY	-BELL AERO- Whirling Arm with Dust or Rain Nozzles	Typical: 8 square inch 1 pound maximum including holder	1000 at 1 atm 3000 at 0.1 atm	0.001 → 2.0	Average density low. Dust concentrated in single jet.	
IMPACT THEORY	-SAI POWDER GUN- Multiple Particle Salvos	6" Square	500 - 5000	Unlimited	N/A	

PARTICLE DENSITY (gm/m^3)	PARTICLE MATERIALS	TEST DURATION	FACILITY STATUS	TEST FREQUENCY	COST PER TEST	COST PER DATA POINT
(average) to 6	MgO Si O_2	800 Feet	Operational	1-2/Day (7 Models/Week)	$2,000 - 4,000	$2,000 - 4,000
1 - 30	MgO $Al_2 O_3$	600 sec Maximum 10 sec Typical	Operational	1 - 2/Week (18 - 36 Models/Week)	$5,000 - 7,000	$ 250 - 350
> 2	ANY		*Six-month* lead time for test program with dust nets	1/Week	$40,000	$ 500 $5,000
TBD	ANY	1,000 to 3,000 feet	Dust nets now	2/Week	$15,000 - 20,000	$1,000 $3,000
density low. ncentrated in jet.	Rain and Dust	Hours	Operational Dust environment calibration required	4-5/Day	Cost for tests up to 2,500 ft/sec $200 - 250	Cost for tests up to 2,500 ft/sec $100 - 125
N/A	ANY	N/A	Operational	25 Shots/Day	$ 150 - 200	$ 150 - 200

5.4 ROCKET SLEDS

From a facilities comparison standpoint, rocket sleds essentially are very large ballistic ranges. In comparison to ballistic ranges, however, cost per model is reduced in most cases because the sleds are large enough to mount many models. Test times substantially longer than those achieved in ballistic ranges are achieved by using longer particle fields, although the high acceleration and deceleration of the sled typically cause large velocity changes during the period of erosion. This fact can be an advantage in designing a system verification test, although it can complicate the use of the data for erosion model development.

To date, most rocket sled dust tests have employed dust nets. These are fine nylon nets with particles bonded to them. However, in a recent test program, shakers were developed which are mounted over the track to provide a uniform free-falling dust environment to provide improved simulation of flight conditions.

5.5 ROTATING ARMS

A rotating arm facility consists of a long counterbalanced arm that can be rotated to achieve high tip speeds. Rotating arms typically operate in sub-atmospheric chambers to reduce air drag on the arm. Such facilities at both Bell Aerospace Corporation and Sandia Laboratories have been investigated; however, only the Bell facility appears capable of duplicating an ascent flight environment. The Bell facility is designed for model speeds up to 3,000 ft/sec, although in its most commonly used configuration; only 2,500 ft/sec can be achieved. Provisions for both rain and dust erosion exist; however, tests to date have been primarily rain erosion, and the dust dispensing system is unsophisticated and not well calibrated. The dust is introduced into a near-sonic airstream by a metering unit and injected down and into the path of the model. The dust velocity relative to the model is the vector sum of the dust and model velocities. This will have a very minor effect on impact velocity (typically 3 percent) but will affect model holder design.

The most commonly used model holder mounts two 2-inch square flat models on either side of a wedge with a horizontal metal leading edge. This holder design has the disadvantage that particle impact angle is strongly affected by particle injection velocity, as shown in Figure 40. This is a serious disadvantage because particle injection velocity is not only difficult to measure accurately, but is also a function of particle size and type. To avoid this problem, a new model holder with a vertical leading edge should be designed. As shown in Figure 40, impact angle is almost independent of particle injection velocity with this holder design except at very high particle velocities. The models are clamped to the holder with metal strips. Mass loss of these strips can provide a mass loss reference for each model.

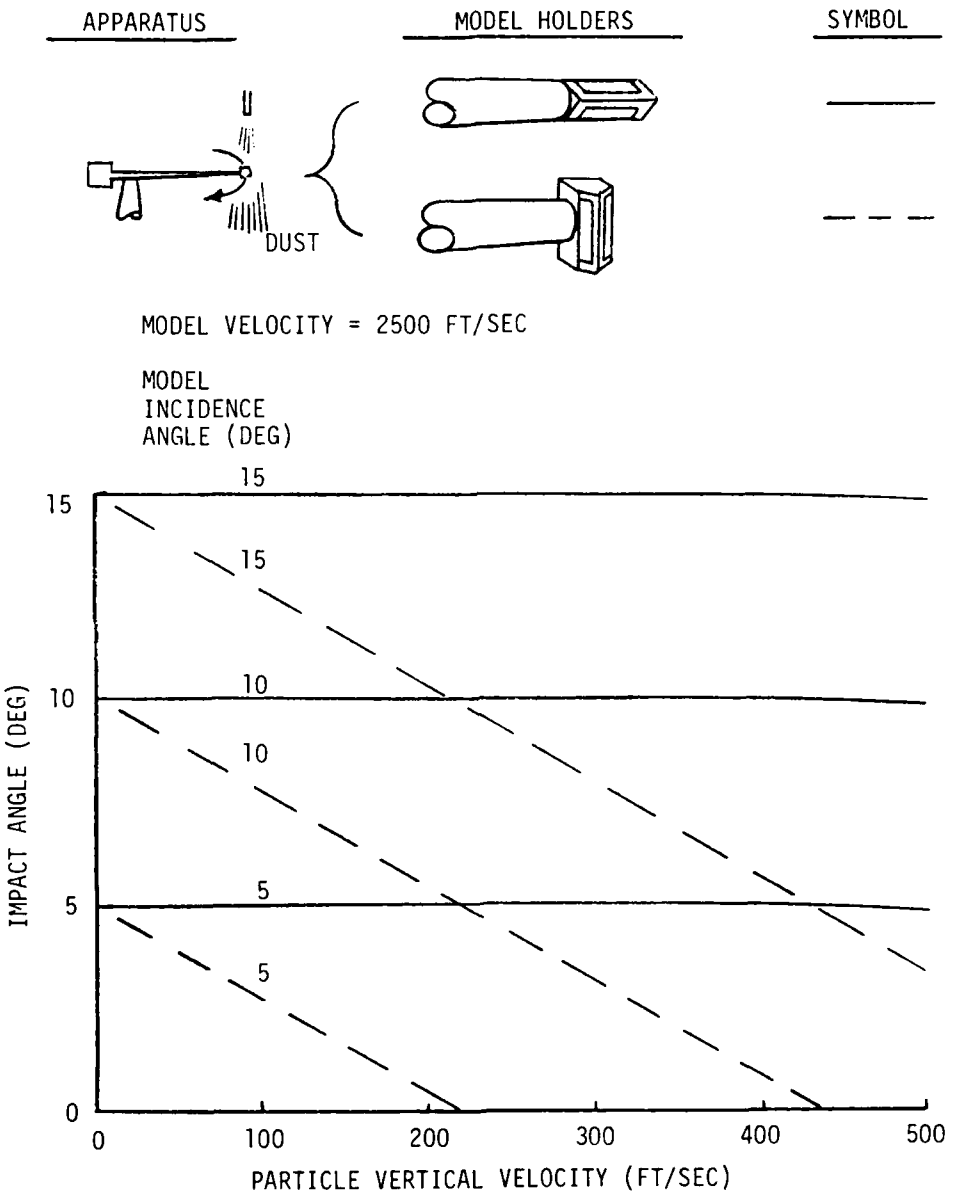

Figure 40. Particle impact parameters in Bell rotating arm facility.

This facility can provide very long run times and has the potential of duplicating the flight velocities and particle size regime with accurately determined impact velocities. Due to the low absolute velocity of the particles in this facility, they can be trapped easily to measure dispersion patterns and flow rates and to evaluate particle break-up. In addition, the cost per model may be lower than at any of the other facilities. This facility has two disadvantages: 1) to achieve this capability, a calibration program is required to characterize the dust field; and 2) its velocity regime is only of limited interest to the reentry missile community. However, the velocity regime may be applicable to erosion tests of many tactical missile materials. Although it is ideal for motorcase material testing, it cannot simulate the peak erosion conditions on the shroud.

5.6 FACILITY RECOMMENDATIONS

Based on the evaluations summarized in the preceding section, recommendations have been made for the selection of erosion test facilities for developing and characterizing materials for external thermal protection of a missile system during ascent flight. The selections reflect the different types of test objectives and simulation requirements such as: 1) screening and evaluation of materials for different vehicle locations, and 2) establishing data bases for developing analytical erosion models. The recommendations are listed in Table 5 and are discussed briefly in the following paragraphs.

Table 5. Erosion facilities recommendations.

APPLICATION	MATERIAL CATEGORY	VARIABLE	RANGE	RECOMMENDED FACILITY
SCREENING	MOTORCASE	MATERIAL	--	BELL ROTATING ARM
	SHROUD COMPOSITE	MATERIAL	--	DET
	SHROUD METALLIC	MATERIAL	--	DET
IMPACT THEORY AND EROSION MODEL DEVELOPMENT	ALL	VELOCITY IMPACT ANGLE PARTICLE SIZE PARTICLE MATERIAL	0 - 2500 fps 0 - 90 deg 0 - 2.0 mm --	BELL ROTATING ARM
	ALL	VELOCITY PARTICLE SIZE TARGET TEMPERATURE	2500 - 5000 fps 2.0 mm ROOM TEMP	SAI POWDER GUN
	SHROUD METALLIC	COUPLED HEATING AND CONTINUOUS EROSION	--	DET
SYSTEM VERIFICATION		PROGRAMMED VELOCITY, PARTICLE SIZE AND IMPACT ANGLE HISTORY	--	ROCKET SLED

The Bell Aerospace rotating arm facility potentially offers a unique erosion capability for the motorcase ascent environment at a very low cost per sample. It is recommended that a pilot program be initiated to calibrate this facility and to obtain preliminary erosion data. Following this program, the Bell facility should be used as the primary facility for screening motorcase materials and for the impact theory and erosion model development tests that fall within its range of capabilities. The SAI powder gun should be used as an alternate facility for this latter purpose and for other impact theory and erosion model development tests, particularly those requiring higher impact velocities. The DET is recommended for materials screening tests and for all tests of shroud metallic and composite materials. Rocket sleds are best suited for system and materials performance verification tests.

Finally, it is recognized that many other facilities are available for performing material erosion tests. The present study was limited in scope and therefore considered only those facilities believed to be of most interest for ascent flight erosion problems. Consideration of other test facilities, along with a more detailed examination of the facilities evaluated herein, can be accomplished at a later date if warranted by subsequent design studies and system performance analyses.

5.7 RECOMMENDATIONS FOR FUTURE TESTING

The following recommendations are made concerning erosion testing of MX motorcase insulation materials:

- More data should be obtained at velocities below 2,500 ft/sec. If these data are obtained in the DET, the particle cloud should be surveyed using holography.
- No data should be obtained at impact angles in excess of 20 degrees.
- DET models with wedge angles greater than 9 degrees should not be pre-heated. Higher dust concentrations should be used (since debris shielding has been found not to be a problem) to allow shorter test times and, thereby, lower surface temperatures.

REFERENCES

1. Lewis, H. F., et al., "Description and Calibration Results of the AEDC Dust Erosion Tunnel," AEDC-TR-73-74, May 1973.

2. Lewis, H. F., "DNA MX Material Evaluation Test," AEDC-TSR-78-P35, 20 September 1978.

3. Spangler, P. S., et al., "Advanced Booster Propulsion System Hardening Program Final Draft Report,"MDAC. Unpublished.

4. Zimmerman, A. W. and J. W. Nienberg, "Results of Dust Erosion Tests for MX Validation," TRW Vulnerability and Hardness Laboratory, 79.4735.9-02, January 1979.

5. Kong, S. J., "Interim Technical Report on Ranking of Shroud Alternate Materials," MDAC. Unpublished.

6. Spangler, P. S. (MDAC), personal communication with D. H. Smith (PDA), 13 February 1979.

7. Johnson, G. P. (MDAC), personal communication with D. H. Smith (PDA).

8. Dunn, J. E. (PDA), letter to Capt. A. T. Hopkins (DNA), 20 September 1979.

9. Schlichting, H., Boundary Layer Theory, McGraw-Hill, New York, New York, 1960.

10. Johnson, G. P., "DET/Track G Test Summary," Advanced Missile Flyout Survivability Programs Review," SAMSO/NAFB, 13-14 June 1979.

11. Spangler, P. S., "Advanced Booster Hardening Technology Program Fourth Monthly Progress Letter," DNA001-79-C-0135, June 1979.

12. "Advanced Booster Hardening Technology Program – Hardcopy of Viewfoils," MDAC, Contract DNA001-77-C-0135, 16 October 1979.

Blank

APPENDIX A

DATA

APPENDIX A

DATA

Erosion data for materials for four sections of an advanced missile vehicle were gathered. These sections are:

1. Extendible Nozzle Exit Cone (ENEC).
2. Motorcase.
3. Shroud.
4. Shroud nosetip.

To simplify cataloguing the many materials considered, the numbering system used by MDAC in Reference 3 has been adopted. The materials are identified by a four-digit number:

Digit	Meaning
1	Material Application: 1. ENEC 2. Motorcase 3. Shroud 4. Shroud nosetip
2	Base Material Number
3, 4	Material Variation Number

The material descriptions and data from the DET and pebble impact tests are given in Sections A1 through A4 for the four sections of the vehicle considered. The salvo particle impact data for all materials are given in Section A5.

A-1. ENEC MATERIALS

Two types of ENEC materials were tested: metals and carbon-carbons. The metal samples were all Nb1OHf, with the following coatings:

Sample	Coating
M1	None
M2	H_fO_2
M3	Silver-moly enriched silicide
M4	Aluminide
M5	Hafnium-modified silicide

The carbon-carbon materials were provided by Aerojet Solid Propulsion Company and the specimens were machined by MDAC.

DET test data for the ENEC materials are listed in the following tables. Sample thickness changes during testing are listed for the metal models, while the more conventional mass losses and mass loss ratios are listed for the carbon-carbon models.

Table A-1. ENEC metal model DET data.

MTL NO.	MTL NAME	REF.	RUN NO.	P_o (LB/IN^2)	h_o (BTU/LBM)	d_p μ	V_p (FT/SEC)	P_d (G/M^3)	θ (DEG)	t_{CA} (SEC)	t_D (SEC)	ΔS* (MILS)
M1	METAL	4	11	1000	1614	100	5400	0.53	15	45.47	4.55	0.25
										45.46	5.20	1.00
									30	6.54	5.60	-0.50
										6.21	5.42	0.25
M2									15	45.39	4.90	4.00
										45.39	4.90	3.25
									30	6.05	4.92	2.75
M3									15	45.16	5.06	3.25
										45.16	5.06	2.35
			11A	992	1509			0.56	30	6.44	4.90	2.50
										6.44	4.90	3.00
M4			12	1000	1678			0.51	15	10.96	4.60	2.30
										10.80	5.22	1.80
									30	0.39	4.98	-0.25
										0.38	5.01	-0.25
M5									15	10.40	4.79	1.42
										10.42	4.79	0.30
									30	0.33	4.60	1.20
										0.33	4.60	1.50

*NEGATIVE INDICATES THICKNESS GAIN

Table A-2. ENEC carbon-carbon model DET data.

MTL NO.	MTL NAME	REF.	RUN NO.	P_o (LB/IN^2)	h_o (BTU/LBM)	d_p μ	V_p (FT/SEC)	P_d (G/M^3)	θ (DEG)	t_{CA} (SEC)	t_D (SEC)	Δm (MILS)	G
A1	C-C	4	12	1000	1678	100	5400	0.51	15	10.31	4.67	6.062	2.94
												4.762	2.30
A2			13	992	1542			0.48		10.97	4.73	7.850	3.89
										10.95	5.03	5.176	2.42
A3										10.97	4.73	2.758	1.37
										10.95	5.03	2.639	1.24
A4										10.64	4.50	4.434	2.31
										10.70	4.75	4.352	2.15
A5										10.64	4.50	4.536	2.41
										10.48	4.20	4.490	2.53

Blank

A-2. MOTORCASE MATERIALS

Materials designed to protect the motorcase, as well as the Kevlar-epoxy motorcase material itself, are described in Tables A-3 through A-7. One series of DET tests evaluated VAMAC 25 models with gaps and holes. Figure A-1 shows the model geometries. Some pebble impact test models employed 2024 T-6 aluminum isogrid substrates. The isogrid panel was machined from a plate, resulting in a 0.038-inch thick skin stiffened by 0.5-inch deep by 0.064-inch thick ribs in a pattern of equilateral triangles, all having leg lengths of 3.5 inches.

Tables A-8 and A-9 list the DET test data, and Tables A-10 and A-11 list pebble impact data for the motorcase materials.

Table A-3. VAMAC materials.

REFERENCE NUMBER	OTHER DESIGNATIONS	RELATIVE PARTS BY WEIGHT[a]					VENDOR DESIGNATION FOR VAMAC BASE POLYMER	REINFORCEMENT	COMMENTS
		SPECIAL CARBON (4.16)[b]	CURING SYSTEM		CARBON BLACK				
			DPG (4.10)	MDA (4.11)	SAF (4.07)	SRF (4.08)			
2101A		0.0	2.5	0.75	0	55	VAMAC B-124 (4.04)	NONE	CHEMLOCK 402 PRIMER
2101B		0.0	2.5	0.75	0	55	VAMAC B-124	KEVLAR 49, STYLE 350	
2101C		0.0	2.5	0.75	0	55	VAMAC B-124	KEVLAR 49, STYLE 350	NO PRIMER
2102		0.0	2.5	0.75	15	20	VAMAC B-124	NONE	
2103		0.0	2.5	0.75	35	20	VAMAC B-124		
2104A		0.0	2.5	0.75	55	20	VAMAC B-124		
2104B		0.0	2.5	0.75	55	20	VAMAC B-124	KEVLAR FABRIC UNDER 0.25mm VAMAC	
2104C		0.0	2.5	0.75	55	20	VAMAC B-124	10 VOL % (18.5 WT %) KEVLAR FIBERS	
2104D		0.0	2.5	0.75	55	20	VAMAC B-124	10 VOL % (20.1 WT %) GRAPHITE FIBERS	
2105	VAMAC 15J	0.0	2.5	0.75	75	20	VAMAC B-124	NONE	
2106		0.0	4.0	1.25	35	20	VAMAC B-124		
2107		0.0	2.5	0.75	35	0	VAMAC VMX-5067 (4.05)		
2108		0.0	2.5	0.75	55	0	VAMAC VMX-5067		
2109		0.0	2.5	0.75	75	0	VAMAC VMX-5067		
2110		0.0	2.5	0.75	95	0	VAMAC VMX-5067		
2111		0.0	4.0	1.25	55	0	VAMAC VMX-5067		
2112		0.0	4.0	0.00	75	0	VAMAC VMX-5067		
2113		0.0	4.0	1.25	95	0	VAMAC VMX-5067		
2114	VAMAC [10-70][c]	453.0	2.5	0.75	0	20	VAMAC B-124		
2115	VAMAC [WC8-70][d]	424.3	2.5	0.75	0	20	VAMAC B-124		
2116	VAMAC 25	0.0	2.5	0.75	50	45	VAMAC B-124		
2116A	VAMAC 25 FOAM	0.0	2.5	0.75	50	45	VAMAC B-124		2/3 DENSE FOAM
2116B	VAMAC 25 FOAM	0.0	2.5	0.75	50	45	VAMAC B-124		1/2 DENSE FOAM
2116C	UNCURED VAMAC	0.0	2.5	0.75	50	45	VAMAC B-124		
2117		0.0	4.0	1.25	50	45	VAMAC B-124		

a. ALL FORMULATIONS CONTAIN 100 PARTS OF VAMAC BASE POLYMER PLUS FOUR PARTS OF PROCESSING AIDS SUPPLIED BY VENDOR.

b. NUMBERS IN PARENTHESES ARE COMPONENT REFERENCES IN TABLE A-7.

c. FIRST NUMBER IS WEIGHT PERCENTAGE OF CARBIDE LOADING IN SPECIAL CARBON PARTICLE. SECOND NUMBER IS VOLUME PERCENTAGE OF PARTICLES IN COMPOSITE.

d. WC8 REFERS TO A SPECIAL CARBON PARTICLE MADE BY CARBONIZING AND GRINDING TBR[6]. THE FINAL PRODUCT CONTAINS 8 WEIGHT-PERCENT METAL AND HAS A DENSITY OF 2.0 g/cm^3.

Table A-3. VAMAC materials - (Continued).

Materials tested in DET.

REFERENCE NUMBER	OTHER DESIGNATIONS	RELATIVE PARTS BY WEIGHT[a]									
		DPG (4.10)	MDA (4.11)	DIAk #1	DOTG (4.25)	MDM	ISAF (4.26)	FEF (4.27)	SAF (4.07)	SRF (4.08)	OTHER
2118		4		1.25				75		20	
2119		3		1.00				75		↓	
2120				1.25	4			75			
2121		2.5				0.75		75			
2122	VAMAC N-123	25.0	0.75								CABOSIL M57
2123		2.5	0.75				75				
2124	LOW RESISTIVITY VAMAC	2.5	0.75								75 N472
2125									40	35	
2126									30	25	
2127									?	20	XC-72
2128	FLAME RETARDANT VAMAC										

a. ALL FORMULATIONS CONTAIN 100 PARTS OF VAMAC BASE POLYMER PLUS FOUR PARTS OF PROCESSING AIDS SUPPLIED BY VENDOR.

b. NUMBERS IN PARENTHESES ARE COMPONENT REFERENCES IN TABLE A-7.

Table A-3. VAMAC materials - (Continued).
Materials tested in DET.

REFERENCE NUMBER	OTHER DESIGNATIONS	COMMENTS
2129	VAMAC 17	HEAVY DAMAGE
2130	VAMAC 28C	34.7 VOLUME PERCENT TBR
2131	VAMAC 28D	34.7 VOLUME PERCENT LC110
2132	VAMAC 18217-32LC	LOW CARBON
2133	15 PERCENT VAMAC SPONGE	
2134	25 PERCENT VAMAC SPONGE	
2135	VAMAC 25 HERCULES	
2136	VAMAC 32LC	100 PARTS VAMAC, 20 PARTS CARBON, 4 PARTS ADDITIVES
2137	MM2	MM2 - VAMAC - 151A
2138	MM3	MM3 - VAMAC - 151B
2139	MM4	MM4 - VAMAC - 151B
2140	MM1	HERCULES KEVLAR MM1 - VAMAC - 151A

Table A-4. Viton materials.

REFERENCE NUMBER	OTHER DESIGNATIONS	SPECIAL CARBON[b] (4.16)	CURING SYSTEM (DIAK #1) (4.09)	CARBON BLACK MT (4.06)	CARBON BLACK SAF (4.07)	CARBON BLACK SRF (4.08)	VENDOR DESIGNATION FOR VITON BASE POLYMER	REINFORCEMENT	COMMENTS
2201A		0.0	1.00	20	0	0	VITON B (4.02)	NONE	
2201B								KEVLAR 49, STYLE 350	
2202A		0.0	1.00	0	10	0	VITON B	NONE	
2202B								8.0 WT % CARBON FIBERS	
2202C								7.8 WT % KEVLAR 49 FIBERS	
2202D								8.6 WT % GRAPHITE FIBERS	
2203A	VITON B	0.0	1.00	0	20	0	VITON B	NONE	
2203B	VITON 2B	0.0	1.00	0	20	0	VITON B	KEVLAR FABRIC UNDER 0.25mm VITON	
2203C	VITON 2B	0.0	1.00	0	20	0	VITON B	10 VOL % KEVLAR FIBERS	
2203D	VITON 2B	0.0	1.00	0	20	0	VITON B		APPLIED OVER SPONGE
2204		0.0	1.00	0	30	0	VITON B	NONE	
2205		0.0	1.00	0	40	0	VITON B	↓	
2206		0.0	2.50	0	20	0	VITON B	↓	
2207A		0.0	1.25	15	0	0	VITON B-50 (4.03)	↓	
2207B		0.0	1.25	15	0	0	VITON B-50	KEVLAR 49, STYLE 350	APPLIED OVER AN EQUALLY THICK LAYER OF VITON [10-70]
2208A	VITON 2B12	0.0	1.00	0	10	10	VITON B	NONE	
2208B	VITON 2B12	0.0	1.00	0	10	10	VITON B	↓	
2208C	VITON FOAM	0.0	1.00	0	10	10	VITON B	↓	2/3 DENSE FOAM
2208D	VITON FOAM							↓	1/2 DENSE FOAM
2209		0.0	1.00	0	20	0	VITON B-50	↓	
2210	VITON [WC8-70][c]	278.0	1.00	0	0	0	VITON B	↓	
2211		0.0	1.00	0	10	10	VITON B-50	↓	
2212	VITON [10-70]	250.00	1.00	0	0	0	VITON B	↓	
2213	VITON [10-34.7]	57.5	1.00	0	0	0	VITON B	↓	

a. ALL FORMULATIONS CONTAIN 100 PARTS OF BASE POLYMER AND 15 PARTS OF MAGOLITE D (MgO) (PART OF CURING SYSTEM).

b. NUMBERS IN PARENTHESES ARE COMPONENT MATERIAL REFERENCES TO TABLE A-7.

c. SEE NOTE d TO TABLE A-3.

Table A-4. Viton materials - (Continued).

MATERIALS TESTED IN DET MARCH 1979		
REFERENCE NUMBER	OTHER DESIGNATION	COMMENTS
2214		100 VITON + 15 XC-72 (BY WEIGHT)
2215		100 VITON + 30 XC-72 (BY WEIGHT)
MATERIALS TESTED IN DET DECEMBER 1978		
2216		34.7 VOLUME PERCENT TBR
2217	VITON 28P	34.7 VOLUME PERCENT LC110
2218	VITON MOSITES	
PEBBLE IMPACT TEST MATERIALS FEB - APR 1979		
2219	WHITE VITON	

Table A-5. Tungsten-bearing resin (TBR) materials.

REFERENCE NUMBER	HITCO FORMULATION NUMBER	CURE TEMPERATURE K	REINFORCEMENT	COMMENTS
2301A	46-26	366	NONE	
2301B	46-26	366	KEVLAR 49 FABRIC, STYLE 350	
2302A	46-74	366	NONE	
2302B	46-74	366	GRAPHITE FABRIC, 200-400 MESH	
2303	46-74A	366	↓	
2304	46-74B	366		
2305	46-74	450		
2306A	51-006	366	NONE	
2306B	51-006	366	10.0 WT % KEVLAR 49 FIBERS	
2306C	51-006	366	NONE	10.0 WT % SAF CARBON BLACK
2307	58-79	339		
2308A	58-82	339		
2308B	58-82	339	10 PLIES KEVLAR 49 FABRIC, STYLE 350	
2308C	58-82	339	10 PLIES KEVLAR 49 FABRIC, STYLE 350 FABRIC PLIES CONCENTRATED AT TBR MID-PLANE	
2310	51-027	394	KEVLAR 49 FABRIC, STYLE 350	EPOXY RESIN ADDED
2311	51-027	394	NONE	EPOXY REPLACED WITH NBR
2312	51-027	394	KEVLAR 49 FABRIC, STYLE 350	EPOXY REPLACED WITH NBR

ALL MATERIALS PRODUCED BY HITCO, 1600 WEST 135th STREET, GARDENA, CA 90249 AND ARE 7.0 $\pm$ 0.5 WEIGHT PERCENT METAL.

Table A-5. Tungsten-bearing resin (TBR) materials (Continued).

Materials tested in DET.

REFERENCE NUMBER	OTHER DESIGNATION	COMMENTS
2313	TBR 3 (504N-54)	HITCO ADVANCED EPS MATERIAL
2314	TBR 3 (504N-55)	↓
2315	TBR 3 (504N-56)	
2316	TBR 3 (504N-57)	

Table A-6. Other materials.

REFERENCE NUMBER	OTHER DESIGNATIONS	RELATIVE PARTS BY WEIGHT			REINFORCEMENT	COMMENTS
2001	KEVLAR-EPOXY MOTORCASE	HRBF-241 RESIN: 100	RD-2 RESIN 14	TONOX 6040 CURING AGENT 17	KEVLAR 49	CUT FROM ADP MOTORCASE FABRICATED BY HERCULES, INC.
2401	NBR	CARBON		49.0		BUTADIENE ACRYLO-NITRILE ELASTOMERIC COMPOUND MADE BY B. F. GOODRICH ACCORDING TO TO U. S. AIR FORCE SPECIFICATION 67A60754 (VENDOR DESIGNATION 72-069).
		HYDROGEN		6.1		
		NITROGEN		4.2		
		OXYGEN		21.1		
		SULPHUR		1.6		
		SILICON		9.7		
		SODIUM		0.2		
		ZINC		2.1		
		TITANIUM		6.0		
2601	ALUMINUM					2024-T6

Table A-6. Other materials - (Continued).

MATERIALS TESTED IN DET		
REFERENCE NUMBER	OTHER DESIGNATION	COMMENTS
2002	KEVLAR-EPOXY MOTORCASE	STAGE 3 MOTORCASE MATERIAL
2402	NBR 68	
2403	NBR 69	
2404	NBR-19709-6A (60/40)	
2405	NBR-19709-6B (75/25)	
2406	NBR-19707-7 020 VINYL	
2501	KPN	ROCKETDYNE
2502	HERCULES	KEVLAR 49 FIBERS PERPENDICULAR TO FLOW
2503	HERCULES DOME	LARGE STRIPWRAP
2504	AEROJET INNER	INNER PLY HELICAL WRAP
2505	AEROJET OUTER	OUTER PLY
2506	ROCKETDYNE	
2507	MM5	MM5-ROYACRIL 930 USCM 252
2508	HERCULES KEVLAR	
2509	ROYACRIL 25	ROYACRIL #25 19709-13
2510	EPDM 1	EPDM NECP-19709-9A (80/20)
2511	EPDM 2	EPDM-19709-2B
PEBBLE IMPACT TEST MATERIALS		
2132	LOW CARBON LOADING VAMAC	
2133	VAMAC SILICA	CARBON REPLACED BY 95 PARTS CABOSIL MS-7-4 PER 100 PARTS VAMAC

Table A-7. Material constituents.

REFERENCE NUMBER	DESCRIPTION	SOURCE
4.01	NBR (Nitrile butadiene rubber)	B. F. Goodrich Aerospace and Defense Products 500 South Main Street Akron, Ohio 44318 per Air Force Specification 67A60754
4.02	Viton B (Ethylene acrylic elastomer)	DuPont Company Elastomer Chemical Department Wilmington, Delaware 19898
4.03	Viton B-50	Same as Viton B
4.04	VAMAC B-124	Same as Viton B
4.05	VAMAC VMX 5067	Same as Viton B
4.06	MT-NS Carbon black	R. T. Vanderbilt Company 30 Winfield Street East Norwalk, Connecticut 06855
4.07	SAF Carbon black (Vulcan 9)	Cabot Corporation Carbon Black Division Boston, Massachusetts 02110
4.08	SRF Carbon black (Sterling S-1)	Same as SAF Carbon black
4.09	Diak #1	Same as Viton B
4.10	DPG (Diphenylquanidine)	Same as Viton B
4.11	MDA (Methyl dianiline)	Same as Viton B
4.12	MgO (Magolite D)	C. P. Hall Company 444 Alaska Avenue Torrance, California 90503
4.13	Kevlar-epoxy motorcase segments	Hercules Incorporated Systems Group Post Office Box 98 Magna, Utah 84044
4.14	Graphite-epoxy	McDonnell Douglas Astronautics Company 5301 Bolsa Avenue Huntington Beach, California 92647
4.16	Special carbon LC10, LC20, LC37	Celanese Research Post Office Box 1000 Summit, New Jersey 07901

Table A-7. Material constituents - (Continued).

REFERENCE NUMBER	DESCRIPTION	SOURCE
4.17	Carbon Fiber "High Modulus Reinforcing Carbon, Type II"	Modmor Morgan Morganite Modmore, Ltd. Buttersea Church, London, England
4.18	Graphite fiber KGF 200, CF-01	Kureha Carbon Fiber Kureha Chemical Industry Company, Ltd. Tokyo, Japan
4.19	Kevlar 49 CS 800 finish	Fiberglass Reinforcements, Inc. 14530 South Anson Santa Fe Springs, California 90670
4.20	Chemlock C-328 bond	Hughson Chemicals Division of Lord Corporation Erie, Pennsylvania
4.21	Bostik 1142 adhesive	Bostik Division USM Corporation Boston Street Middleton, Maine
4.22	Bostik 1107P primer	Same as Bostik 1142
4.23	PVF (Polyvinyl formal)	---
4.24	EpNor (Epoxy noralac)	---
4.25	DOTG (diorthotolylguanidine)	---
4.26	ISAF Carbon black (ASTM designation N220)	---
4.27	FEF Carbon black (ASTM designation N550)	---

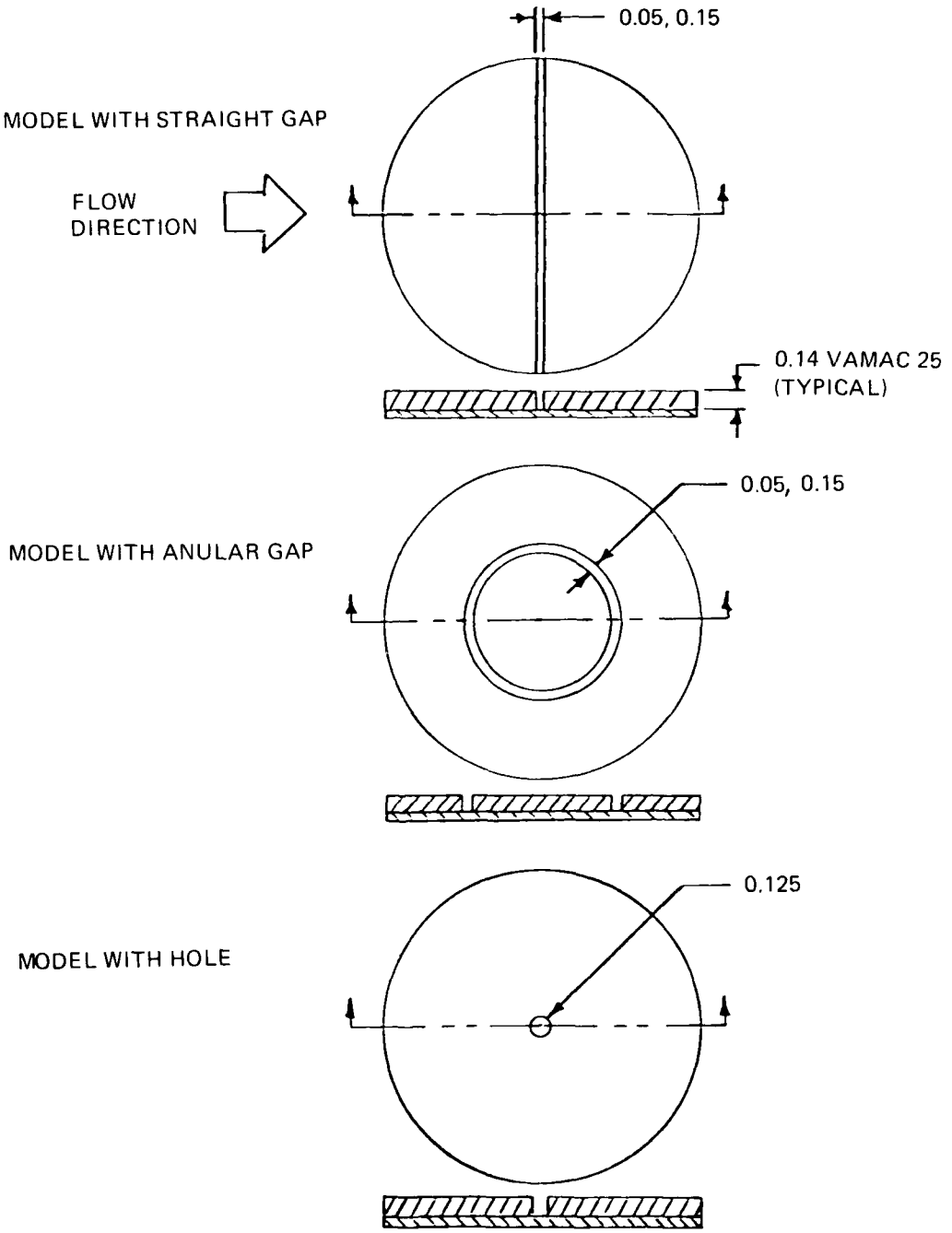

Figure A-1. DET models with gaps and holes.

Table A-8. DET notes.

1	– QUESTIONABLE – TARE SAMPLES IN RUN 3 CHARRED AND LOST SUBSTANTIAL MASS IN 20 SECONDS.
2	– QUESTIONABLE – HIGH MASS LOSS.
3	– QUESTIONABLE – MASS LOST DURING CLEAR AIR TIME (LAYERS PEELED OFF BY SHEAR/AEROHEATING).
4	– QUESTIONABLE – FRONT EDGE OF RETAINER MATERIAL PEELED UP SO AS TO SHIELD SAMPLE.
5	– SAMPLE DIAMETER QUESTIONABLE DUE TO EROSION/THERMAL DEGRADATION AROUND EDGE OF 2-INCH DISC.
6	– QUESTIONABLE – HIGH MASS LOSS AND ERODED THROUGH.
7	– SPECIMEN WAS A TRAPEZOID RATHER THAN A 2-INCH DISC SURROUNDED BY A TRAPEZOIDAL RETAINER. G VALUES MAY BE HIGH DUE TO EDGE EFFECTS.
8	– PRE-DAMAGED SPECIMEN.
9	– QUESTIONABLE – RESULTS INCONSISTENT WITH OTHER RESULTS FOR RUN.
10	– SINGLE LAYER LOST DURING CLEAR AIR TIME.
11	– QUESTIONABLE – LAYERS BEGAN PEELING OFF BEFORE MODEL WAS ON CENTERLINE.
12	– MASS LOSS CALCULATED FOR 2.00-DIAMETER SPECIMEN.
13	– NO HOLOGRAPHIC CALIBRATION FOR THIS CONDITION. NOMINAL PARTICLE SITE AND PARTICLE VELOCITY CALCULATED BY AEDC LISTED.
14	– EROSION FOR ALL MODELS ON THIS RUN APPROXIMATELY HALF THAT SEEN ON OTHER RUNS.

Table A-9. Motorcase material DET data.

MTL NO.	MTL NAME	REF.	RUN NO.	P_o (LB/IN^2)	h_o (BTU/LBM)	d_p μ	V_p (FT/SEC)	P_d (G/M^3)	θ (DEG)	t_{CA} (SEC)	t_D (SEC)	Δm (G)	G	NOTES
2001	KEVLAR MOTOR-CASE	4	8	996	505	94	4125	0.559	9	25.15	30.1	6.380	0.984	
									9	25.15	30.1	6.720	1.05	
									14	15.65	10.05	4.640	1.39	
									14	15.25	10.45	4.414	1.29	
			10	992	511	438	2950	0.649	4	15.71	15.29	0.524	0.498	
										15.80	15.40	0.163	0.158	4
			10A	1000	492			0.596	9	25.48	20.28	4.042	1.40	
												4.721	1.65	
			10	992	511			0.649	14	15.71	15.29	4.56	1.24	
										15.80	15.40	5.278	1.47	
			12	300	486		2140	0.695	9	0.38	40.60	3.700	0.888	
												3.326	0.802	
									14		14.90	2.179	0.948	
										0.40	15.15	2.486	1.04	
			14	1000	484		2950	0.561	9	17.53	20.60	4.583	1.68	
									14	9.57	10.34	3.817	1.81	

Table A-9. Motorcase material DET data - (Continued).

MTL NO.	MTL NAME	REF.	RUN NO.	P_o (LB/IN^2)	h_o (BTU/LBM)	d_p μ	V_p (FT/SEC)	P_d (G/M^3)	θ (DEG)	t_{CA} (SEC)	t_D (SEC)	$\dot{a}_m$ (G)	G	NOTES
2002	KEVLAR MOTOR-CASE	7	4	1000	583	438	2950	0.54	14	15	40	11.13	1.168	12
									4	15	40	1.73	0.630	
									9	20	31	5.93	1.243	
									20	2	5.5	3.83	2.070	
									4	2	5.5	0.56	1.495	
									30	0	2.46	3.00	2.48	
									30	0	2.46	2.82	2.33	
									9	10	31	5.27	1.104	
									9	10	31	5.79	1.213	
									14	0	8.97	2.62	1.226	
									4	0	8.97	0.44	0.718	
									14	15	31	10.34	1.401	
									4	15	31	0.99	0.472	
									9	0	20.67	3.02	0.949	

Table A-9. Motorcase material DET data - (Continued).

MTL NO.	MTL NAME	REF.	RUN NO.	P_o (LB/IN^2)	h_o (BTU/LBM)	d_p μ	V_p (FT/SEC)	P_d (G/M^3)	θ (DEG)	t_{CA} (SEC)	t_D (SEC)	Δm (G)	G	NOTES
2101A	VAMAC	1	5	1000	552	438	2950	0.633	9.0	10	30	2.47	0.56	12
2101A	↓		6A	1006	493			1.115				4.27	0.55	
2101B	Ke/VAMAC		5	1000	552			0.633				3.35	0.76	
2101B			6A	1006	493			1.115				3.65	0.47	
2101C			5	1000	552			0.633				3.97	0.90	
2101C			6A	1006	493			1.115				6.29	0.81	
2102	VAMAC		10	1000	472			0.577				2.09	0.52	
2103												1.45	0.36	
2104A												1.49	0.37	
2105	VAMAC 15J											0.88	0.22	
			14A	999	506			0.581			15	0.49	0.24	
			20	995	449			0.621	8.5			0.45	0.22	
		4	7	298	514		2140	0.666	30	0.38	10.88	1.493	0.463	
												1.203	0.368	
			14	1000	484		2950	0.561	9	17.71	19.95	0.803	0.327	
									30	0.41	5.25	2.939	1.41	
			13	998	461	54	4125	1.32	4	16.02	5.20	0.146	0.128	
											5.60	0.080	0.065	
									9	25.40	15.27	2.900	0.382	
												2.264	0.299	
									14	16.02	5.20	5.461	1.35	9
											5.60	6.028	1.38	
									30	7.56	3.74	5.449	0.913	
												5.181	0.868	

Table A-9. Motorcase material DET data - (Continued).

MTL NO.	MTL NAME	REF.	RUN NO.	P_o (LB/IN^2)	h_o (BTU/LBM)	d_p μ	V_p (FT/SEC)	P_d (G/M^3)	θ (DEG)	t_{CA} (SEC)	t_D (SEC)	Δm (G)	G	NOTES
2105	VAMAC 15J	4	5 (pt.1)	1000	441	94	4125	0.658	4	30.78	10.03	0.256	0.233	
			5 (pt.2)	999	501					30.59	10.85	0.240	0.200	
									9	50.11	30.70	3.976	0.524	
												4.295	0.570	
			5 (pt.1)	1000	441				14	30.78	10.03	3.127	0.811	
			5 (pt.2)	999	501					30.59	10.85	3.194	0.767	
			4	1000	470	438	2950	0.682	4	30.84	15.29	0.063	0.059	
										30.0	15.56	0.155	0.144	
			4A	998	414			0.601	9	50.05	19.99	1.215	0.444	
												1.187	0.438	
			4	1000	470			0.682	14	30.84	15.29	2.672	0.726	
										30.0	15.56	2.762	0.734	
			4A	998	414			0.601	30	15.34	5.81	6.257	2.43	1
												6.351	2.45	1
			7	298	514		2140	0.666	4	0.38	20.21	0.027	0.033	
										0.35	20.61	0.011	0.013	
									9	0.37	40.40	0.493	0.132	
												0.427	0.114	
									14	0.38	20.21	0.403	0.139	
										0.35	20.61	0.469	0.160	
2106	VAMAC	2	10	1000	472		2950	0.577	9.0	10	30	3.53	0.88	12
2107												1.20	0.30	12

Table A-9. Motorcase material DET data - (Continued).

MTL NO.	MTL NAME	REF.	RUN NO.	P_o (LB/IN^2)	h_o (BTU/LBM)	d_p	V_p (FT/SEC)	P_d (G/M^3)	θ (DEG)	t_{CA} (SEC)	t_D (SEC)	a_m (G)	G	NOTES
2108	VAMAC	1	10	1000	472	438	2950	0.577	9	10	30	2.28	0.57	12
2109			11	510				0.525				1.53	0.42	
2110			10	472				0.577				1.49	0.37	
2111	VAMAC 27		11	510				0.525				0.91	0.25	
2111	VAMAC 27		20	995	449			0.621	8.5		15	0.49	0.24	
2112	VAMAC								9			0.54	0.25	
2113	VAMAC											0.73	0.34	
2114	VAMAC 10-70											0.80	0.37	
2115	VAMAC WC8-70											0.89	0.41	
2116	VAMAC 25											0.37	0.17	
												0.41	0.19	
		7	1	988	472			0.491	14	15	40.23	5.23	0.60	
									4	15	40.23	0.186	0.074	
									9	20	31.04	1.26	0.29	
			2	1000	490	200	3100	2.94	20	0.35	2.2	2.16	0.51	12,13
									4	0.35	2.2	0.033	0.038	
									9	0.35	3.7	0.53	0.164	
									9	10.0	5.75	1.31	0.26	
									9	10.0	5.75	1.16	0.23	
									14	0.4	2.55	1.34	0.39	
									4	0.4	2.55	0.044	0.044	
									14	15.0	6.0	4.58	0.56	
									30	1.6	2.0	3.94	0.70	
									30	1.6	2.0	3.71	0.66	

Table A-9. Motorcase material DET data - (Continued).

MTL NO.	MTL NAME	REF.	RUN NO.	P_o (LB/IN^2)	h_o (BTU/LBM)	d_p	V_p (FT/SEC)	P_d (G/M^3)	θ (DEG)	t_{CA} (SEC)	t_D (SEC)	Δm (G)	G	NOTES
2116	VAMAC 25	7	5	994	522	438	2950	0.561	8.5	0.30	20.78	0.41	0.132	12
			5	994	522			0.561	9	0.29	20.55	0.51	0.155	
			6	982	508			0.461	9	0.30	21.16	0.50	0.179	
			6	982	508			0.461	8.5	0.31	20.72	0.38	0.146	
	VAMAC 25 0.05 STR. GAP		1	990	463			0.503	9	10.0	12.0	0.40	0.23	
	VAMAC 25			988	472			0.491	20	2	5.26	0.76	0.47	
									4	2	5.26	0.020	0.061	
									30	0	5.18	3.11	1.34	
									30	0	5.18	2.90	1.25	
									11	10	30.64	1.83	0.35	
									7	10	30.64	0.74	0.22	
									14	0	30.69	3.66	0.55	
									4	0	30.69	0.115	0.060	
									14	15	31.17	3.98	0.59	
									4	15	31.17	0.13	0.067	
									9	20	20.30	0.50	0.175	
			2	1000	490	200	3100	2.94	14	15	7.0	6.39	0.67	12,13
									4	15	7.0	0.20	0.074	
									9	20	5.7	1.21	0.24	
	VAMAC 25 0.05 STR. GAP		1	990	463	438	2950	0.503	9	10.0	12.0	0.40	0.23	12
	VAMAC 25 0.15 STR. GAP											0.48	0.28	

Table A-9. Motorcase material DET data - (Continued).

MTL NO.	MTL NAME	REF.	RUN NO.	P_o (LB/IN^2)	h_o (BTU/LBM)	d_p μ	V_p (FT/SEC)	P_d (G/M^3)	θ (DEG)	t_{CA} (SEC)	t_D (SEC)	Δm (G)	G	NOTES
2116	VAMAC 25 0.15 GAP	7	1	990	463	438	2950	0.503	8.5	10.0	12.0	0.46	0.28	12
	VAMAC 25 0.05 ANN. GAP								9			0.45	0.26	
	VAMAC 25 0.05 ANN. GAP											0.38	0.22	
	VAMAC 25 0.15 ANN. GAP											0.52	0.30	
	VAMAC 25 0.15 ANN. GAP											0.43	0.25	
	VAMAC 25 0.125 HOLE		2	980	491			0.582				0.60	0.30	
	VAMAC 25 0.125 HOLE											0.46	0.23	
	VAMAC 25	12	7	1000	472			0.386		0.31	21.12	0.274	0.118	
			7	1000	472			0.386		0.31	20.70	0.280	0.123	
			8	986	460			0.461		0.30	21.11	0.558	0.201	
			8	986	460			0.461	8.5	0.28	21.53	0.471	0.176	
	0.04 VAMAC 25 0.01 SPONGE		9	990	465			0.433	9	0.31	20.76	0.528	0.206	
										0.31	20.76	0.610	0.238	
	VAMAC 25									0.30	21.16	0.473	0.181	
									8.5	0.31	20.60	0.514	0.214	

Table A-9. Motorcase material DET data - (Continued).

MTL NO.	MTL NAME	REF.	RUN NO.	P_o (LB/IN^2)	h_o (BTU/LBM)	d_p	V_p (FT/SEC)	P_d (G/M^3)	α (DEG)	t_{CA} (SEC)	t_D (SEC)	Δm (G)	S	NOTES
2116	VAMAC 25	12	12	1000	458	1000	2100	0.863	4	10.15	10.59	0.036	0.044	12
									9	10.66	20.69	0.912	0.252	
									4	10.59	10.55	0.049	0.060	
									20	0.28	5.85	1.040	0.464	
									4		5.85	-0-	-0-	
									12		11.13	0.544	0.210	
									6		11.13	0.153	0.105	
									15		10.17	1.238	0.420	
									15		10.17	1.076	0.365	
									9	0.23	6.49	0.121	0.106	
									9	0.23	6.49	0.086	0.076	
			13	1000	598	438	2950	2.14	9	0.24	4.24	0.442	0.171	
									9	0.22	4.36	0.599	0.225	
									4	0.24	3.02	0.005	0.006	
									14	0.24	2.85	1.200	0.446	
									4	0.22	2.71	0.014	0.019	
									20	0.24	2.63	3.56	1.013	
									15	0.26	3.57	2.45	0.679	
									30	0.23	2.51	6.21	1.268	
			14	996	491			2.30	15	9.86	3.68	2.37	0.594	
									9	10.87	5.12	1.07	0.318	
									15	10.47	3.44	2.59	0.693	
									6	0.26	4.84	0.210	0.099	
									12	0.26	4.84	2.27	0.538	
									9	0.20	4.75	0.601	0.192	
									9	0.20	4.75	0.642	0.206	

AD-A090 216 PROTOTYPE DEVELOPMENT ASSOCIATES INC SANTA ANA CA F/G 21/8
DUST EROSION PERFORMANCE OF CANDIDATE MOTORCASE THERMAL PROTECT--ETC(U)
MAR 80 D H SMITH DNA001-79-C-0179
UNCLASSIFIED PDA-TR-1473-00-05 DNA-5286F NL

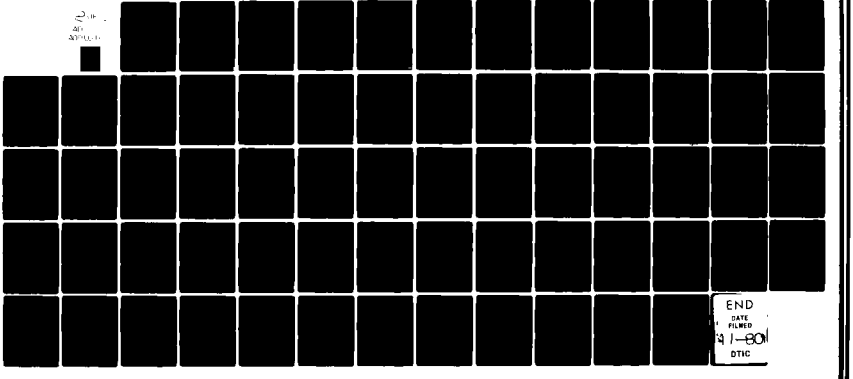

END
DATE FILMED
9-80
DTIC

Table A-9. Motorcase material DET data - (Continued).

MTL NO.	MTL NAME	REF.	RUN NO.	P_o (LB/IN^2)	h_o (BTU/LBM)	d_p μ	V_p (FT/SEC)	P_d (G/M^3)	θ (DEG)	t_{CA} (SEC)	t_D (SEC)	Δm (G)	G	NOTES
2116	VAMAC 25	12	14	996	491	438	2950	2.30	20	0.32	4.09	5.70	0.971	12
									15	0.25	3.59	1.68	0.431	
									15	0.25	3.59	1.53	0.393	
			18	976	492			0.569	9	0.21	20.33	0.835	0.253	
			18	976	492			0.569		0.26	10.47	0.365	0.215	
			19	994	513			3.40		0.25	5.77	1.31	0.234	
2117		1	20	995	449			0.621		10	15	0.43	0.20	
2117		1	20	995	449			0.621		10	15	0.43	0.20	
2118		7	5	994	522			0.561		0.27	20.43	0.44	0.135	
2118										0.27	20.43	0.50	0.153	
2119										0.29	20.95	0.47	0.139	
2119										0.29	20.95	0.43	0.129	
2120										0.29	20.55	0.59	0.180	
2120									8.5	0.30	20.78	0.46	0.146	
2121									9	0.29	20.75	0.45	0.136	
2121									8.5	0.27	20.96	0.43	0.135	
2122	VAMAC N-123								9	0.29	20.75	0.48	0.145	
2122	VAMAC N-123								8.5	0.27	20.96	0.41	0.128	
2123	VAMAC								9	0.28	21.03	0.52	0.154	
2123	VAMAC									0.28	21.03	0.60	0.177	
2124	LO RESIS. VAMAC									0.27	20.76	0.58	0.176	
2124	LO RESIS. VAMAC									0.27	20.76	0.63	0.189	

Table A-9. Motorcase material DET data - (Continued).

MTL NO.	MTL NAME	REF.	RUN NO.	P_o (LB/IN^2)	h_o (BTU/LBM)	d_p μ	V_p (FT/SEC)	P_d (G/M^3)	θ (DEG)	t_{CA} (SEC)	t_D (SEC)	Δm (G)	G	NOTES
2125	VAMAC	7	9	990	463	438	2950	0.503	9	10.0	12.0	0.32	0.185	12
2125												0.38	0.223	
2126												0.47	0.274	
2126												0.37	0.217	
2127			6	982	508			0.461		0.30	20.84	0.44	0.160	
2127									8.5		21.24	0.47	0.180	
2128	FLAME RET. VAMAC								9		20.81	0.56	0.205	
2128	FLAME RET. VAMAC								8.5		21.24	0.49	0.187	
2129	VAMAC 17		2	980	491			0.582	9	10.0	12.0	0.50	0.252	
2130	VAMAC 28C											0.75	0.375	
2130	VAMAC 28C											0.81	0.405	
2131	VAMAC 28D											0.67	0.337	
2131	VAMAC 28D											0.62	0.310	
2132	VAMAC	12	7	1000	472			0.386	4	0.40	20.74	0.017	0.017	12,14
									20	0.40	20.74	3.44	0.689	
									9	0.30	20.92	0.322	0.140	
									15	0.31	20.72	1.98	0.525	
			9	990	465			0.433	9	0.31	20.23	0.587	0.235	12
									9	0.31	20.36	0.588	0.234	

Table A-9. Motorcase material DET data - (Continued).

MTL NO.	MTL NAME	REF.	RUN NO.	P_o (LB/IN^2)	h_o (BTU/LBM)	d_p μ	V_p (FT/SEC)	P_d (G/M^3)	θ (DEG)	t_{CA} (SEC)	t_D (SEC)	Δm (G)	G	NOTES
2133	15% VAMAC SPONGE	12	9	990	465	438	2950	0.433	9	0.30	21.16	0.651	0.249	12
2133	15% VAMAC SPONGE									0.31	20.39	0.609	0.242	
2134	25% VAMAC SPONGE									0.31	20.39	0.549	0.218	
2134	25% VAMAC SPONGE									0.31	20.23	0.635	0.254	
2135	VAMAC 25 HERC.									0.30	20.83	1.42	0.552	
2136	VAMAC 32 LC		13	1000	598			2.14		0.24	4.24	0.652	0.252	
										0.22	4.36	0.836	0.314	
									14	0.24	3.02	1.94	0.680	
									4	0.24	2.85	0.002	0.003	
									20	0.22	2.71	2.82	0.780	
									4	0.24	2.63	0.019	0.027	
									15	0.26	3.57	2.68	0.745	
									30	0.23	2.51	>6.21	>1.268	
			18	976	492			0.569	14	10.21	40.41	6.93	0.683	
									4	10.21	40.41	1.56	0.533	
									6	15.36	40.66	0.772	0.175	
									12	15.36	40.66	7.14	0.814	

Table A-9. Motorcase material DET data - (Continued).

MTL NO.	MTL NAME	REF.	RUN NO.	P_o (LB/IN^2)	h_o (BTU/LBM)	d_p μ	V_p (FT/SEC)	P_d (G/M^3)	θ (DEG)	t_{CA} (SEC)	t_D (SEC)	Δm (G)	G	NOTES
2136	VAMAC 32 LC	12	18	976	492	438	2950	0.569	9	0.21	20.33	1.27	0.386	12
									30	0.22	2.54		2.125	
									30	0.22	2.54	2.41	1.830	
									20	0.24	2.90	1.21	1.180	
									4	0.24	2.90	0.006	0.029	
									9	0.26	10.47	0.625	0.368	
									14	39.90	41.00	11.38	1.106	
									4	39.90	41.00	0.026	0.091	
									14	0.26	3.48	0.734	0.841	
									4	0.26	3.48	0.008	0.032	
			19	994	513			3.40	14	30.29	4.67	5.32	0.760	
									4	30.29	4.67	0.123	0.061	
									6	20.15	5.00	0.716	0.221	
									12	20.15	5.00	5.67	0.880	
									9	10.22	5.79	2.67	0.475	
									9	10.22	5.79	1.82	0.325	
									30	0.24	2.95	BURN	THRU	
									30	0.24	2.95	BURN	THRU	
									20	0.20	3.19	4.52	0.669	
									4	0.20	3.19	0.044	0.032	
									9	0.25	5.77	1.96	0.351	
									14	10.34	6.33	6.72	0.708	
									4	10.34	6.33	0.153	0.056	
									14	0.24	3.72	3.66	0.657	
									4	0.24	3.72	0.066	0.041	

Table A-9. Motorcase material DET data - (Continued).

MTL NO.	MTL NAME	REF.	RUN NO.	P_o (LB/IN^2)	h_o (BTU/LBM)	d_p μ	V_p (FT/SEC)	P_d (G/M^3)	θ (DEG)	t_{CA} (SEC)	t_D (SEC)	Δm (G)	G	NOTES
2137	MM2	12	7	1000	472	438	2950	0.386	9	0.31	20.52	0.307	0.136	12
2138	MM3										21.00	0.356	0.154	
2139	MM4										20.88	0.317	0.138	
2140	MM1										20.88	0.299	0.130	
2201A	VITON	1	5		552			0.633		10	30	1.45	0.33	
			6A		493			1.115				1.71	0.22	
			10		472			0.577				1.33	0.33	
2201B	Ke/VITON		5		552			0.633				5.90	1.34	
			6A	1006	493			1.115				6.67	0.86	
			11		510			0.525				3.07	0.84	
2202A	VITON		10		472			0.577				1.41	0.34	
2202B	C/VITON		15		506			0.600			15	0.52	0.25	
2202C	Ke/VITON											0.56	0.27	
2202D	G/VITON											0.58	0.28	
2203	VITON 2B		10		472			0.577			30	0.92	0.23	
2203	VITON 2B		15		506			0.600			15	0.46	0.22	
2203D	VITON 2B	7	2	980	491			0.582			12	0.31	0.154	
	VITON 2B LT SCUFF											0.61	0.306	
	VITON 2B HEAVY DAMAGE											0.50	0.251	
2204	VITON		10	1000	472			0.577			30	0.96	0.24	
2205	VITON		10	1000	472			0.577			30	1.00	0.25	

Table A-9. Motorcase material DET data - (Continued).

MTL NO.	MTL NAME	REF.	RUN NO.	P_o (LB/IN^2)	h_o (BTU/LBM)	d_p μ	V_p (FT/SEC)	P_d (G/M^3)	θ (DEG)	t_{CA} (SEC)	t_D (SEC)	Δm (G)	G	NOTES
2206	VITON	1	10	1000	472	438	2950	0.577	9	10	30	2.09	0.52	12
2207A	VITON		11		510			0.525				1.43	0.39	
2207B	Ke/VITON		11		510			0.525				3.80	1.04	
2208	VITON 2312		14A	999	506			0.581			15	0.32	0.16	
			20	995	449			0.621	8.5		15	0.27	0.13	
		7	3	980	551			0.438	14	14	40.85	3.55	0.45	
									4	14	40.85	0.125	0.055	
									9	20	31	0.678	0.175	
									20	2	5.5	0.674	0.449	
									4	2	5.5	0.009	0.030	
									30	0.3	2.55	1.11	1.087	
									30	0.3	2.55	1.02	1.005	
									9	10	31	0.75	0.194	
									9	10	31	0.67	0.173	
			3 (3-79)						14	0.3	8.95	0.45	0.258	
									4	0.3	8.95	0.025	0.051	
									14	14.4	30.3	2.83	0.484	
									4	14.4	30.3	0.088	0.052	
									9	0.3	21.2	0.34	0.129	
2209	VITON	1	14A	999	506			0.581		10	15	0.38	0.19	
2210	VITON WC8-70		20	995	449			0.621				1.38	0.64	
2211	VITON		20	995	449			0.621				0.39	0.18	

Table A-9. Motorcase material DET data - (Continued).

MTL NO.	MTL NAME	REF.	RUN NO.	P_o (LB/IN^2)	h_o (BTU/LBM)	d_p μ	V_p (FT/SEC)	P_d (G/M^3)	θ (DEG)	t_{CA} (SEC)	t_D (SEC)	Δm (G)	G	NOTES
2214	VITON	7	6	982	508	438	2950	0.461	9	0.27	20.4	0.31	0.114	12
2214										0.30	20.75	0.40	0.147	
2215										0.30	20.84	0.37	0.135	
2215										0.30	20.75	0.39	0.142	
2216			1	990	463			0.503	8.5	10	12	0.38	0.234	
2216			1	990	463			0.503	8.5	10	12	0.38	0.234	
2217	VITON 28P		2	980	491			0.582	9	10	12	0.57	0.284	
2217	VITON 28P		2	980	491			0.582	9	10	12	0.48	0.243	
2218	VITON MOSITES		4	998	447			0.694	8.5	17	12	0.74	0.330	
2218	VITON MOSITES		4	998	447			0.694	8.5	17	12	1.08	0.480	
2301A	TBR 6	1	5	1000	552			0.633	9	10	30	5.11	1.16	
2301A	TBR 6		6A	1006	493			1.115				7.99	1.03	
2301B	Ke/TBR 6		5	1000	552			0.633				3.79	0.86	
2301B	Ke/TBR 6		6A	1006	493			1.115				6.67	0.86	
2302B	G/TBR 6		10	1000	472			0.577				3.05	0.76	
2302A	B/TBR 6		11		510			0.525				2.48	0.68	
2302A	TBR 6											3.14	0.86	
2303												3.14	0.86	
2305												3.40	0.93	
2306B	Ke/TBR 6		16	1008	505			0.559			15	1.25	0.64	
2306C	C/TBR 6		16	1008	505			0.559			15	1.71	0.88	

Table A-9. Motorcase material DET data - (Continued).

MTL NO.	MTL NAME	REF.	RUN NO.	P_o (LB/IN^2)	h_o (BTU/LBM)	d_p μ	V_p (FT/SEC)	P_d (G/M^3)	θ (DEG)	t_{CA} (SEC)	t_D (SEC)	Δm (G)	G	NOTES
2310	TBR	4	5 (pt.2)	999	501	94	4125	0.658	4	30.39	10.46	0.695	0.600	
									4	30.21	10.54	1.407	1.21	
									9	50.33	30.93	8.974	1.17	
									13	30.39	10.46	6.131	1.64	10
									13	30.21	10.54	6.141	1.63	
			4A	998	414	438	2950	0.601	4	30.42	15.24	1.315	1.39	
									4	30.26	15.19	0.390	0.412	
									9	50.32	20.62	4.444	1.54	
									13	30.42	15.24	5.321	1.74	
									13	30.26	15.19	5.853	1.90	
			7	298	514		2140	0.666	4	0.38	20.24	0.035	0.040	
									9	0.38	40.43	3.496	0.894	
									9	0.38	40.43	2.946	0.749	
									13	0.38	20.24	2.572	0.905	
									30	0.38	10.37	4.909	1.528	
									30	0.38	10.37	6.980	2.162	11
			14	1000	484		2950	0.561	4	9.93	15.55	0.931	1.03	
									9	17.71	19.95	4.838	1.87	
									13	9.93	15.55	4.492	1.54	
2311			11		516			0.530	4	15.45	15.25	0.102	0.121	
									9	25.09	15.46	1.269	0.661	
									13	15.45	15.25	3.683	1.36	

Table A-9. Motorcase material DET data - (Continued).

MTL NO.	MTL NAME	REF.	RUN NO.	P_o (LB/IN^2)	h_o (BTU/LBM)	d_p μ	V_p (FT/SEC)	P_d (G/M^3)	θ (DEG)	t_{CA} (SEC)	t_D (SEC)	Δm (G)	G	NOTES
2312	TBR	4	11	1000	516	438	2950	0.530	4	15.53	15.10	0.071	0.085	
									9	25.09	15.46	2.043	1.06	
									13	15.53	15.10	3.292	1.22	
2313	TBR 3	7	6	982	508			0.461	9	0.30	20.81	0.95	0.349	12
2314									8.5	0.31	20.72	0.93	0.360	
2315									9	0.30	20.69	0.88	0.322	
2316										0.30	20.69	0.93	0.342	
2401	NBR	5	17	1000	500	94	4125	0.60		0	15	2.05	0.570	NEW,12
												2.08	0.580	NEW,12
												1.81	0.504	NEW,12
												1.69	0.472	NEW,12
												1.04	0.289	OLD,12
												1.32	0.369	NEW,12
			18		468-495	438	2950	0.45	8.5	10		0.46	0.252	NEW,12
			18		468-495	438	2950	0.45	9			0.71	0.368	NEW,12
			19		456	94	4125	0.58				1.17	0.338	OLD,12
												1.47	0.424	NEW,12
												1.27	0.367	NEW,12
												1.12	0.322	NEW,12
		4	8	996	505			0.559		25.25	29.90	4.391	0.722	
			5 (pt. 2)	999	501			0.658		50.33	30.93	9.321	1.22	6
			10A	1000	492	438	2950	0.596		25.52	20.35	2.249	0.762	

Table A-9. Motorcase material DET data - (Continued).

MTL NO.	MTL NAME	REF.	RUN NO.	P_o (LB/IN^2)	h_o (BTU/LBM)	d_p μ	V_p (FT/SEC)	P_d (G/M^3)	θ (DEG)	t_{CA} (SEC)	t_D (SEC)	Δm (G)	G	NOTES
2401	NBR	4	4A	998	414	438	2950	0.601	9	50.32	20.62	2.024	0.718	
			13	998	461	94	4125	1.32	9	25.17	15.56	3.298	0.427	
			11	1000	516	438	2950	0.530	9	10.24	15.22	1.118	0.608	
			C-2	992	1509	100	5400	0.559	9	45.58	4.68	1.909	1.41	
										45.58	4.68	1.965	1.45	
										45.56	5.05	2.062	1.40	
										45.56	5.05	2.05	1.40	
		7	1 (12-78)	990	463	438	2950	0.503	8.5	10.0	12.0	0.40	0.247	12
2402	NBR 68		3 (12-78)	996	462			0.532	9			0.72	0.393	
			3 (12-78)	996	462			0.532				0.51	0.279	
			4 (12-78)	998	447			0.694	8.5	17	12	0.82	0.367	
			4 (12-78)	998	447			0.694	8.5	17	12	0.79	0.350	
2403	NBR 69		1 (12-78)	990	463			0.503	9	10.0	12.0	0.60	0.349	
			2 (12-78)	980	491			0.582	8.5			0.52	0.275	
			2 (12-78)	980	491			0.582	8.5			0.50	0.265	
2404	NBR-6A	12	8	986	460			0.461	9	0.28	21.20	0.747	0.268	
2404	NBR-6A											0.658	0.236	
2405	NBR-6B									0.26	20.82	0.711	0.260	
2405	NBR-6B									0.26	20.82	0.728	0.266	
2406	NBR-020									0.26	20.77	0.467	0.171	
2406	NBR-020								8.5	0.28	21.53	0.358	0.134	

Table A-9. Motorcase material DET data - (Continued).

MTL NO.	MTL NAME	REF.	RUN NO.	P_o (LB/IN^2)	h_o (BTU/LBM)	d_p μ	V_p (FT/SEC)	P_d (G/M^3)	θ (DEG)	t_{CA} (SEC)	t_D (SEC)	Δm (G)	G	NOTES
2501	KPN	7	6	982	508	438	2950	0.461	9	0.27	20.4	0.96	0.358	12
		7	6	982	508			0.461		0.30	21.16	1.51	0.455	
		12	9	990	465			0.433		0.31	20.36		0.792	
		12	9	990	465			0.433	8.5	0.31	21.21		0.858	
2502	HERC.	7	4	998	447			0.694	9	17	12	1.50	0.632	
												2.40	1.012	
												1.38	0.582	
												1.27	0.536	
2503	HERC. DOME											2.03	0.857	
2503	HERC. DOME											1.97	0.828	
2504	AEROJET INNER											1.45	0.612	
2504	AEROJET INNER											1.97	0.830	
2505	AEROJET OUTER											2.31	0.974	
2505	AEROJET OUTER											1.95	0.823	
2506	ROCKET-DYNE											1.11	0.469	
2506	ROCKET-DYNE											1.19	0.499	
2507	MM5	12	7	1000	472			0.386		0.31	20.52	0.407	0.180	

Table A-9. Motorcase material DET data - (Continued).

MTL NO.	MTL NAME	REF.	RUN NO.	P_o (LB/IN^2)	h_o (BTU/LBM)	d_p μ	V_p (FT/SEC)	P_d (G/M^3)	θ (DEG)	t_{CA} (SEC)	t_D (SEC)	Δm (G)	G	NOTES
2508	HERC. KEVLAR	12	7	1000	472	438	2950	0.836	9	0.31	20.52	0.407	0.180	12
										0.31	21.12	1.29	0.555	
			9	990	465			0.433	8.5	0.31	20.60	1.37	0.568	
2509	ROYACRIL 25		8	986	460			0.461	9	0.28	20.98	0.667	0.242	
2509	ROYACRIL 25		8							0.28	20.98	0.670	0.243	
2510	EPDM 1									0.29	20.94	0.743	0.270	
2510	EPDM 1									0.29	20.94	0.785	0.285	
2511	EPDM 2									0.30	21.11	0.735	0.265	
2511	EPDM 2								8.5	0.23	20.90	0.582	0.224	
2601	ALUMINUM		7	1000	472			0.386	15	0.31	20.74	0.223	0.059	
			8	986	460			0.461	9	0.26	20.77	0.142	0.052	
			8	986	460			0.461	8.5	0.23	20.90	0.283	0.042	
			9	990	465			0.433	9	0.30	20.83	0.113	0.044	
			9	990	465			0.433	8.5	0.31	21.21	0.106	0.043	
			10	1006	442			0.562	9	10.27	20.0	0.090	0.028	
			11	1000	437			0.380	9	-0-	19.46	0.089	0.042	
			11	1000	437			0.380	9	-0-	19.46	0.093	0.044	

Table A-10. Pebble test notes.

DEGREE OF SEVERITY	CODE NO.	DAMAGE DESCRIPTION OF TARGET
↓	1	NO PENETRATION • FRONT FACE CRATER OF DIMENSIONS INDICATED • SOME EVIDENCE OF SLIGHT DELAMINATION (BACK FACE BULGE)* • DENT (APPLICABLE TO Ti TARGET) OF DIMENSIONS INDICATED
	2	NO PENETRATION • FRONT FACE CRATER OF DIMENSIONS INDICATED • DELAMINATION • SOME BACK FACE FIBER BREAKAGE*
	3	NEAR PENETRATION (BALLISTIC LIMIT) • FRONT FACE CRATER OF DIMENSIONS INDICATED • BACK FACE FIBER BREAKAGE* • DELAMINATION
MOST SEVERE	4	PENETRATION • OPEN HOLE OF DIMENSIONS INDICATED

OTHER CODES:
- I - PEBBLE REMAINED INTACT AFTER STRIKING TARGET
- S - PEBBLE SHATTERED OR PULVERIZED AFTER STRIKING TARGET
- R1 - REMOVED SURFACE MATERIAL DOWN TO REINFORCEMENT
- R2 - REMOVED MATERIAL DOWN TO SUBSTRATE
- C - DEEP CRACK IN DAMAGED AREA
- * - ONLY FOR SAMPLES WITH NO SUBSTRATE

Table A-10. Motorcase material pebble test data.

MTL NO.	MTL NAME	REF.	SHOT NO.	PEB. MTL	d_p (IN)	W_p (GM)	θ (DEG)	V_p (FT/SEC)	MATERIAL TEMP (°K)	MATERIAL THICK (IN)	SUBSTRATE MTL TYPE	SUBSTRATE THICK (IN)	MASS LOSS (GM)	DAMAGE DATA NOTES	DENT OR CRATER L(IN)	DENT OR CRATER W(IN)	DENT OR CRATER D(IN)	OPEN HOLE L(IN)	OPEN HOLE W(IN)
2104B	Ke/VAMAC	1	112101	TON.	0.625	-	21	980	RT	0.153	Ke/Ep	0.51	-	3,R1	1.00	0.50	0.01		
			120501			-		1240	RT	0.144			-	3,R1	1.75	0.60	0.01		
			120502			-		1230	RT	0.137			-	3	1.65	0.65	-		
			120508			-		1200	RT	0.140			-	3,R1	1.60	0.55	0.01		
			10402		0.135	-	5.5	2700	394	0.139			0.0	1	-	-	-		
2104C			112102		0.625	-	21	961	RT	0.133			-	1	1.40	0.45	-		
			10501		0.120	-	5.5	2560	394	0.134			0.0	1	-	-	-		
2104D	G/VAMAC		41107		0.625	-	21	950	RT	0.140			-	2	1.50	0.50	-		
2105	VAMAC 15J		110801			-	18	932	RT	0.142			0.0	1	-	-	-		
			110802			-	18	860	464	0.140			-	4,R2				1.20	0.35
			111001		0.130	-	5.5	2510	RT	0.144			0.0	1	-	-	-		
2116	VAMAC 25		7891106		0.625	-	21	990	RT	0.147	Gr/Ep	0.182	-	1	1.35	0.35	0.005		
2203A	VITON 2B		112201			-	21	980	RT	-	Ke/Ep	0.51	0.0	1	1.40	0.40	-		
			120503			-	21	1240	RT	-			-	2	1.30	0.45	-		
			10503		0.125	-	5.5	2600	394	-			-	1	0.45	0.05	-		
			10902		0.625	-	5.5	2550	408	-			-	2	3.10	0.30	-		
			7891105				21	990	RT	0.147	Gr/Ep	0.18	-	1	1.50	0.42	0.04		
			7890501					2200	RT	0.147	Gr/Ep	0.22	-	4				0.57	0.25
2203B	Ke/VITON		112201			-		951	RT	-	Ke/Ep	0.51	-	3,R1	1.30	0.40	0.01		
			120504			-		1220	RT	-			-	3,R1	1.20	0.45	0.01		
			10601		0.120	-	5.5	2500	394	-			-	3,R1	0.10	0.02	0.01		
2203C			112202		0.625	-	21	980	RT	-			-	1	1.40	0.40	-		
			120505		0.625	-	21	928	RT	-			-	2	1.00	0.40	-		

Table A-10. Motorcase material pebble test data - (Continued).

MTL NO.	MTL NAME	REF.	SHOT NO.	PEB. MTL	d_p (IN)	W_p (GM)	θ (DEG)	V_p (FT/SEC)	MATERIAL TEMP (°K)	MATERIAL THICK (IN)	SUBSTRATE MTL TYPE	SUBSTRATE THICK (IN)	MASS LOSS (GM)	DAMAGE DATA NOTES	DENT OR CRATER L(IN)	DENT OR CRATER W(IN)	DENT OR CRATER D(IN)	OPEN HOLE L(IN)	OPEN HOLE W(IN)
2208A	VITON 2B12	1	7890102	TON.	0.625	-	21	990	RT	0.140	Gr/Ep	0.22	-	1	1.70	0.40	0.01		
			7890105			-		942		0.244		0.21	-	1	1.50	0.45	0.03		
			7890502			-		1968		0.140		0.22	-	4				1.35	0.40
			7890505			-		1400		0.244		0.21	-	2	1.63	0.68	-		
2208B			7890103			-		890		0.120*		0.22	-	1	1.25	0.38	0.005		
			7890106			-		928		0.120*		0.24	-	1	1.55	0.52	0.015		
			7890503			-		1260		0.120*		0.22	-	1	1.70	0.40	-		
			7890601			-		1460		0.125*	Ke/Ep	0.47	-	1	1.80	0.80	-		
			7890506			-		1460		0.125*	Gr/Ep	0.23	-	2	2.03	0.98	-		
2213	VITON [10-34.7]		7890104			-		890		0.232	Gr/Ep	0.21	-	1	1.30	0.39	0.005		
			7890504			-		1500		0.233	Gr/Ep	0.21	-	2	1.62	0.44	-		
2306A	OLD TBR		10903			-		1090		0.140	Ke/Ep	0.51	LARGE	-				-	-
			10904			-		925					LARGE	-				-	-
			41103			-		800					-	3,C	1.45	1.40	-		
2306B	OLD TBR/ Ke		41101			-		928					-	3	1.00	0.45	0.06		
			41108			-		942					-	3	1.50	0.50	0.04		
2306C			41104			-		814					-	3,C	0.90	0.60	-		
			41105			-		850					-	4,R2	1.00	0.50	0.14		
2307	NEW TBR		7890107					918					-	1	1.83	0.38			
			7890108					918					-	1	1.25	0.38	0.005		
2308A	NEW TBR		7890508					1460		0.160	Gr/Ep	0.210	-	4,R2	2.03	0.70	0.16		
			7890507					1515		0.160	Ke/Ep	0.462	-	4,R2	2.61	0.92	0.16		

*APPLIED OVER AN EQUAL THICKNESS OF VITON [10-70]

Table A-10. Motorcase material pebble test data - (Continued).

MTL NO.	MTL NAME	REF.	SHOT NO.	PEB. MTL	d_p (IN)	W_p (GM)	θ (DEG)	V_p (FT/SEC)	MATERIAL TEMP (°K)	MATERIAL THICK (IN)	SUBSTRATE MTL TYPE	SUBSTRATE THICK (IN)	MASS LOSS (GM)	DAMAGE DATA NOTES	DENT OR CRATER L(IN)	DENT OR CRATER W(IN)	DENT OR CRATER D(IN)	OPEN HOLE L(IN)	OPEN HOLE W(IN)
2308B	NEW TBR/Ke	1	7890110	TON.	0.625	-	21	925	RT	0.160	Ke/Ep	0.51	-	1	1.40	0.48	-		
			7890111			-		945			Gr/Ep	0.23	-	1	1.30	0.62	0.005		
2308C	NEW TBR/Ke		7890603			-		1440			Gr/Ep	0.25		2	1.95	0.95	-		
			7890602			-		1500			Ke/Ep	0.51		2	2.35	1.40	-		
2401	NBR		102801			-	18	950		0.130			<0.4	3,R2	0.11	0.16	0.13		
			103102			-	25	1050					<0.4	3,R2	0.11	0.39			
			110201			-	18	978	339				<0.4	3,R2	0.16	0.51			
			11040			-	18	950	389				<0.4	3,R2	0.11	0.90			
			10605		0.120	-	5.5	2600	408				1.3	1,S?	-	-	-		
			10901		0.625	-	5.5	2588	408				0.4	1	0.31	3.14	-		
			7891104		0.625	-	21	1000	RT	0.140	Gr/Ep	0.18	-	4,R2	1.15	0.23	0.11		

Table A-11. Motorcase material pebble test data (Feb - Apr 1979).

MTL NO.	MTL NAME	REF.	SHOT NO.	PEB. MTL	d_p (IN)	W_p (GM)	θ (DEG)	V_p (FT/SEC)	OUTER MATERIAL TEMP (°K)	OUTER MATERIAL THICK (IN)	SECOND MATERIAL MTL NO.	SECOND MATERIAL THICK (IN)	SUBSTRATE MTL TYPE	SUBSTRATE THICK (IN)	SUBSTRATE DENT (IN)	DAMAGE DATA
2116	VAMAC 25	7,8	79022101	TON.	0.625	5.28	33.5	469	RT	0.06	2116A	0.08	ISOGRID	0.038		VAMAC LAYERS CUT ISOGRID CORNER SHEARED
			79022103			5.42	33.5	371								SURFACE SCUFF
			79033001			5.50	15	925								SURFACE SCUFF
			79033002			5.48	20	640								SURFACE SCUFF
			79033003			5.52	20	650							ENLARGED	HIT ON TOP OF 79033003. DENT ENLARGED. NO OTHER EFFECT.
			79032601			5.53	20	666		0.14	-	-	ALUMINUM	0.071	0.065	SURFACE SCUFF
			79032801			5.61	20	610		0.10	-	-			0.078	
			79022701			5.50	33.3	410		0.10	2116A	0.04			0.045	
			79022707			5.50	20	636							0.085	
			79040201			5.51	20	850							0.094	
			79022702			5.49	33.5	380			2116B				0.049	
			79022708			5.51	20	650							0.092	
			79040202			5.50	15	1000							0.110	
			79022703			5.50	33.5	303		0.025	2133	0.11			0.040	
			79022801			5.50	20	670		0.025	2133	0.11			0.90	
			79032901			5.41	20	680		-	2501	-	ISOGRID	0.038	SLIGHT	VAMAC SCRAPED OFF
			79040603			5.51	33.5	330		-		-				SURFACE SCUFF
2116C	UNCURED VAMAC		79032902			5.41	20	640		-		-				VAMAC SCRAPED OFF
			79040602			5.50	33.5	360		-		-				SURFACE SCUFF

Table A-11. Motorcase material pebble test data (Feb - Apr 1979) - (Continued).

MTL NO.	MTL NAME	REF.	SHOT NO.	PEB. MTL	d_p (IN)	W_p (GM)	θ (DEG)	V_p (FT/SEC)	OUTER MATERIAL TEMP (°K)	OUTER MATERIAL THICK (IN)	SECOND MATERIAL MTL NO.	SECOND MATERIAL THICK (IN)	SUBSTRATE MTL TYPE	SUBSTRATE THICK (IN)	SUBSTRATE DENT (IN)	DAMAGE DATA
2124	LOW RESISTANCE VAMAC	7,8	79032803	TON.	0.625	5.50	20	630	RT	0.14	-	-	ALUMINUM	0.071	0.075	SURFACE SCUFF
			79040203		0.625	5.50	20	950			-	-			0.094	
			79040401		0.250	0.40	6	2310							0.059	
2132	LOW CARBON VAMAC		79032802		0.625	5.58	20	607			-	-			0.070	
2208	VITON 2B12		79032804			5.50	20	750		0.10	-	-			0.083	
			79032805			5.51	20	650		0.06	-	-			0.075	
			79022706			5.51	33.5	331		0.10	2298C	0.04			0.029	
			79040204			5.51	15	1000		0.10	2208C	0.04			0.070	
			79022704			5.49	33.5	365		0.06	2208C	0.08			0.015	
			79022802			5.51	20	675							0.080	
			79040205			5.50	15	860							0.020	
			79040402		0.250	0.39	6	2280							NONE	
			79022705		0.625	5.51	33.5	335		0.10	2208D	0.04			0.001	
			79022803			5.50	15	690							0.025	
			79040206			5.51	15	975							0.043	
2219	WHITE VITON		79032809			5.51	20	750			2208				0.167	
2501	KPN		79032903			5.40	20	690			-	-	ISOGRID	0.038		CRACK IN CORNER OF ISOGRID
			79032904			5.48	15	880			-	-			SLIGHT	SURFACE SCUFF
			79040302		0.125	0.066	6	2300			-	-			NONE	
			79040601		0.625	5.49	33.5	351			-	-			SLIGHT	
			79032808		0.625	5.49	20	700			-	-	ALUMINUM	0.071	SLIGHT	

Table A-11. Motorcase material pebble test data (Feb - Apr 1979) - (Continued).

MTL NO.	MTL NAME	REF.	SHOT NO.	PEB. MTL	d_p (IN)	W_p (GM)	θ (DEG)	V_p (FT/SEC)	OUTER MATERIAL TEMP (°K)	OUTER MATERIAL THICK (IN)	SECOND MATERIAL MTL NO.	SECOND MATERIAL THICK (IN)	SUBSTRATE MTL TYPE	SUBSTRATE THICK (IN)	SUBSTRATE DENT (IN)	DAMAGE DATA
2501	KPN	7,8	79040604	TON.	0.625	5.50	33.5	350	RT		-	-	ALUMINUM	0.071	SLIGHT	SURFACE SCUFF
2501	KPN	↓	79040403	↓	0.250	0.40	6	2330	↓		-	-	ALUMINUM	0.071	NONE	FIRST FABRIC LAYER SCRAPED THROUGH
2601	2024-T6 ALUMINUM	↓	79033004	↓	0.625	5.51	20	635	↓	0.071	-	-	-	-	0.10	SURFACE SCUFF

Blank

A-3. SHROUD MATERIALS

Candidate shroud materials including titanium are described in Tables A-12 and A-13. Tables A-14 and A-15 list the DET test data, while Tables A-16 and A-17 list the pebble impact data.

Table A-12. Shroud materials identification.

REFERENCE NO.	MATERIAL	PANEL NO.	NOMINAL THICKNESS* (INCHES)	DENSITY (g/cm^3)
3001	Kevlar/Phenolic	G-1	0.115	1.36
		G-2	0.230	1.33
3002	Titanium	---	0.020	4.45
		---	0.063	4.45
3003	Graphite (Cloth)/Phenolic	F-2	0.110	1.54
		F-1	0.220	1.51
3004	Graphite (Tape)/Polyimide	E-2	0.115	1.56
		E-1	0.230	1.58
3005	Kevlar-Graphite/Phenolic	H-2	0.115	1.39
		H-1	0.230	1.35
3006	Kevlar Tape/5208 Epoxy	---	0.240	1.36
3007	Kevlar Cloth/E759 Epoxy	---	0.230	1.33
3008	Kevlar/Epoxy Novalac	---	0.240	1.12
3009	Carbon/Phenolic (20° Shingle)	---	0.240	1.47
3010	Layered Viton with Carbon Black	---	0.033	1.94
	Kevlar/Phenolic	---	0.045	1.36
	Syntactic Foam (Phenolic)	---	0.125	0.38
	Graphite/Polyimide	---	0.128	1.54
3011	Layered Viton with Carbon Black	---	0.108	1.94
	Graphite/Polyimide	---	0.122	1.54
3012	Layered Graphite Phenolic (15° Shingle)	---	0.112	1.54
	Graphite Polyimide	---	0.100	1.54
3014	Graphite (Cloth) PVF/0.75 PVF + 0.25 Epoxy	---	0.250	1.30
3015	Layered Graphite (Cloth) PVF/0.50 PVF			
	+ 0.50 Epoxy	---	0.177	1.52
	Graphite (Tape)/Polyimide		0.120	1.53
3016	V1 + MW (Natural)	---	0.120	0.94
	Marinite	---	0.120	

Table A-12. Shroud materials identification - (Continued).

REFERENCE NO.	MATERIAL	PANEL NO.	NOMINAL THICKNESS* (INCHES)	DENSITY (g/cm^3)
3017	Layered Kevlar 329/Epoxy Novalac	---	0.135	1.28
	Syntactic Foam (Phenolic)	---	0.100	0.38
	Graphite/Polyimide	---	0.120	1.54
3018	Kevlar 329 PVF/0.75 PVF + 0.25 Phenolic	---	0.090	1.25
	Syntactic Foam (Glass)	---	0.103	0.32
	Kevlar 328/Epoxy	---	0.125	1.33
3019	Kevlar 49 PVF/0.50 PVF + 0.50 Epoxy	---	0.23	1.26
3020	Thin Kevlar 49/0.75 PVF + 0.25 Epoxy	---	0.23	1.28
3023	Layered Ke PVB/0.25 PVB + 0.75 Ph.	---	0.231	1.25
	Syntactic Foam (Phenolic)	---	0.106	0.38
	Graphite/Polyimide	---	0.110	1.54
3024	Layered Ke PVB/0.25 PVB + 0.75 Ph (15° Shingle)	7A	0.230	1.30
	Graphite/Polyimide	7B	0.103	1.59
3025	Hybrid 0.25 Graphite 0.75 Kevlar/Phenolic	5-2	0.230	1.36
3026	Hybrid 0.75 Graphite 0.25 Kevlar/Phenolic	5-1	0.230	1.44
3027	Ultra-High Molecular Weight Polymer (Natural)	---	0.12	0.94
3028	Ultra-High Molecular Weight Polymer (Cross-linked)	---	0.12	0.94
3029	Kevlar 328 PVF/0.75 PVF + 0.25 Epoxy Novalac	---	0.127	1.25
3031	Kevlar 329 PVF/0.75 PVF + 0.25 Epoxy Novalac (Same as 3029 with Style 329 Cloth)			
3032	3:1 NEAT PVF/Epoxy	---	----	----
3033	50-50 NEAT PVF/Epoxy	---	----	----
3034	Kevlar/L100	---	----	----
3035	Nomex/PVF-Epoxy	---	----	----
3036	Kevlar 350 0.75 PVF + 0.25 Epoxy	---	----	----
3037	Kevlar 350 0.50 PVF + 0.50 Epoxy	---	----	----

Table A-12. Shroud materials identification - (Continued).

REFERENCE NO.	MATERIAL	PANEL NO.	NOMINAL THICKNESS* (INCHES)	DENSITY (g/cm^3)
3038	Kevlar 329 0.75 PVF + 0.25 Epoxy	---	----	----
3039	Kevlar 329 0.50 PVF +0.50 Epoxy	---	----	----
3040	0.75 PVF + 0.25 Epoxy NEAT	---	----	----
3041	0.50 PVF + 0.50 Epoxy NEAT	---	----	----
3042	0.75 PVF + 0.25 Epoxy	---	----	----
3043	0.50 PVF + 0.50 Epoxy	---	----	----

Table A-13. Shroud program composite materials process summary.

PANEL	MATERIAL		CURE TEMPERATURE	CURE PRESSURE	POST CURE	LAMINATE CONFIGURATION
E-1	F-178/T-300	TAPE	350°F 1-1/2 HRS	100 PSI	5 HRS 485°F	40 PLY $(0,90,+45,-45,090,+45,-45,0,90,0,90,+45,-45,0,90,+45,-45,0,90)_S$
E-2	F-178/T-300	TAPE	350°F 1-1/2 HRS	100 PSI	5 HRS 485°F	20 PLY $(0,90,+45,-45,0,90,+45,-45,0,90)_S$
F-1	F-502/T-300	CLOTH	350°F 2 HRS	150 PSI		14 PLY (0/90,0/90,±45,0/90,0/90,±45,0/90,0/90,±45,0/90,0/90,±45,0/90,0/90)
F-2	F-502/T-300	CLOTH	350°F 2 HRS	150 PSI		7 PLY (0/90,0/90,±45,0/90,±45,0/90,0/90)
G-1	CPH2280/K-49	CLOTH	350°F 3 HRS	100 PSI		25 PLY $(0/90,0/90,\pm45,0/90,0/90,0/90,\pm45,0/90,0/90,0/90,\pm45,0/90,0/90,\pm45,0/90_L)_S$
G-2	CPH2280/K-49	CLOTH	350°F 3 HRS	100 PSI		13 PLY (0/90,0/90,±45,0/90,0/90,0/90,±45,0/90,±45,0/90,0/90,0/90,±45,0/90)
H-1	K-49/T-300/PHENOLIC	CLOTH	350°F 3 HRS	100 PSI		24 PLY $(0/90,0/90,\pm45,0/90,\pm45,0/90,0/90,0/90,\pm45,0/90,+45,0/90,0/90)_S$
H-2	K-49/T-300/PHENOLIC	CLOTH	350°F 3 HRS	100 PSI		12 PLY $(0/90,0/90,\pm45,0/90,\pm45,0/90)_S$
5	K-49/T-300/PHENOLIC	CLOTH	350°F 3 HRS	100 PSI		24 PLY $(0/90,0/90,\pm45,0/90,0/90,0/90,\pm45,0/90,0/90,0/90,\pm45,0/90,0/90,\pm45)_S$
7	K-49/CPH2280/PVB F-178/T-300	CLOTH TAPE	350°F 2 HRS 350°F 1-1/2 HRS	100 PSI 100 PSI	 5 HRS 485°F	+45-15° SHINGLES 20 PLY $(0,90,+45,-45,0,90,+45,-45,0,90)_S$

Table A-14. DET test notes.

1	–	QUESTIONABLE – TARE SAMPLES IN RUN 3 CHARRED AND LOST SUBSTANTIAL MASS IN 20 SECONDS.
2	–	QUESTIONABLE – HIGH MASS LOSS.
3	–	QUESTIONABLE – MASS LOST DURING CLEAR AIR TIME (LAYERS PEELED OFF BY SHEAR/AEROHEATING).
4	–	QUESTIONABLE – FRONT EDGE OF RETAINER MATERIAL PEELED UP SO AS TO SHIELD SAMPLE.
5	–	SAMPLE DIAMETER QUESTIONABLE DUE TO EROSION/THERMAL DEGRADATION AROUND EDGE OF 2-INCH DISC.
6	–	QUESTIONABLE – HIGH MASS LOSS AND ERODED THROUGH.
7	–	SPECIMEN WAS A TRAPEZOID RATHER THAN A 2-INCH DISC SURROUNDED BY A TRAPEZOIDAL RETAINER. G VALUES MAY BE HIGH DUE TO EDGE EFFECTS.
8	–	PRE-DAMAGED SPECIMEN.
9	–	QUESTIONABLE – RESULTS INCONSISTENT WITH OTHER RESULTS FOR RUN.
10	–	SINGLE LAYER LOST DURING CLEAR AIR TIME.
11	–	QUESTIONABLE – LAYERS BEGAN PEELING OFF BEFORE MODEL WAS ON CENTERLINE.
12	–	MASS LOSS CALCULATED FOR 2.00-DIAMETER SPECIMEN.

Table A-15. Shroud material DET data.

MTL NO.	MTL NAME	REF.	RUN NO.	P_o (LB/IN^2)	h_o (BTU/LBM)	d_p μ	V_p (FT/SEC)	P_d (G/M^3)	θ (DEG)	t_{CA} (SEC)	t_D (SEC)	Δm (G)	G	NOTES
3001	Ke-Ph	5	7	1000	550	94	4125	0.62	9	20	0	-	-	
									15	0	10	4.75	1.160	12
									20	10	10	7.73	1.430	
									9	10	10	1.88	0.760	
									4	10	10	0.24	0.216	
									15	10	10	4.48	1.095	
			8		495-555	438	2950	0.42	9	20	0	-	-	
									15	0	5	0.39	0.390	
									20	10	10	3.16	1.208	
									9	10	10	0.73	0.610	
									4	10	10	0.13	0.240	
									15	10	10	1.96	0.987	
			9		491-560	94	4125	1.08	9	?	0	-	-	
									9	10	7	2.80	0.930	12
									4	10	7	0.40	0.298	
									15	10	7	5.42	1.087	
									15	10	7	5.37	1.072	
			17		500			0.60	9	0	15	2.05	0.571	
			17		500			0.60	15	0	15	4.73	0.797	
			19		456			0.58	15	10	15	4.41	0.768	
			19		456			0.58	9	10	15	1.84	0.530	
3002	Ti		7		550			0.62	9	10	10	GAINED	-	
									20				-	
									15				-	

Table A-15. Shroud material DET data - (Continued).

MTL NO.	MTL NAME	REF.	RUN NO.	P_o (LB/IN^2)	h_o (BTU/LBM)	d_p μ	V_p (FT/SEC)	P_d (G/M^3)	θ (DEG)	t_{CA} (SEC)	t_D (SEC)	Δm (G)	G	NOTES
3002	Ti	5	8	1000	495-555	438	2950	0.42	9	10	10	GAINED	-	
									20			0.08	0.029	12
									15			0.05	0.026	12
			21		480			0.48	30		15	0.04	0.0064	8,12
3003	Gr/Ph		7		550	94	4125	0.62	9	20	0	-	-	
									15	0	10	4.16	1.017	12
									4	10	10	0.74	0.670	
									9	10	10	1.54	0.623	
									15	10	10	5.19	1.269	
			8		495-555	438	2950	0.42	9	20	0	-	-	
									15	0	5	0.26	0.259	12
									4	10	10	0.10	0.189	
									9	10	10	0.42	0.350	
									15	10	5	0.55	0.557	
			9		491-560	94	4125	1.08	15	10	7	6.19	1.240	
			9		491-560			1.08	9	10	7	1.49	0.494	
3004	Gr/Pl		7		550			0.62	9	10	10	0.94	0.379	
			7		550			0.62	15	10	10	3.62	0.885	
			8		495-555	438	2950	0.42	9	10	10	0.35	0.297	
			8		495-555	438	2950	0.42	15	10	5	0.56	0.594	
			9		491-560	94	4125	1.08	20	10	10	13.8	1.463	
			9		491-560	94	4125	1.08	15	10	10	6.61	0.928	
			12A		500	438	2950	0.51	4	10	20	0.09	0.071	
			19		456	94	4125	0.58	9	10	15	1.17	0.322	

Table A-15. Shroud material DET data - (Continued).

MTL NO.	MTL NAME	REF.	RUN NO.	P_o (LB/IN^2)	h_o (BTU/LBM)	d_p μ	V_p (FT/SEC)	P_d (G/M^3)	θ (DEG)	t_{CA} (SEC)	t_D (SEC)	Δm (G)	G	NOTES
3004	Gr/Pl	5	19	1000	456	94	4125	0.58	15	10	15	3.90	0.680	12
↓	↓	↓	21	↓	480	438	2950	0.48	9	10	15	0.58	0.281	8,12
↓	↓	↓	21	↓	480	438	2950	0.48	9	10	15	0.75	0.365	12
3005	Ke-Gr/Ph	↓	9	↓	491-560	94	4125	1.08	9	?	0		-	
↓	↓	↓	↓	↓	↓	↓	↓	↓	15	10	7	5.84	1.170	12
↓	↓	↓	↓	↓	↓	↓	↓	↓	20	↓	↓	11.60	1.760	↓
↓	↓	↓	↓	↓	↓	↓	↓	↓	4	↓	↓	0.93	0.690	↓
↓	↓	↓	↓	↓	↓	↓	↓	↓	9	↓	↓	2.29	0.760	↓
↓	↓	↓	↓	↓	↓	↓	↓	↓	9	↓	↓	2.56	0.852	↓
↓	↓	↓	↓	↓	↓	↓	↓	↓	15	↓	↓	5.35	1.072	↓
3006	Ke(Tape)/ 5208	↓	12A	↓	500	438	2950	0.51	9	↓	20	2.00	0.689	↓
↓	↓	↓	↓	↓	↓	↓	↓	↓	15	↓	↓	3.68	0.764	↓
↓	↓	↓	↓	↓	↓	↓	↓	↓	20	↓	↓	7.60	1.195	↓
↓	↓	↓	↓	↓	↓	↓	↓	↓	14	↓	↓	3.93	0.874	↓
↓	↓	↓	17	↓	↓	↓	↓	0.60	15	0	15	2.79	0.657	↓
3007	Ke(Cloth)/ E759	↓	12A	↓	↓	↓	↓	0.51	9	10	20	0.55	0.190	↓
↓	↓	↓	↓	↓	↓	↓	↓	↓	15	↓	↓	2.82	0.587	↓
↓	↓	↓	↓	↓	↓	↓	↓	↓	4	↓	↓	0.69	0.536	↓
↓	↓	↓	17	↓	↓	↓	↓	0.60	15	0	15	2.90	0.684	↓
↓	↓	↓	18	↓	468-595	↓	↓	0.45	9	10	↓	0.40	0.206	↓
↓	↓	↓	18	↓	468-495	↓	↓	0.45	8.5	↓	↓	0.50	0.273	↓
↓	↓	↓	21	↓	480	↓	↓	0.48	9	↓	↓	1.01	0.494	↓
↓	↓	↓	21	↓	480	↓	↓	0.48	15	↓	↓	2.93	0.863	↓

Table A-15. Shroud material DET data - (Continued).

MTL NO.	MTL NAME	REF.	RUN NO.	P_o (LB/IN^2)	h_o (BTU/LBM)	d_p μ	V_p (FT/SEC)	P_d (G/M^3)	θ (DEG)	t_{CA} (SEC)	t_D (SEC)	Δm (G)	G	NOTES
3007	Ke(Cloth)/ E759	5	22	1000	495-648	438	2950	0.54	15	10	15	2.90	0.759	12
3007	Ke(Cloth)/ E759		22		495-648			0.54	9		15	0.77	0.333	
3008	Ke/Ep *Nov 1*		12A		500			0.51	15		20	3.28	0.683	
3009	CP 20°		12A		500			0.51	20		20	5.25	0.826	
3009	CP 20°								15		20	2.62	0.545	
3010	VITON SYS		18		468-595			0.45	9		15	1.35	0.701	
3011	VITON SYS		19		456	94	4125	0.58	15			3.39	0.590	
3011	VITON SYS		22		495-648	438	2950	0.54	15			2.70	0.706	
3012	Gr/Ph 15°		18		468-595	438	2950	0.45	9			2.59	1.348	
3012	Gr/Ph 15°		19		456	94	4125	0.58	15			-	HIGH SAMPLE DESTROYED	
3014	Gr/PVF 1		18		468-595	438	2950	0.45	8.5			2.14	0.205	12
3014	Gr/PVF 1		19		456	94	4125	0.58	15			1.96	0.342	
3015	G/PVF 2		18		468-595	438	2950	0.45	9			0.36	0.186	
			21		480			0.48	9			0.64	0.312	
			21		480			0.48	15			2.38	0.702	
			22		495-648			0.54	15			3.56	0.931	
			22		495-648			0.54	9			1.09	0.470	
3016	V1		17		500	94	4125	0.60	15	0		3.78	0.636	
3016	VI		19		456	94	4125	0.58	15	10		3.26	0.568	

Table A-15. Shroud material DET data - (Continued).

MTL NO.	MTL NAME	REF.	RUN NO.	P_o (LB/IN^2)	h_o (BTU/LBM)	d_p μ	V_p (FT/SEC)	P_d (G/M^3)	θ (DEG)	t_{CA} (SEC)	t_D (SEC)	Δm (G)	G	NOTES
3017	Ke/Ep Nov 2	5	18	1000	468-595	438	2950	0.45	9	10	15	0.52	0.269	12
			21		480			0.48	9			0.36	0.176	
			21		480			0.48	15			3.06	0.902	
			22		495-648			0.54	15			3.34	0.873	
			22		495-648			0.54	9			0.89	0.384	
3018	Ke/PVF 1		18		468-595			0.45	9			0.20	0.102	
			19		456	94	4125	0.58	9			0.63	0.182	
			19		456	94	4125	0.58	15			2.87	0.501	
			21		480	438	2950	0.48	9			0.13	0.061	
			21		480			0.48	15			2.10	0.618	
	Ke/PVF 2		22		495-648			0.54	12			1.77	0.578	
									6			0.17	0.107	
									9			0.61	0.264	
									15			2.81	0.735	
		7	3	996	462			0.532	9		12	0.54	0.295	
												0.31	0.173	
										0		0.95	0.522	9,12
										0		0.93	0.510	
										20		1.10	0.604	
										20		0.98	0.539	
										30		0.40	0.220	
										30		1.47	0.807	
									15	0		2.33	0.775	12
										0		2.10	0.698	
										10		3.14	1.042	
										10		2.75	0.914	

Table A-15. Shroud material DET data - (Continued).

MTL NO.	MTL NAME	REF.	RUN NO.	P_o (LB/IN^2)	h_o (BTU/LBM)	d_p μ	V_p (FT/SEC)	P_d (G/M^3)	θ (DEG)	t_{CA} (SEC)	t_D (SEC)	Δm (G)	G	NOTES
3019	K3/PVF 3	5	18	1000	468-595	438	2950	0.45	9	10	15	0.42	0.219	12
3020	Thin Ke/PVF		18		468-595	438	2950	0.45	8.5			0.33	0.181	
3023	Ke/PVB 1		18		468-595	438	2950	0.45	9			0.99	0.503	
3023	Ke/PVB 1		19		456	94	4125	0.58	15			HIGH SAMPLE DESTROYED		
3024	Ke/PVB 2		17		500	94	4125	0.60	15	0		4.41	0.742	12
3024	Ke/PVB 2		18		468-595	438	2950	0.45	9	10		4.11	0.334	
3025	Gr/Ke Ph 1		18		468-595	438	2950	0.45	9			1.43	0.743	
3025	Gr/Ke Ph 1		19		456	94	4125	0.58	15			4.94	0.862	
3026	Gr/Ke Ph 2		17		500	94	4125	0.60	9	0		2.91	0.812	
3026	Gr/Ke Ph 2		18		468-595	438	2950	0.45	9	10		1.51	0.783	
3027	UHMW		17		500	94	4125	0.60	15	0		3.86	0.651	
			21		480	438	2950	0.48	15	10		5.06	1.492	
			21		480	438	2950	0.48	9	10		1.46	0.429	
3028	UHMW-X		17		500	94	4125	0.60	15	0		5.77	0.972	
3029	Ke/PVF 4		22		495-648	438	2950	0.54	9	10		0.70	0.304	
									15			2.69	0.704	
									12			1.71	0.556	
									6			0.15	0.098	

Table A-15. Shroud material DET data - (Continued).

MTL NO.	MTL NAME	REF.	RUN NO.	P_o (LB/IN^2)	h_o (BTU/LBM)	d_p μ	V_p (FT/SEC)	P_d (G/M^3)	θ (DEG)	t_{CA} (SEC)	t_D (SEC)	Δm (G)	G	NOTES
3031	Ke/PVF 5	4	8	996	505	50	3900	0.559	9	25.25	29.90	3.178	0.515	
									15	15.50	10.10	2.039	0.590	
									15	15.50	10.10	2.773	0.808	
									30	7.10	5.50	4.923	1.33	3
									30	7.10	5.50	5.217	1.42	3
			10A	1000	492	650	2400	0.596	9	0.38	10.63	0.087	0.061	
									9	25.52	20.35	0.718	0.260	
									15	0.38	10.63	1.603	0.672	
									15	15.60	10.29	1.468	0.634	
									15	15.60	10.29	1.590	0.693	
									30	0.38	5.53	2.605	1.08	
									30	7.49	5.27	2.832	0.937	3
									30	7.49	5.27	3.331	1.09	3
			12	300	486	650	1725	0.695	9	0.41	40.40	0.674	0.170	
									9	0.41	40.40	0.784	0.195	
									15	0.38	15.60	0.954	0.375	
									15	0.38	15.60	0.712	0.280	
									30	0.40	10.37	1.572	0.478	
									30	0.40	10.37	1.235	0.378	
			14	1000	484	650	2400	0.561	9	17.53	20.60	1.256	0.531	
									13	9.19	10.48	1.318	0.766	
									30	1.59	5.21	1.863	0.968	
			13	998	461	50	3900	1.32	9	25.17	15.56	3.015	0.441	
									13	15.73	5.16	1.590	0.490	
									13	15.51	5.21	1.167	0.357	
									30	7.21	3.06	3.955	0.920	3,5
									30	7.21	3.06	3.641	0.838	3,5

Table A-15. Shroud material DET data - (Continued).

MTL NO.	MTL NAME	REF.	RUN NO.	P_o (LB/IN^2)	h_o (BTU/LBM)	d_p μ	V_p (FT/SEC)	P_d (G/M^3)	θ (DEG)	t_{CA} (SEC)	t_D (SEC)	Δm (G)	G	NOTES
3032	3:1 NEAT	12	10	1006	442	438	2950	0.562	9	10.49	20.30	0.560	0.172	12
									15	10.70	10.90	1.93	0.666	
									4	10.27	10.27	-0-	-0-	
									20	10.27	10.27	2.61	0.989	
3033	50-50 NEAT								9	10.49	20.30	0.774	0.238	
									15	10.70	10.90	1.56	0.538	
									4	10.39	10.50	0.013	0.017	
									20	10.39	10.50	2.38	0.646	
3034	KEVLAR L100								9	10.17	20.55	1.84	0.558	
3034	KEVLAR L100								9	10.17	20.55	1.64	0.499	
3035	NOMEX								15	10.09	10.62	2.17	0.772	
									4	10.19	10.97	0.038	0.049	
									20	10.19	10.97	3.76	0.979	
									9	10.27	20.00	0.952	0.297	
3036	Ke 5		11	1000	437			0.380	9	10.00	20.28	0.554	0.252	
									4	10.00	10.57	0.022	0.043	
									15	10.00	10.53	1.39	0.735	
									20	10.00	10.57	1.97	0.787	
3037	Ke 6								9	10.00	19.10	1.19	0.576	

Table A-15. Shroud material DET data - (Continued).

MTL NO.	MTL NAME	REF.	RUN NO.	P_o (LB/IN^2)	h_o (BTU/LBM)	d_p μ	V_p (FT/SEC)	P_d (G/M^3)	θ (DEG)	t_{CA} (SEC)	t_D (SEC)	Δm (G)	G	NOTES
3038	Ke 7	12	11	1000	437	438	2950	0.380	9	10.00	20.28	0.666	0.303	12
									15	10.00	10.53	1.46	0.772	
									9	-0-	20.82	0.806	0.357	
										20.00	21.09	0.517	0.226	
			12		458	1000	2100	0.863		10.28	20.40	1.46	0.410	
			14	996	491	438	2950	2.30		10.29	4.72	3.23	1.044	
3039	Ke 8		11	1000	437			0.380		10.00	19.10	1.14	0.550	
									4	10.00	10.00	-0-	-0-	
									20	10.00	10.00	1.42	1.235	
3040	NEAT 1		12		458	1000	2100	0.863	20	10.15	10.59	4.50	1.11	
					458	1000	2100	0.863	9	10.66	10.69	1.06	0.280	
					437	438	2950	0.380	9	-0-	20.82	0.275	0.122	
					437	438	2950	0.380	9	20.00	21.09	0.178	0.078	
3041	NEAT 2				458	1000	2100	0.863	20	10.59	10.55	3.90	0.965	
					458	1000	2100	0.863	9	10.28	20.44	0.752	0.210	
3042	PVF-Ep 1		14	996	491	438	2950	2.30	15	9.86	3.68	1.86	0.467	
3043	PVF-Ep 2				491				9	10.87	5.12	1.43	0.426	
									15	10.47	3.44	2.83	0.757	
									9	10.29	4.72	2.08	0.672	

Table A-16. Pebble test notes.

DEGREE OF SEVERITY	CODE NO.	DAMAGE DESCRIPTION OF TARGET
↓	1	NO PENETRATION • FRONT FACE CRATER OF DIMENSIONS INDICATED • SOME EVIDENCE OF SLIGHT DELAMINATION (BACK FACE BULGE)* • DENT (APPLICABLE TO Ti TARGET) OF DIMENSIONS INDICATED
	2	NO PENETRATION • FRONT FACE OF CRATER DIMENSIONS INDICATED • DELAMINATION • SOME BACK FACE FIBER BREAKAGE*
	3	NEAR PENETRATION (BALLISTIC LIMIT) • FRONT FACE CRATER OF DIMENSIONS INDICATED • BACK FACE FIBER BREAKAGE* • DELAMINATION
MOST SEVERE	4	PENETRATION • OPEN HOLE OF DIMENSIONS INDICATED

OTHER CODES:
- I - PEBBLE REMAINED INTACT AFTER STRIKING TARGET
- S - PEBBLE SHATTERED OR PULVERIZED AFTER STRIKING TARGET
- R1 - REMOVED SURFACE MATERIAL DOWN TO REINFORCEMENT
- R2 - REMOVED MATERIAL DOWN TO SUBSTRATE
- C - DEEP CRACK IN DAMAGED AREA
- * - ONLY FOR SAMPLES WITH NO SUBSTRATE

Table A-17. Shroud material pebble test data.

MTL NO.	MTL NAME	REF.	SHOT NO.	PEB. MTL	d_p (IN)	W_p (GM)	θ (DEG)	V_p (FT/SEC)	MATERIAL TEMP (°K)	MATERIAL THICK (IN)	SUBSTRATE MTL TYPE	SUBSTRATE THICK (IN)	MASS LOSS (GM)	DAMAGE DATA NOTES	DENT OR CRATER L(IN)	DENT OR CRATER W(IN)	DENT OR CRATER D(IN)	OPEN HOLE L(IN)	OPEN HOLE W(IN)
3001	Ke/Ph	5	72803	TON.	0.365	1.092	12	1886	RT	0.120	NONE	-	0.04	1	1.711	0.458	0.024		
			80202			1.104	6	2138		0.115			0.01	1,I	1.457	0.302	0.021		
			80206			1.140	12	2095					0.11	4,S				0.853	0.149
			80303		0.370	1.133	30	1681					0.13	4,S				0.666	0.343
			80304		0.365	1.096		1352					0.03	1,S	1.277	0.577	0.038		
			80305		0.370	1.160		1676					0.12	4,S				0.643	0.328
			80306		0.365	1.120		1375					0.05	1,S	1.361	0.509	0.064		
			80502		0.630	5.557	12	1735					0.27	3,S	3.515	0.784	0.175		
			80503			5.816		1244					0.04	1,I	2.430	0.330	0.018		
			80801			5.403		1837		0.230			0.18	1,I	2.566	0.661	0.061		
			80802			5.797		2040					0.28	4,S				0.883	0.185
			80803			5.925		2019					0.34	3,I	2.957	0.832	0.250		
			80903		0.370	1.140	30	943					0.01	1,S	0.585	0.312	0.020		
			81001		0.630	5.677	6	1731		0.120			0.03	1,I		0.370	0.030		
			81002			5.816		2012					0.16	1,I		0.505	0.055		
			81003					2387					0.14	1,I		0.525	0.035		
			81101			5.719		2346					0.28	4,I				1.582	0.296
			81102			5.641		2219					0.10	3,I	4.065	0.486	0.068		
			81104			5.933	12	1560					0.29	1,I	3.641	0.714	0.022		
			81105			5.784		2038					1.63	4,S				2.767	0.710
			81106		0.365	1.087		2142					0.08	1,I	1.853	0.430	0.041		
			81107		0.370	1.122		2168					0.09	4,I				0.769	0.081
			81504		0.370	1.107		1669		0.230			0.01	1,I	1.102	0.276	0.023		
			81505		0.630	5.720		1243		0.230			0.02	1,I	1.892	0.402	0.017		
			81904		0.380	1.339	6	2350		0.115			0.48	1,S	1.395	0.329	0.031		
			81905		0.380	1.386	6	2522		0.115			0.51	1,S	1.695	0.376	0.043		

Table A-17. Shroud material pebble test data - (Continued).

MTL NO.	MTL NAME	REF.	SHOT NO.	PEB. MTL	d_p (IN)	W_p (GM)	θ (DEG)	V_p (FT/SEC)	MATERIAL TEMP (°K)	MATERIAL THICK (IN)	SUBSTRATE MTL TYPE	SUBSTRATE THICK (IN)	MASS LOSS (GM)	DAMAGE DATA NOTES	DENT OR CRATER L(IN)	DENT OR CRATER W(IN)	DENT OR CRATER D(IN)	OPEN HOLE L(IN)	OPEN HOLE W(IN)
3001	Ke-Ph	5	81906	TON.	0.630	5.479	6	2370	RT	0.230	NONE	-	-	1,S	2.305	0.457	0.065		
			82201			5.698		2690					-	1,S	1.880	0.470	0.082		
			82205			5.568		2872					-	1,S	2.235	0.450	0.054		
			82302			5.595	30	1726					0.19	4,S				0.713	0.159
			82303			5.702		1061		0.115			1.23	4,S				1.510	0.460
			82304		0.380	1.451		1970		0.230			0.10	1,S	1.090	0.537	0.113		
			82401		0.630	5.691		1094		0.115			1.75	4,S				1.485	0.505
			100301		0.380	1.312	20	2200		0.135			0.59	4,S				0.575	0.365
			100302		0.380	1.346	20	1720		0.135			1.13	4,S				0.680	0.147
			82501		0.380	1.383	12	2645		0.230			0.07	1,S	-	-	-		
			82502		0.630	5.764	30	1254		0.115			1.43	1,S	-	-	-		
			82503		0.380	1.377	12	2877		0.230			0.04	1,S	-	-	-		
			92801	GLASS	0.375	1.119		2160		0.120			0.09	1,S	-	-	-		
			92802		0.625	5.207		1640		0.120			0.99	4,I				-	-
			92803			5.109		1870		0.230			0.17	1,I	-	-	-		
			92901			5.205		1260		0.115			0.02	1,I	-	-	-		
			92902			5.208		2040		0.230			0.37	1,I	-	-	-		
			101201	TON.	0.380	1.314	20	1380		0.135			0.54	1,S	-	-	-		
			101202		0.625	5.563		1040		0.135			0.35	1,I	-	-	-		
			101203			5.562		1550		0.135			2.66	4,S				-	-
			101204			5.602		1660		0.230			0.20	1,S	-	-	-		
			101301			5.681		1830		0.230			0.51	4,S				-	-
3002	Ti		72601	GLASS	0.370	1.74	30	1539		0.019			-	4				1.236	0.477
			72602	TON.	0.370	1.118	20	1871		0.020			-	4,S				1.575	0.557
			72802		0.360	1.043	12	1897		0.019			0.25	4,I				1.020	0.270
			72901		0.370	1.154	6	1853		0.020			0.0	1	2.298	0.892	0.050		

Table A-17. Shroud material pebble test data - (Continued).

MTL NO.	MTL NAME	REF.	SHOT NO.	PEB. MTL	d_p (IN)	W_p (GM)	θ (DEG)	V_p (FT/SEC)	MATERIAL TEMP (°K)	MATERIAL THICK (IN)	SUBSTRATE MTL TYPE	SUBSTRATE THICK (IN)	MASS LOSS (GM)	NOTES	DAMAGE DATA: DENT OR CRATER L(IN)	DENT OR CRATER W(IN)	DENT OR CRATER D(IN)	OPEN HOLE L(IN)	OPEN HOLE W(IN)
3002	Ti	5	80103	TON.	0.365	1.073	12	1359	RT	0.020	NONE	-	0.0	1,I	2.353	0.746	0.063		
			80104		0.362	1.105	12	1678					0.33	4,S				1.258	0.375
			80203		0.365	1.095	6	2092					0.24					0.926	0.226
			80204		0.365	1.107	12	2150		0.063			0.02	1,S	1.870	0.716	0.009		
			80301		0.370	1.149	20	1448		0.020			0.38	4,S				1.201	0.421
			80302		0.360	1.060	20	999		0.020			0.0	1,I	1.780	1.163	0.066		
			80403		0.625	5.779	30	2111		0.063			0.45	4,S				2.115	0.760
			80404		0.625	5.763	30	1781		0.063			0.37	4,S				1.343	0.747
			80407		0.625	5.736	20	1069		0.020			0.10	4,I				2.670	0.205
			80501		0.630	5.853	12	1079						3,S				1.995	0.002
			81502		0.360	1.085	6	1673					0.0	1,I	1.630	0.503	0.050		
			81503		0.630	5.978		1587					0.0	1,I	3.270	1.100	0.069		
			81603			5.796		1715					0.70	4,S				2.187	1.135
			81604			5.869		1745					0.88	4,S				2.041	0.564
			81805			5.642	12	1344					0.07	4,S				1.183	0.079
			81806			5.617	12	785					0.01	1,I	2.603	1.210	0.062		
			81901		0.380	1.295	30	1770		0.063			0.01	1,S	1.050	0.468	0.009		
			81902		0.380	1.279	30	2165		0.063			0.02	1,S	2.153	0.983	0.023		
			81903		0.630	5.670	20	1472		0.020			0.09	4,I				1.997	0.809
3003	Gr/Ph		72801		0.365	1.115	12	1780		0.110			0.68	4				0.765	0.179
			72805		0.370	1.141	6	1881		0.115			0.15	3	1.404	0.254	0.[illegible]		
			72906		0.370	1.134	12	1380		0.115			0.30	4,I				0.623	0.104
			80101		0.375	1.196	12	1118		0.120			0.13	3,I	1.414	0.251	0.037		
			80106		0.370	1.140	6	1387		0.115			0.15	1,I	1.455	0.207	0.008		
			80201		0.370	1.109	6	2160		0.115			0.32	4,I				0.586	0.110

Table A-17. Shroud material pebble test data - (Continued).

MTL NO.	MTL NAME	REF.	SHOT NO.	PEB. MTL	d_p (IN)	W_p (GM)	θ (DEG)	V_p (FT/SEC)	MATERIAL TEMP (°K)	MATERIAL THICK (IN)	SUBSTRATE MTL TYPE	SUBSTRATE THICK (IN)	MASS LOSS (GM)	DAMAGE DATA NOTES	DENT OR CRATER L(IN)	DENT OR CRATER W(IN)	DENT OR CRATER D(IN)	OPEN HOLE L(IN)	OPEN HOLE W(IN)
3003	Gr/Ph	5	81004	TON.	0.630	5.808	6	1066	RT	0.120	NONE	-	0.11	1,I	-	0.299	0.014		
			81005		0.630	5.859	6	1209		0.120			0.14	2,I	3.018	0.415	0.028		
			81201		0.630	5.900	12	959		0.115			2.12	4,I				2.020	0.360
			81501		0.365	1.143		1347		0.115			0.38	4,I				0.638	0.147
			81602		0.365	1.118		1701		0.230			0.09	1,S	0.840	0.270	0.023		
			81605		0.630	5.877	6	1700		0.114			2.45	4,I				1.920	0.311
			81606		0.630	5.798	6	1662		0.114			2.13	4,I				1.855	0.328
			81701		0.370	1.135	12	2192		0.245			0.19	2,S	0.710	0.320	0.033		
			81702		0.365	1.125		2578		0.240			0.38	4,S				0.035	0.025
			81703		0.370	1.158		2356		0.240			0.32	3,S	0.855	0.305	0.073		
			82202		0.630	5.878	6	1870		0.230			0.88	3,I	2.020	0.380	0.150		
			82203		0.380	1.363		2351					0.08	1,S	1.005	0.350	0.031		
			82204		0.630	5.527		1756					0.15	2,I	2.236	0.283	0.032		
			82301		0.380	1.342		3089					0.06	1,S	0.811	0.312	0.013		
			82504		0.630	5.771	12	1564					1.20	4,S				-	-
			82505		0.630	5.702		1245					1.30	4,I				-	-
3004	Gr/Pl	6	72701		0.370	1.121		1883		0.107			0.69	4				0.880	0.173
			72804		0.370	1.131	6	1853		0.107			0.30	2				0.465	0.078
			72902		0.365	1.099	12	1880		0.205			0.16	2	0.868	0.281	0.046		
			72904		0.365	1.21		870		0.106			0.02	1,I	0.986	0.155	0.030		
			80102		0.370	1.146		1369		0.108			0.32	4,I				0.590	0.116
			80105		0.375	1.184	6	1360		0.108			0.15	1,I	1.330	0.139	0.014		
			80205		0.370	1.136	12	2183		0.230			0.36	3,S	0.761	0.312	0.085		
			80805		0.630	5.808		1384		0.205			1.92	4,S				1.250	0.201
			80806		0.630	5.865		1084		0.205			0.44	2,I	2.477	0.427	0.125		

Table A-17. Shroud material pebble test data - (Continued).

MTL NO.	MTL NAME	REF.	SHOT NO.	PEB. MTL	d_p (IN)	W_p (GM)	θ (DEG)	V_p (FT/SEC)	MATERIAL TEMP (°K)	MATERIAL THICK (IN)	SUBSTRATE MTL TYPE	SUBSTRATE THICK (IN)	MASS LOSS (GM)	DAMAGE DATA NOTES	DENT OR CRATER L(IN)	DENT OR CRATER W(IN)	DENT OR CRATER D(IN)	OPEN HOLE L(IN)	OPEN HOLE W(IN)
3004	Gr/Pl	6	80901	TON.	0.630	5.890	12	1169	RT	0.205	NONE	-	0.52	3,I	2.420	0.400	0.160		
			80906		0.630	5.792	6	1202		0.205			0.02	1,I	1.811	0.297	0.012		
			81704			5.930	12	1406		0.105			3.35	4,S				2.437	0.483
			81705			5.715		1137		0.105			2.14	4,S				2.045	0.415
			81706			5.636		1157		0.230			1.00	4,S				0.487	0.230
			81801		0.380	1.213		2190					0.28	3,S	0.627	0.309	0.063		
			81802			1.218		2401					0.16	2,S	0.586	0.282	0.013		
		5	81803			1.266		2541					0.19	4,S				0.050	0.037
			81804		0.385	1.290		1307		0.115			0.46	4,I				0.675	0.230
			101302		0.380	1.309	20	1890		0.230			0.32	4,S				-	-
			101303			1.296		1810					1.34	4,S				-	-
			101304			1.386		1350					0.09	2,S	-	-	-		
			101403			1.340		1030		0.115			0.0	4,S				-	-
			101404			1.318		860					0.26	4,S				-	-
			101405			1.308		580					0.01	1,I	-	-	-		
			101701			1.317	30	1370		0.230			0.41	2,S	-	-	-		
			101702			1.306		1620		0.230			0.55	4,S				-	-
			101703			1.305		450		0.115			0.01	1,S	-	-	-		
			101704			1.304		660					0.11	2,S	-	-	-		
			101801			1.302		990					0.76	4,S				-	-
			93001	GLASS	0.375	1.117	12	2160		0.230			0.26	2,S	-	-	-		
			93002	GLASS	0.375	1.116	12	1380		0.115			0.58	4,I				-	-
3005	Ke-Gr/Ph		80902	TON.	0.365	1.120	30	1169		0.235			0.08	1,S	0.857	0.385	0.035		
			81506		0.630	5.652	12	1205		0.230			0.11	1,I	2.069	0.410	0.041		
			81601		0.375	1.181	12	1705		0.230			0.05	1,S	1.151	0.307	0.025		

Table A-17. Shroud material pebble test data - (Continued).

MTL NO.	MTL NAME	REF.	SHOT NO.	PEB. MTL	d_p (IN)	W_p (GM)	θ (DEG)	V_p (FT/SEC)	MATERIAL TEMP (°K)	MATERIAL THICK (IN)	SUBSTRATE MTL TYPE	SUBSTRATE THICK (IN)	MASS LOSS (GM)	DAMAGE DATA NOTES	DENT OR CRATER L(IN)	DENT OR CRATER W(IN)	DENT OR CRATER D(IN)	OPEN HOLE L(IN)	OPEN HOLE W(IN)
3007	Ke(Cloth)/ E759	5	51501	TON.	0.625	5.487	20	1115	RT	0.230	NONE	-	-0.03	2,S	1.663	0.470	0.011		
			51601		0.380	1.273		1510		0.230			0.05	2,S	0.930	0.440	0.030		
			51607		0.380	1.275		2310		0.235			0.05	2,S	0.990	0.480	0.035		
			62203		0.625	5.512		1550					-0.25	4,S				-	-
			62303		0.380	1.280		2540					0.15	2,S	-	-	-		
3010	VITON SYS		51504		0.625	5.553		1080		0.340			0.60	2,S	2.365	0.615	0.065		
			51603		0.380	1.323		1500		0.340			0.20	1,S	1.375	0.510	0.035		
			51608		0.380	1.247		2400		0.350			0.10	2,S	1.180	0.395	0.150		
			62204		0.625	5.556		1400		0.355			1.25	1,S	-	-	-		
3011	VITON SYS		51502			5.518		1150		0.245			0.20	2,S	1.410	0.440	0.021		
			51503			5.543		1140					0.0	2,S	2.095	0.497	0.022		
			51602		0.380	1.333		1460					0.40	2,S	0.745	0.300	0.040		
			51611		0.380	1.409		2100		0.240			0.0	3,S	0.920	0.450	0.150		
			62205		0.625	5.526		1460		0.240			1.90	4,S				-	-
3015	G/PVF 2		51505		0.625	5.570		1040		0.300			0.05	3,S	0.955	0.525	0.070		
			51604		0.380	1.273		1490		0.300			0.15	1,S	0.490	0.250	0.010		
			51612		0.380	1.271		2000		0.305			0.05	2,S	0.575	0.295	0.010		
			62206		0.625	5.519		1430		0.305			0.35	3,S	-	-	-		
			62304		0.380	1.123		2340		0.305			0.10	2,S	-	-	-		
3017	Ke/Ep Nov 2		51506		0.625	5.499		1100		0.370			0.05	2,I	2.610	0.725	0.035		
			51605		0.380	1.351		1520		0.370			0.20	1,S	1.325	0.515	0.025		
			51609		0.380	1.343		2460		0.355			0.15	2,S	1.325	0.595	0.105		
			62301		0.625	5.500		1440		0.350			1.20	4,S				-	-

Table A-17. Shroud material pebble test data - (Continued).

MTL NO.	MTL NAME	REF.	SHOT NO.	PEB. MTL	d_p (IN)	W_p (GM)	θ (DEG)	V_p (FT/SEC)	MATERIAL TEMP (°K)	MATERIAL THICK (IN)	SUBSTRATE MTL TYPE	SUBSTRATE THICK (IN)	MASS LOSS (GM)	DAMAGE DATA NOTES	DENT OR CRATER L(IN)	DENT OR CRATER W(IN)	DENT OR CRATER D(IN)	OPEN HOLE L(IN)	OPEN HOLE W(IN)
3018	Ke/PVF 1	5	51507	TON.	0.625	5.488	20	1100	RT	0.370	NONE	-	0.0	2,S	1.620	0.550	0.015		
↓	↓	↓	51606	↓	0.380	1.280	↓	1460	↓	0.370	↓	↓	0.0	1,S	0.880	0.455	0.035		
↓	↓	↓	51610	↓	0.380	1.339	↓	2460	↓	0.355	↓	↓	0.05	2,S	0.935	0.485	0.050		
↓	↓	↓	62302	↓	0.625	5.502	↓	1400	↓	0.355	↓	↓	0.10	1,S	-	-	-		
↓	↓	↓	62305	↓	0.380	1.270	↓	2650	↓	0.355	↓	↓	-0.15	1,S	-	-	-		
3027	UHMW	↓	112204	↓	↓	1.365	↓	2130	↓	0.110	↓	↓	0.14	1/4,S	-	-	-	-	-
↓	↓	↓	112301	↓	↓	1.335	↓	1590	↓	0.110	↓	↓	0.01	1/2,S	-	-			
↓	↓	↓	112302	↓	↓	1.351	↓	1620	↓	0.140	↓	↓	0.21	1/4,S	-	-	-	-	-

Blank

A-4. SHROUD NOSETIP MATERIAL

Several three-inch diameter, 0.05-inch thick metal nosetips were tested in the DET. The nosetips were made of stainless steel, Inconel, or titanium. Most of the nosetips experienced melt-through at the stagnation point before the end of the test. The data are summarized in Table A-18.

Table A-18. Shroud nosetip DET data.

MATERIAL	REF.	RUN NO.	P_o (LB/IN^2)	h_o (BTU/LBM)	d_p	V_p (FT/SEC)	p_d (G/M^3)	(DEG)	t_{CA} (SEC)	t_d (SEC)	TEST RESULT	NOTES
STAINLESS	4	14	1000	1645	100	5400	0.59	90	2.59	3.15	7/8-INCH HOLE	
									1.82	5.94	2-INCH HOLE	
									2.16	9.05	2 1/2-INCH HOLE	
		15	1025	1695			0.25		2.56	3.07	SURVIVED	1
									1.87	4.58	1 1/8-INCH HOLE	1
									2.16	4.87	1-INCH HOLE	1
INCONEL		14	1000	1645			0.59		2.31	2.74	SURVIVED	
									1.73	5.74	1 5/8-INCH HOLE	
									2.25	9.32	2 3/8-INCH HOLE	
		15	1025	1695			0.25		2.34	3.07	SURVIVED	2
									1.95	4.42	SURVIVED	2
									2.23	5.54	SURVIVED	2
	7	5	1000	800		4450	0.45		6	6	SURVIVED	
									6	12	BURN-THROUGH: 7-8 SEC	
									6	24	BURN-THROUGH: 7-8 SEC	
TITANIUM									6	6	IGNITION: 2.5 SEC	
									6	6	IGNITION: 2.5 SEC	
									6	6	IGNITION: 2.5 SEC	

NOTES: 1 DUE TO BLOCKAGE, DUST HIGHER THAN 0.25 G/M^3

2 DUE TO BLOCKAGE, DUST LOWER THAN 0.25 G/M^3

A-5. SALVO PARTICLE DATA

A large body of data was obtained on VAMAC 25 for varying surface temperature, particle material and size, and impact velocity and angle. In addition, screening data, all at the same set of conditions, were obtained for 25 other materials. These data are all listed in Table A-19. Material samples were all provided by McDonnell Douglas Astronautics Company, and information regarding the materials tested may be obtained from that source.

Table A-19. Salvo particle data.

Run No.	Material	Particle Type	Particle Size	T	Angle	Velocity	G	$\bar{G}/\sigma$
790612-09	Vamac 25	MgO	2.0	RT	20	3075	.12	
-10						3000	.20	
-11						3000	.21	
-12						3075	.15	
-13						3000	.32	.216/.062
-14						3075	.23	
-15						3000	.18	
-16						3000	.26	
-17						3000	.27	
790611-01			3.0			2770	.06	
-02						2950	.10	
-03						2950	.20	
-04						2950	.20	
-05						2950	.06	
-06						2950	.12	.183/.094
-07						2950	.29	
-08						2820	.28	
-09						2820	.21	
-10						3075	.31	
790530-16		Glass	1.65			2500	.06	
						2700	.09	
						2080	.03	
790604-01						2000	.03	
-03						1900	.16	
-04						1950	.18	.109/.064
790605-03						2500	.17	
-04						1800	.08	
-06						2220	.11	
790606-05						2700	.245	
-06						2800	.487	
-07						3010	.381	
-08						3075	.479	.441/.179
-09						3010	.531	
790607-01						3200	.22	
-02						3400	.742	
790530-01						4370	.46	
-05						4160	.29	
-06						4510	.32	
-09						4350	.42	
-10						4100	.39	.473/.150
-11						4670	.67	
-13						4450	.54	
-14						4180	.69	

Table A-19. Salvo particle data - (Continued).

Run No.	Material	Particle Type	Particle Size	T	Angle	Velocity	G	$\bar{G}/\sigma$
790613-01	Vamac 25	Glass	1.65	RT	20	3050	.34	
-02						3000	.30	
-03						3000	.33	
-04						3000	.26	.329/.052
-06						3000	.42	
-07						3050	.27	
-08						3000	.36	
-09						3000	.35	
790524-05			0.325			4360	.5	
790706-01			1.65		9	2825	.04	
-02						3300	.03	
-03						3000	.08	
-05						3200	.06	
-06						3200	.06	
-07						3200	.04	
-08						3200	.07	.058/.018
-09						3200	.06	
-10						3100	.07	
-12						3100	.09	
-14						3200	.05	
-15						3375	.04	
790705-01		MgO	0.65			2180	.14	
-02						2940	.22	
-03						2700	.16	
-04						2800	.21	
-05						2575	.19	
-06						2700	.19	.186/.025
-07						2700	.20	
-08						2600	.21	
-09						2250	.16	
-10						2450	.18	
-11						2500	.19	
790716-02				200	20	2800	.40	
790716-01		Glass	1.65			2800	.67	
790713-04		MgO	0.65			3200	.41	
790713-03		Glass	1.65			2800	.43	
790713-01						2900	.92	
790713-02				150		2900	.49	
790619-09				RT		4925	.83	
-10						5000	.63	.745/.087
-11						4900	.79	
-12						4900	.73	
790618-01			0.325			3000	.26	
-02						3050	.12	
-03						3050	.17	
-04						3000	.12	
-05						3000	.12	.159/.052
-06						2850	.19	
-07						3000	.18	
-08						2500	.11	

Table A-19. Salvo particle data - (Continued).

Run No.	Material	Particle Type	Particle Size	T	Angle	Velocity	G	$\bar{G}/c$
790618-09	Vamac 25	Glass	1.65	RT	20	4500	.28	
-10						4925	.33	
-11						5100	.76	
-12						5200	.72	.639/.232
-13						5500	.75	
790619-01						5400	.77	
-02						~5000	.86	
790614-12			0.50			3050	.19	
-14						3000	.27	.227/.04
790615-02						3050	.22	
790612-04		MgO	0.65			3000	.20	
-05						3000	.19	
-06						3000	.18	.188/.008
-07						3000	.19	
-08						3075	.18	
790605-09		Glass	1.65			1600	.03	
-10						1700	.01	
-12						1600	.02	
790606-02						1100	.06	
790830-02	K/EA9332-1	MgO	0.65	400		3000	2.267	
790830-01	K/L100-1					3000	.875	
790829-02	NOMEX 438EP					3000	2.215	
790829-01	KEVLAR/CIBA					2440	.736	

Table A-19. Salvo particle data - (Continued).

All at 20°, RT, 1.0 mm Glass

Run Number	Material	Velocity	G	$\bar{G}$	σ
0790815-07	T300, Lol, Item 4	3000	.726		
-08		2980	.696		
-09		2960	.887		
-10		2980	.632	.792	.127
-11		2980	.964		
-12		2980	.844		
0790815-01	T300, Hil, Item 4	2980	.642		
-02		2980	.677		
-03		2980	.738		
-04		2980	.669	.732	.105
-05		2980	.931		
-06		2980	.735		
0790814-04	R-2051Al, Item 3	2980	.374		
-05		3080	.529		
-06		3000	.906		
-07		2850	.927		
-08		2960	.892		
-09		3290	.724	.771	.280
-10		3200	1.118		
-11		3200	.305		
-12		3200	.659		
0790813-01	329K, Lol, Item 2	2565	.071		
-02		2760	.082		
-03		3240	.054		
-04		3079	.464		
-05		2980	.214		
0790814-01		2980	.288	.426	.217
-02		2950	.775		
-03		2900	.389		
0790810-01	329K, Hi2, Item 2	3015	.411		
-02		3030	.298		
-03		3105	.140		
-04		3030	.360	.424	.214
-05		3000	.596		
-06		3030	.739		
0790809-01	Kevlar 353, Hil	3030	.526		
-02		3030	.289		
-03		3100	.640	.488	.128
-04		3015	.465		
-05		3030	.521		
0790809-06	Kevlar 353, Lol	3030	.238		
-07		3225	.492	.490	.231
-08		3050	.796		
-09		3030	.435		
0790716-04	P1700 PS	3000	.20		
-05		2800	.21		
-06		3125	.15	.260	.114
-07		3200	.44		
-08		2825	.30		

Table A-19. Salvo particle data - (Continued).
All at 20°, RT, 1.0 mm Glass

Run Number	Material	Velocity	G	$\bar{G}$	σ
0790711-01	KE PVF .75 PVF + .25 EP	----	.312		
-02		3300	.487		
-03		----	.659		
-04		3100	.770		
-05		3200	.721		
-06		3200	.680		
-07		----	1.006	.821	.111
0790712-01		3200	.850		
-02		----	.903		
-03		3100	.820		
0790703-12	KE PVF .75 PVF + .25 EP	3300	.668		
-13	Composite	3300	.956	.839	.313
-14		3400	.513		
-15		3400	1.220		
0790703-08	Kevlar Phenolic Composite	3300	.362		
-09		3300	.587	(0)1	
-10		3300	.815		
-11		3300	1.022		
0790629-17	KETBR Composite	3200	.522		
-18		3200	1.211	>1	
0790702-01		3200	1.016		
0790629-14	KE/EA 9323	3000	.418		
-15		3400	.394		
-16		3225	.625		
0790703-16		3400	.750		
0790803-03		3070	.816		
-04		3240	1.327	.916	.222
-05		3370	.966		
-06		3090	.722		
-07		3020	.912		
0790629-07	KE/ADX 3130	3200	.185		
-08		----	.139		
-09		3200	.353		
-10		3200	.544		
0790806-01		3125	.419		
-02		3075	.610	.701	.269
-03		3000	1.197		
-04		3150	.745		
-05		3050	.688		
0790629-01	TBR - Carbon Filled	3225	.403		
-02		3100	.309		
-03		3200	.457	.424	.128
-04		3200	.623		
-05		3200	.485		
-06		3100	.268		
0790628-10	TBR - Unfilled	2700	.300		
-11		3000	.430		
-12		3200	.418		

Table A-19. Salvo particle data - (Continued).

All at 20°, RT, 1.0 mm Glass

Run Number	Material	Velocity	G	$\bar{G}$	σ
0790628-13	TBR - Unfilled	3000	.601		
-14		3200	.670		
-15		3300	.384	.527	.136
-16		3375	.378		
-17		3010	.600		
0790628-03	.75 PVF + .25 EP Res.	3200	.117		
-04		3000	.148		
-05		3250	.131		
-06		3250	.198		
-07		3350	.229	.263	.076
-08		3250	.371		
-09		3100	.254		
0790703-04	CIBA Epoxy	3300	.338		
-05		3300	.398		
-06		3300	.720		
-07		3300	.777		
0790801-01		3320	1.041		
-02		3070	.244	.694	.268
-03		3170	.589		
-04		3170	.646		
0790802-01		3170	.874		
-02		3060	.682		
-03		3120	1.014		
-04		3170	1.007		
0790702-07	KE/EA 9332 Comp.	3300	.064		
-08		3375	.087		
-09		3300	.136		
0790703-01		?	.202		
-02		3300	.262		
-03		3225	.574		
0790807-01		3000	.167	.314	.174
-02		3030	.167		
-03		3225	.400		
0790702-02	KE/L-100 Comp.	3225	.055		
-03		----	.168		
-04		3300	.615		
-05		3300	.117		
-06		3300	.505		
0790802-05		3080	.223		
-06		3240	.348	.366	.178
-07		3100	.215		
-08		3070	.634		
0790803-01		3160	.524		
-02		3080	.360		
0790629-11	KE 759 EP Comp.	2477	.294		
-12		3300	.416	(0)1	
-13		3000	1.000		

Table A-19. Salvo particle data - (Continued).
All at 20°, RT, 1.0 mm Glass

Run Number	Material	Velocity	G	$\bar{G}$	σ
0790626-01	HYSOL ADX 3130	3000	.184		
-02		----	.037		
-03		3000	.453		
-04		3010	.322		
-05		3100	.354		
-06		3100	.362	.378	.046
-07		3100	.426		
-08		3100	.426		
0790622-04	HYSOL EA 9323	3200	.391		
-05		2900	.374		
-06		3200	.432		
-07		2800	.410	.507	.190
-08		2800	.566		
-09		3200	.461		
-10		2850	.912		
0790621-09	HYSOL EA 9309 ER	2600	.161		
-10		3000	.290		
-11		2700	.207		
-12		2750	.293	.263	.064
-13		2700	.310		
-14		2700	.318		
0790620-01		----	----		
-02		2600	.156		
-03		2700	.185		
-04		2850	.133		
-05		2600	.229		
-06		2700	.121		
-07		3185	.302		
0790621-01		2850	.280		
-02		----	----	.177	.073
-03		2750	.045		
-04		----	.098		
-05		2700	.125		
-06		2600	.214		
-07		2600	.221		
-08		2600	.193		

APPENDIX B

ASSESSMENT OF SHIELDING OF EROSION IN REGIONS OF HIGH POTENTIAL FLUX

APPENDIX B
ASSESSMENT OF SHIELDING OF EROSION IN REGIONS OF HIGH POTENTIAL FLUX

B-1. INTRODUCTION

Particle erosion of missiles has been the subject of a great deal of study and testing. For much of the testing, particularly in ballistic ranges and rocket sled facilities, it is desirable to compress the particle density. In doing this, there is a possibility that rebounded particles and debris (referred to herein simply as "debris") from upstream locations will collide with incoming particles and effectively shield downstream locations on the test sample. A simple method of assessing the probability of debris shielding on a flat plate has been developed. This method has been used to derive a dimensionless parameter that can be used to determine whether or not shielding is probable.

B-2. ANALYTICAL METHOD

The analysis was performed for a flat plate* at some angle-of-attack (θ) to the flow, moving at a velocity, V_p, through the particle field. The following assumptions were made to allow the prediction of the onset of shielding:

Assumptions:

1. Debris particles are all of the same size and density.
2. All incoming particles impact the surface.
3. Debris particles do not collide with one another.
4. The debris leaves the surface at an angle equal to the angle of incidence of the incoming particles.
5. The debris layer depth is much less than its length.

The principal task in predicting shielding is the calculation of the concentration of debris in the path of an incoming particle. For the situation under evaluation, this reduces to simply the calculation of the transit time of debris from the leading edge of the surface to the point under examination (see Figure B-1). This can be shown by the following argument: assume that the surface in front of the point under examination is divided into equal segments of area, $(\Delta X)^2$. Each segment produces a streamtube of debris. Due to assumptions 2 and 3, all streamtubes are identical. Consequently, the debris in streamtube volume element, ν_2, in the second streamtube is identical to that in ν_2' in the first streamtube. ν_3 is identical to ν_3' and similarly, each volume element in the tube τ

*If the impacted surface is a cone or a yawed cylinder, debris shielding will begin at higher particle densities than predicted by this method, due to the effects of streamline divergence.

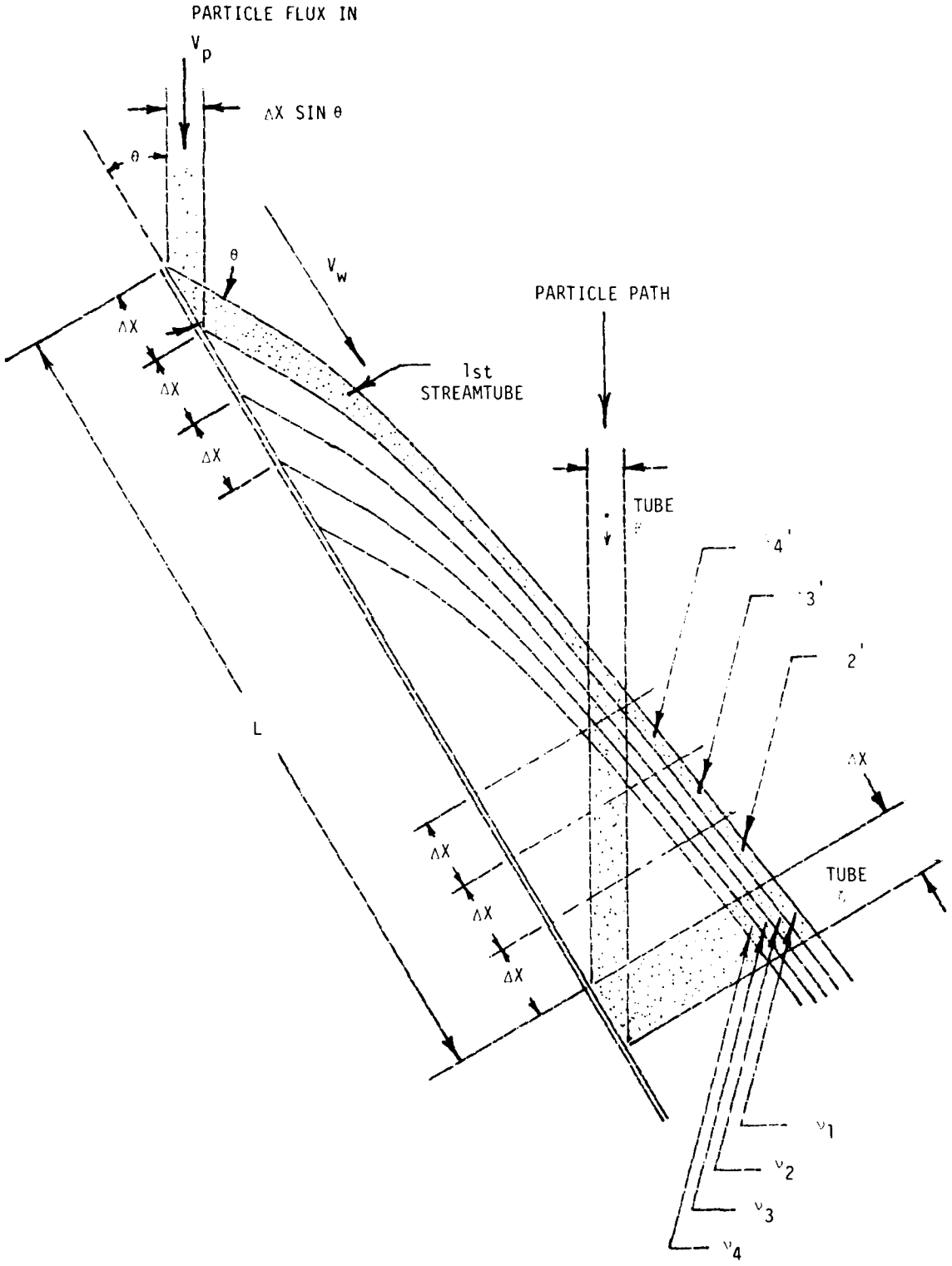

Figure B-1. Debris shielding geometry.

is matched by an identical element in the first streamtube. If the debris layer length is much greater than its height, the number (N) of debris particles along the path of an incoming freestream particle (tube β) is approximately equal to the number in tube ζ which has been shown to be equal to the total number in the first streamtube.

$$N = \frac{(\text{Mass flux per unit surface area})\ \Delta X^2\ (1 + G)\ t_L}{(\text{Mass of debris fragment})}$$

where t_L is the transient time from X = 0 to X = L.

So: $$N = \frac{6\ \rho_\infty\ \Delta X^2\ \sin\theta\ (1 + G)\ V_p\ t_L}{\rho_d\ \pi\ D_d^3} \tag{A1}$$

The transit times to each station L are obtained by solving the following equation numerically:

$$L = (V_e - V_{ox})\ t_L - 1/B\ \ln[(V_e - V_{ox})\ Bt_L + 1] \tag{A2}$$

in which

$$B = \frac{\rho_e\ C_{D_d}\ A_d}{2\ M_d} \tag{A3}$$

Assuming that the residual kinetic energy is equally shared by the debris:

$$V_{ox} = \sqrt{\frac{V_p^2\ (1 - C_{KE})}{1 + G}}\ \cdot \cos\theta \tag{A4}$$

From statistics, the probability that an incoming particle collides with debris is

$$P = 1 - \left(\frac{1}{e}\right)^E \tag{A5}$$

where $$E = \frac{\text{Total cross sectional area of debris in Tube } \beta}{\text{Area of Tube } \beta}$$

so $$E = \frac{N\ A_{eff}}{\Delta X^2\ \sin\theta} \tag{A6}$$

where A_e is the effective cross section area of a single debris particle. Since Equation (5) is based on incoming particles of infinitesimal size, the diameter of the incoming particle is superimposed upon that of the debris particle, so:

$$A_{eff} = \frac{\pi}{4}\ (D_d + D_p)^2 \tag{A7}$$

Substituting Equations (1) and (7) into (6):

$$E = \frac{3\rho_\infty (D_d + D_p)^2 (1 + G) V_p t_L}{\rho_d D_d^3} \tag{A8}$$

B-3. DERIVATION OF DIMENSIONLESS PARAMETER

A dimensionless parameter is derived such that if the parameter is less than one, the probability of an incoming particle striking a debris fragment is less than 10 percent. The expression for the probability of such a collision [Equations (5) and (8)] is straightforward with the exception of the transit time. Consequently, the principal task in the derivation of the dimensionless parameter becomes the identification of an explicit function for the transit time. Using the conservative assumption that the debris initial velocity is zero, the expression for the debris displacement is:

$$X = V_e t - 1/B \ln (B V_e t + 1) \tag{A9}$$

The problem then is to find a function f(X) such that $f(X) \geq t$ for all X. A two-branched function for f(X) is found. The first branch uses:

$$f(X) = \frac{K}{V_e} \left(\frac{X}{B}\right)^{\frac{1}{2}} \tag{A10}$$

K is evaluated from the requirement that for all X:

$$X \leq V_e f(X) - 1/B \ln [B V_e f(X) + 1] \tag{A11}$$

Substituting for f(X) and multiplying through by B:

$$XB \leq K(XB)^{\frac{1}{2}} - \ln [K(XB)^{\frac{1}{2}} + 1] \tag{A12}$$

Now let

$$K(XB)^{\frac{1}{2}} = \zeta \tag{A13}$$

which yields:

$$\frac{1}{K^2} \leq \frac{\zeta - \ln (\zeta + 1)}{\zeta^2} \tag{A14}$$

Over the range $0 \leq \zeta \leq 1$, the right hand side is a minimum at $\zeta = 1$ and has a value of $1 - \ln(2)$. Thus

$$\frac{1}{K^2} \leq 0.307 \tag{A15}$$

That is, the function selected is always less than t as required, as long as

$$K \geq \left(\frac{1}{0.307}\right)$$

$$\geq 1.81 \qquad \text{(A16)}$$

For the second branch of the function, let:

$$f(X) = \frac{XK}{V_e} \qquad \text{(A17)}$$

Substituting for f(X) in Equation (11) and multiplying through by B yields:

$$XB \leq XKB - \ell n\,(XKB + 1) \qquad \text{(A18)}$$

This branch will be valid over the range:

$$\zeta = K(XB)^{\frac{1}{2}} > 1 \qquad \text{(A19)}$$

Substituting the value from Equation (16) for K yields

$$XB > 0.307 \qquad \text{(A20)}$$

Substituting Equation (20) into Equation (18) and solving yields

$$K > 3.26$$

Since a 10 percent probability of collision corresponds to an exponent E of 0.1, the shielding parameter can be stated:

$P \leq 0.1$ if:

$$\frac{30\rho_\infty (D_d + D_r)^2 (1 + G) V_p f(X)}{\rho_d D_d^3} \leq 1.0$$

$$f(X) = \frac{1.81}{V_e} (XB)^{\frac{1}{2}} \qquad (XB \leq 0.307)$$

$$f(X) = \frac{3.26\ X}{V_e} \qquad (XB > 0.307)$$

NOMENCLATURE

(Applicable to main text and appendices)

SYMBOL	MEANING	UNITS
A	Cross section area	ft^2
B	Particle deceleration parameter defined in Equation A3	---
C_D	Drag coefficient	---
C_{KE}	Kinetic energy accommodation coefficient	---
D	Diameter	ft
e	Base of natural logarithms	---
E	Exponent defined in Equation A6	---
G	Erosion mass loss ratio (mass removed/impacting mass)	---
h	Enthalpy	Btu/lbm
L	X distance to station under analysis	ft
M	Mass	lbm
N	Number	---
p	Pressure	lbf/in^2
P	Probability	---
$\dot{q}$	Heat flux	Btu/ft^2-sec
t_L	Transit time from X = 0 to X = L	sec
T	Temperature	deg F
V	Velocity	ft/sec
X	Streamwise coordinate	ft
GREEK		
ρ	Density	lbm/ft^3*
θ	Impact angle	deg
SUBSCRIPT		
∞	Freestream	
d	Debris	
e	Edge of boundary layer	
eff	Effective	
NOM	Nominal	
o	Initial	
p	Impacting particle	
t	Target	
X	Streamwise component	

* Except freestream particle density, ρ_∞ is given in "conventional" units of g/m^3.

Blank

DISTRIBUTION LIST

DEPARTMENT OF DEFENSE

Defense Advanced Rsch Proj Agency
ATTN: TIO

Defense Communications Agency
ATTN: CCTC

Defense Intelligence Agency
ATTN: DB-4D
ATTN: DT-1C
ATTN: DT-2

Defense Nuclear Agency
ATTN: STSP
ATTN: SPAS, Maj Case
ATTN: SPTD
4 cy ATTN: TITL

Defense Technical Information Center
12 cy ATTN: DD

Field Command
Defense Nuclear Agency
ATTN: FCPR

Joint Strat Tgt Planning Staff
ATTN: JPTM
ATTN: JLTW-2
ATTN: JLA

Under Secy of Def for Rsch & Engrg
ATTN: Engineering Technology, J. Persh
ATTN: Strategic & Space Systems (OS)

DEPARTMENT OF THE ARMY

BMD Advanced Technology Center
Department of the Army
ATTN: ATC-T, M. Capps

BMD Systems Command
Department of the Army
ATTN: BMDSC-H, N. Hurst

Deputy Chief of Staff for Rsch Dev & Acq
Department of the Army
ATTN: DAMA-CSS-N

Harry Diamond Laboratories
Department of the Army
ATTN: DELHD-N-P, J. Gwaltney
ATTN: DELHD-N-TF

U.S. Army Ballistic Research Labs
ATTN: DRDAR-BLE, J. Keefer

U.S. Army Material & Mechanics Rsch Ctr
ATTN: DRXMR-HH, J. Dignam

U.S. Army Materiel Dev & Readiness Cmd
ATTN: DRCDE-D, L. Flynn

U.S. Army Missile Command
ATTN: DRSMI-RKP, W. Thomas
ATTN: DRDMI-TRR, B. Gibson
ATTN: DRDMI-XS

DEPARTMENT OF THE ARMY (Continued)

U.S. Army Nuclear & Chemical Agency
ATTN: Library

U.S. Army TRADOC Systems Analysis Activity
ATTN: ATAA-TDC, R. Benson

DEPARTMENT OF THE NAVY

Naval Research Laboratory
ATTN: Code 2627
ATTN: Code 7908, A. Williams
ATTN: Code 6770, G. Cooperstein

Naval Sea Systems Command
ATTN: SEA-0352, M. Kinna

Naval Surface Weapons Center
ATTN: Code R15, J. Petes
ATTN: Code F31
ATTN: Code K06, C. Lyons

Office of Naval Research
ATTN: Code 465

Office of the Chief of Naval Operations
ATTN: OP 604E14, R. Blaise

Strategic Systems Project Office
Department of the Navy
ATTN: NSP-272

DEPARTMENT OF THE AIR FORCE

Aeronautical Systems Division
Air Force Systems Command
2 cy ATTN: ASD/ENFTV, D. Ward

Air Force Flight Dynamics Laboratory
ATTN: FXG

Air Force Geophysics Laboratory
ATTN: LY, C. Touart

Air Force Materials Laboratory
ATTN: MBC, D. Schmidt
ATTN: MBE, G. Schmitt
ATTN: LLM, T. Nicholas

Air Force Rocket Propulsion Laboratory
ATTN: LKCP, G. Beale

Air Force Systems Command
ATTN: SOSS
ATTN: XRTO

Arnold Engineering Development Center
Air Force Systems Command
ATTN: Library Documents

Ballistic Missile Office
Air Force Systems Command
ATTN: MNRTE
ATTN: MNNR
2 cy ATTN: MNNXH, Blankinship

DEPARTMENT OF THE AIR FORCE (Continued)

Air Force Weapons Laboratory
Air Force Systems Command
ATTN: DYS
ATTN: DYV
ATTN: DYV, A. Sharp
ATTN: DYT
ATTN: NTESB, K. Filippelli
ATTN: SUL
ATTN: HO, W. Minge
ATTN: NTES, G. Ganong
2 cy ATTN: NTQ

Deputy Chief of Staff
Research, Development & Acq
Department of the Air Force
ATTN: AFRDQSM
ATTN: AFRD

Foreign Technology Division
Air Force Systems Command
ATTN: SDBG
ATTN: SDBS, J. Pumphrey
ATTN: TQTD

Headquarters Space Division/YL
Air Force Systems Command
ATTN: AFML, G. Kirschner

Strategic Air Command
Department of the Air Force
ATTN: XPFS
ATTN: DOXT
ATTN: XPQM
ATTN: XOBM

DEPARTMENT OF ENERGY

Department of Energy
ATTN: OMA/RD&T

DEPARTMENT OF ENERGY CONTRACTORS

Sandia National Laboratories
Livermore Laboratory
ATTN: Library & Security Classification Div
ATTN: H. Norris, Jr.

Sandia National Laboratories
ATTN: T. Cook
ATTN: A. Chabai
ATTN: M. Cowan

DEPARTMENT OF DEFENSE CONTRACTORS

Acurex Corp
ATTN: R. Rindal
ATTN: C. Nardo

Aerojet Solid Propulsion Co
ATTN: R. Steele

DEPARTMENT OF DEFENSE CONTRACTORS (Continued)

Aerospace Corp
ATTN: H. Blaes
ATTN: J. McClelland
ATTN: W. Barry
ATTN: R. Crolius

APTEK
ATTN: T. Meagher

AVCO Research & Systems Group
ATTN: J. Stevens
ATTN: Document Control
ATTN: J. Gilmore
ATTN: W. Broding
ATTN: P. Grady

Boeing Co
ATTN: B. Lempriere

California Research & Technology, Inc
ATTN: K. Kreyenhagen

Effects Technology, Inc
ATTN: R. Parisse
ATTN: J. Carlyle

General Electric Co
Space Division
ATTN: G. Harrison
ATTN: D. Edelman
ATTN: C. Anderson

General Electric Co
Re-entry & Environmental Systems Div
ATTN: P. Cline

General Electric Company—TEMPO
ATTN: DASIAC

Hercules, Inc
ATTN: P. McAllister

Kaman Sciences Corp
ATTN: J. Hoffman
ATTN: F. Shelton
ATTN: J. Keith
ATTN: D. Sachs

Lockheed Missiles & Space Co, Inc
ATTN: F. Borgardt

Lockheed Missiles & Space Co, Inc
ATTN: R. Walz

Los Alamos Technical Associates, Inc
ATTN: C. Sparling
ATTN: J. Kimmerly
ATTN: P. Hughes

Martin Marietta Corp
ATTN: J. Potts
ATTN: G. Aiello
ATTN: L. Kinnaird

DEPARTMENT OF DEFENSE CONTRACTORS (Continued)

Martin Marietta Corp
ATTN: E. Strauss

McDonnell Douglas Corp
ATTN: H. Berkowitz
ATTN: P. Lewis, Jr.
ATTN: D. Dean
ATTN: H. Hurwicz
ATTN: J. Garibotti
ATTN: E. Fitzgerald
ATTN: L. Cohen
ATTN: R. Reck
2 cy ATTN: J. Kirby

National Academy of Sciences
National Materials Advisory Board
ATTN: D. Groves

Pacific-Sierra Research Corp
ATTN: H. Brode
ATTN: G. Lang

Physics International Co
ATTN: J. Shea

Prototype Development Associates, Inc
ATTN: J. McDonald
5 cy ATTN: D. Smith
5 cy ATTN: M. Sherman

R & D Associates
ATTN: P. Rausch
ATTN: P. Haas
2 cy ATTN: F. Field

Rand Corp
ATTN: J. Mate

Rockwell International Corp
ATTN: G. Perrone

Science Applications, Inc
ATTN: G. Ray
ATTN: O. Nance
ATTN: D. Hove
ATTN: W. Yengst
ATTN: J. Warner

DEPARTMENT OF DEFENSE CONTRACTORS (Continued)

Science Applications, Inc
ATTN: G. Burghart

Science Applications, Inc
ATTN: W. Layson
ATTN: J. Cockayne

Science Applications, Inc
ATTN: A. Martellucci

Southern Research Institute
ATTN: C. Pears

SRI International
ATTN: G. Abrahamson
ATTN: P. Dolan
ATTN: H. Lindberg
ATTN: D. Curran

System Planning Corp
ATTN: F. Adelman

Systems, Science & Software, Inc
ATTN: G. Gurtman
ATTN: R. Duff

Terra Tek, Inc
ATTN: S. Green

Thiokol Corp
ATTN: W. Shoun

TRW Defense & Space Sys Group
ATTN: R. Bacharach
ATTN: M. Seizew
ATTN: T. Mazzola
ATTN: P. Brandt
ATTN: G. Arenguren
2 cy ATTN: A. Zimmerman

TRW Defense & Space Sys Group
ATTN: V. Blankenship
ATTN: E. Wong
ATTN: D. Kennedy
ATTN: L. Berger
2 cy ATTN: W. Polich


DATE:
TIME